

Salp swarms in the Tasman Sea: Insights into their population ecology

Author:

Henschke, Natasha

Publication Date:

2015

DOI:

<https://doi.org/10.26190/unsworks/18144>

License:

<https://creativecommons.org/licenses/by-nc-nd/3.0/au/>

Link to license to see what you are allowed to do with this resource.

Downloaded from <http://hdl.handle.net/1959.4/54319> in <https://unsworks.unsw.edu.au> on 2024-04-28

Salp swarms in the Tasman Sea: Insights into their population ecology



Natasha Henschke

**Evolution and Ecology Research Centre
School of Biological, Earth and Environmental Sciences
University of New South Wales**

**A thesis in fulfillment of the requirements for the degree of
Doctor of Philosophy**

August 2014

THE UNIVERSITY OF NEW SOUTH WALES

Thesis/Dissertation Sheet

Surname or Family name: **Henschke**

First name: **Natasha**

Other name/s:

Abbreviation for degree as given in the University calendar: **PhD**

School: **Biological, Earth and Environmental Sciences**

Faculty: **Science**

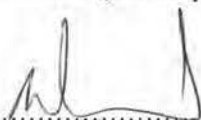
Title: **Salp swarms in the Tasman Sea: Insights into their population ecology**

Salps are gelatinous zooplankton that regularly occur in intermittent swarms, quickly becoming the most dominant organism within an area. However, the factors affecting the occurrence and size of these swarms are still widely unknown and little research attention has been paid to salps in the Tasman Sea. This thesis explores the trophic interactions of salps within the zooplankton community, the environmental drivers that influence the formation of salp swarms, and impact of salp swarm demise on the benthic community. The trophic niche of an oceanic zooplankton community was studied using stable isotopes of carbon and nitrogen. The trophic relationships among the zooplankton were dynamic and responded to different water types depending on food availability. The salp *Thalia democratica* likely competes with copepods for the same food source, however, krill were found to partition the niche to feed on other prey items. The interannual abundance of *T. democratica* was negatively related to the rates of asexual reproduction (buds per chain). *T. democratica* abundance was significantly positively related to food >2 µm in size and negatively related to the proportion of non-salp zooplankton. This suggests that salp swarm abundance may depend on the abundance of larger phytoplankton (prymnesiophytes and diatoms) and competition with other zooplankton. In this thesis, a size-structured population model of the salp, *T. democratica* was developed to understand the relationship between environmental variables (temperature and chlorophyll *a*) and population dynamics. Temperature and chlorophyll *a* were sufficient as environmental variables to predict *T. democratica* population dynamics. The model simulated larger, faster growing salp swarms when availability of chlorophyll *a* (food) was high and temperature was near optimum (20.5°C). This thesis also identified that after the demise of a salp swarm, carcasses can rapidly sink to the benthos as food fall events. Benthic crustaceans and fish were observed feeding on carcasses, and the nutritional value of the salp carcasses were high compared to other gelatinous organisms. The deposition of the mean yearly biomass (4.81 t km⁻² WW) of salps in the Tasman Sea represents a 330% increase to the carbon input normally estimated for this region.

Declaration relating to disposition of project thesis/dissertation

I hereby grant to the University of New South Wales or its agents the right to archive and to make available my thesis or dissertation in whole or in part in the University libraries in all forms of media, now or here after known, subject to the provisions of the Copyright Act 1968. I retain all property rights, such as patent rights. I also retain the right to use in future works (such as articles or books) all or part of this thesis or dissertation.

I also authorise University Microfilms to use the 350 word abstract of my thesis in Dissertation Abstracts International (this is applicable to doctoral theses only).



Signature



Witness

1/08/2014

Date

The University recognises that there may be exceptional circumstances requiring restrictions on copying or conditions on use. Requests for restriction for a period of up to 2 years must be made in writing. Requests for a longer period of restriction may be considered in exceptional circumstances and require the approval of the Dean of Graduate Research.

FOR OFFICE USE ONLY

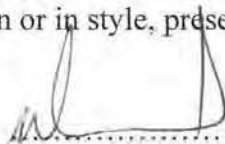
Date of completion of requirements for Award:

Cover image from CL Griffiths

ORIGINALITY STATEMENT

'I hereby declare that this submission is my own work and to the best of my knowledge it contains no materials previously published or written by another person, or substantial proportions of material which have been accepted for the institution, except where due acknowledgement is made in the thesis. Any contribution made to the research by others, with whom I have worked at UNSW or elsewhere, is explicitly acknowledged in the thesis. I also declare that the intellectual content of this thesis is the product of my own work, except to the extent that the assistance from others in the project's design and conception or in style, presentation and linguistic expression is acknowledged'.

Signed



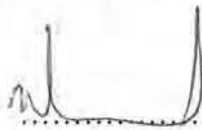
Date

1/08/2014

COPYRIGHT STATEMENT

'I hereby grant the University of New South Wales or its agents the right to archive and make available my thesis or dissertation in whole or part in the University libraries in all forms of media, now or here after known, subject to the provisions of the Copyright Act 1968. I retain all proprietary rights, such as patent rights. I also retain the right to use in future works (such as articles of books) all or part of this thesis or dissertation. I also authorise University Microfilms to use the 350 word abstract of my thesis in Dissertation Abstract International (this is applicable to doctoral theses only). I have either used no substantial portions of copyright material in my thesis or I have obtained permission to use copyright material; where permission has not been granted I have applied/will apply for a partial restriction of digital copy of my thesis or distertation.'

Signed



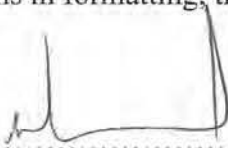
Date

1/08/2014

AUTHENTICITY STATEMENT

'I certify that the Library deposit digital copy is a direct equivalent of the final officially approved version of my thesis. No emendation of content has occurred and if there are any minor variations in formatting, they are the result of the conversion to digital format.'

Signed



Date

1/08/2014

Abstract

Pelagic tunicates, including salps, are an important category of gelatinous zooplankton and yet are relatively understudied. Salps regularly occur in intermittent swarms and can quickly become the most dominant zooplankton within an area. My thesis explores the trophic interactions of salps within the zooplankton community using stable isotope analysis, the environmental drivers of salp population dynamics, and the occurrence of salp deposition on the sea floor.

The trophic niche of salps within the oceanic zooplankton community was investigated using stable isotopes of carbon and nitrogen. Zooplankton and suspended particulate organic matter (POM) were sampled in three different water types: inner shelf (IS), a cold core eddy (CCE; cyclonic) and a warm core eddy (WCE; anti-cyclonic). Recent upwelling in the IS water type resulted in lower than expected trophic enrichment for all zooplankton species (0.53‰ compared to 3.4‰), and the salp *Thalia democratica* was depleted in ^{15}N compared to POM. Trophic enrichment of zooplankton within the CCE (2.74‰) was higher than the IS, and more similar to expected results (3.4‰). Based on chlorophyll *a* and nitrate concentrations, the WCE was characterised as an oligotrophic environment and was associated with an increased trophic level for omnivorous zooplankton (copepods and euphausiids) to a similar level as carnivorous zooplankton (chaetognaths). This study shows that trophic relationships among the zooplankton are dynamic and can vary across water types.

The demographic characteristics of three salp swarms were studied to examine factors influencing variations in salp swarm magnitude. The interannual abundance of *Thalia democratica* during spring was related to the rates of asexual reproduction (buds per chain). *T. democratica* abundance was significantly higher in October 2008 (1312 individuals m^{-3}) than 2009 and 2010 (210 and 92 individuals m^{-3} , respectively). Salp abundance was negatively related to buds per chain and relative growth rates, implying a faster release rate. As *T. democratica* abundance was significantly positively related to food $>2\ \mu\text{m}$ in size and negatively related to the proportion of non-salp zooplankton, salp swarm abundance may depend on the abundance of larger phytoplankton (prymnesiophytes and diatoms) and competition with other zooplankton.

A discrete-time, size-structured *Thalia democratica* population model was developed to investigate the temporal resolution of a salp swarm. The model used size-dependent reproduction and mortality, where growth was dependent on food consumption (chlorophyll *a* biomass) and temperature. Average generation time (12 days) and mean abundances of each stage correspond to previously reported values. Salp ingestion rate and the doubling time of chlorophyll *a* were the most influential parameters, negatively influencing salp biomass and abundances for each individual stage. Forcing the model with a 10-year temperature and chlorophyll *a* time-series identified that salp abundances off the coast of Sydney (34°S) were significantly greater during spring and summer compared to autumn and winter. This is consistent with observations of salp swarms which occur after the spring phytoplankton bloom. Salp swarm abundance appears to be related to the availability of food (chlorophyll *a* per salp) rather than absolute abundance (chlorophyll *a* biomass).

Mass depositions of the large salp *Thetys vagina* were observed on the Tasman Sea floor in 2008 and 2009, prompting examination into the potential of salp carcasses to act as food fall events to the benthos. Over 1700 carcasses were identified on the sea floor and benthic fish and crustaceans were observed feeding on the carcasses. Analysis of a 30-year trawl survey database determined that salp biomass (wet weight, WW) in the eastern Tasman Sea regularly exceeds 100 t km^{-3} . *T. vagina* has a carbon (31% dry weight, DW) and energy ($11 \text{ kJ g}^{-1} \text{ DW}$) content more similar to that of phytoplankton blooms, copepods and fish than to that of jellyfish (cnidarians), with which they are often grouped. Given their abundance, rapid export to the seabed and high nutritional value, salps are likely to be a significant input of carbon to pelagic and benthic food webs, which until now, has been largely overlooked.

Acknowledgements

Firstly I would like to thank my supervisors, Iain Suthers and Jason Everett, for their guidance during the course of this research. Thank you for the encouragement, advice, support and never ending enthusiasm for salps. I am grateful that you both had the confidence in me to pursue my interests in this thesis and the patience to allow me to attend several international “conferences” during the past four years.

I am grateful to James Smith for his significant help in Chapters 2 and 4 of this thesis. Thank you for patiently assisting me with the salp model and answering all my questions. To Sebastian Holmes, thank you for all your assistance. Without your generosity, patience and determination Chapter 5 would not have been possible.

This thesis also relied on the support of individuals from several institutions apart from UNSW, including CSIRO, NIWA, UWS, UTS and Griffith University. In particular, I am grateful to David Bowden, Martina Doblin, Kylie Pitt, Anthony Richardson, Rudy Kloser, Raymond Lee, Matt Taylor, Brian Hunt and Mark Baird for their advice, support, assistance and insight. Collaborating with such a diverse group of enthusiastic scientists has greatly improved this thesis and my capabilities as a researcher.

I also wish to thank the crew and scientists of R.V. *Southern Surveyor* who assisted on the research cruises of October 2008, October 2009 and September 2010; and the Australian Research Council for funding this research. Without their assistance this research would not have been possible. To the FAMER lab, thank you for the proof reading, the friendship and the coffee breaks throughout the years.

To my family and friends, thank you for your endless support and love. I am grateful to my family for always taking care of me and encouraging me to pursue any career path I wish – even if they don’t know what a salp is! A massive thank you to my friends, for the laughter, the good times, the encouragement and your general awesomeness.

Finally, to Josh. Thank you for everything. You have been by my side since the beginning of this thesis and have made every day better.

Table of Contents

Abstract	iv
Acknowledgements	vi
List of Figures	x
List of Tables	xiii
Chapter 1	1
Introduction: Understanding process influencing salp swarms	1
1.1 Gelatinous zooplankton	1
1.2 Pelagic tunicates	2
1.3 The salp life cycle and swarm formation.....	3
1.4 Feeding and trophic role of salps	6
1.5 Salps in the Tasman Sea ecosystem.....	8
1.6 Aims and thesis objectives.....	9
1.7 Thesis chapters.....	10
Chapter 2	13
The zooplankton trophic niche across different water types: a stable isotope analysis.....	13
Abstract	13
2.1 Introduction.....	14
2.2 Methods	16
2.2.1 Field sampling	16
2.2.2 Stable isotope analysis	18
2.2.3 Statistical analyses	19
2.3 Results.....	20
2.3.1 Water type characterisation	20
2.3.2 Particulate organic matter	20
2.3.3 Zooplankton isotope analysis	26
2.3.4 Trophic niche widths across species	30
2.4 Discussion	32
2.4.1 Particulate organic matter	32
2.4.2 Isotopic enrichment of Tasman Sea zooplankton	34
2.4.3 Species-specific trophic niche width	36
2.4.4 Concluding remarks	38
Chapter 3	39
Demography and interannual variability of salp swarms (<i>Thalia democratica</i>)	39
Abstract	39
3.1 Introduction.....	40
3.2 Methods	44
3.2.1 Long-term <i>Thalia democratica</i> sampling	44
3.2.2 Oceanographic sampling procedure	44
3.2.3 Pigment analyses	48
3.2.4 Shipboard zooplankton sampling	48
3.2.5 Shipboard growth experiments.....	49
3.2.6 <i>Thalia democratica</i> demographic analyses.....	51
3.2.7 Data analyses	53
3.3 Results.....	57
3.3.1 Long-term <i>Thalia democratica</i> abundance	57
3.3.2 Hydrographic properties during the sampling period	57
3.3.3 <i>Thalia democratica</i> life history characteristics from ocean voyages.....	59

3.3.4 Zooplankton community composition.....	62
3.3.5 Laboratory growth experiments	64
3.3.6 Relationship between <i>Thalia democratica</i> abundance and the environment.....	64
3.4 Discussion	67
3.4.1 Long-term monitoring	67
3.4.2 Experimental growth comparison	68
3.4.3 <i>Thalia democratica</i> demography.....	71
3.4.4 Oceanographic influence on salp swarm magnitude	71
3.4.5 Concluding remarks	73
Chapter 4	74
Population drivers of a <i>Thalia democratica</i> swarm: Insights from population modelling	74
Abstract	74
4.1 Introduction.....	75
4.2 Methods	78
4.2.1 General approach.....	78
4.2.2 Lefkovich matrix model	80
4.2.3 Size-structured population model.....	81
4.2.4 Standard simulation	89
4.2.5 Sensitivity analysis.....	93
4.2.6 Time-series simulation	93
4.3 Results.....	95
4.3.1 Lefkovich matrix model	95
4.3.2 Standard simulation	96
4.3.3 Sensitivity analysis.....	96
4.3.4 Time-series simulation	98
4.4 Discussion	105
4.4.1 Comparison of the modelled salp population with field estimates.....	105
4.4.2 Pattern of long-term and seasonal salp abundance.....	106
4.4.3 Population dynamics driving salp biomass.....	109
4.4.4 Environmental factors driving salp biomass.....	110
4.4.5 Model limitations.....	110
4.4.6 Predicting <i>Thalia democratica</i> swarms.....	112
4.4.7 Concluding remarks	113
Chapter 5	114
Salp-falls in the Tasman Sea: a major food input to deep sea benthos.....	114
Abstract	114
5.1 Introduction.....	115
5.2 Methods	118
5.2.1 Study region.....	118
5.2.2 Trawl data analysis	118
5.2.3 Benthic sample collection and analysis.....	120
5.2.4 Biochemical analyses	121
5.3 Results.....	123
5.3.1 Observations of <i>Thetys vagina</i> on the sea floor	123
5.3.2 Abundance of <i>Thetys vagina</i> and other large salps in the Tasman Sea	125
5.3.3 Biochemical composition of <i>Thetys vagina</i>	127
5.4 Discussion	129
5.4.1 Observations of <i>Thetys vagina</i> on the sea floor	129
5.4.2 Abundance of <i>Thetys vagina</i> and other large salps in the Tasman Sea	129
5.4.3 Biochemical composition of large salps.....	131
5.4.4 Contribution to the benthic food web	132

5.4.5 Potential carbon standing stock.....	134
5.4.6 Concluding remarks	135
Chapter 6	136
Conclusion: Understanding processes influencing salp swarms	136
6.1 General discussion	136
6.2 Avenues for future research.....	138
6.2.1 Defining “optimal conditions”	138
6.2.2 The fate of small salp carcasses.....	139
6.2.3 Incorporation of salps into biogeochemical models	140
6.2.4 Salps are not jellyfish!	141
References.....	142

List of Figures

Figure 1.1 Life cycle of the salp *Thalia democratica*, demonstrating alternation between aggregated sexual (A1 to A3) and solitary asexual (S1 and S2) generations (Heron & Benham 1985). Blastozooid female buds (A1) are fertilised immediately upon release by mature male blastozooids (A3). These female buds then grow an embryo internally (A2). Once the embryo is released, the blastozooid female develops testes and functions as a male (A3). The embryo is the start of the oozoid generation. The immature oozoid (S1) develops up to 3 chains of between 20 and 80 blastozooid buds, released by mature oozoids (S2). Dashed lines represent the shift in generation. Dotted line represents external fertilization. Figure from Henschke et al. (2011). 4

Figure 2.1 Location plot with satellite-derived sea surface temperature (°C; left) and chlorophyll *a* ($\mu\text{g L}^{-1}$; right) overlaid on best representing conditions occurring during sampling (Table 2.1). Geostrophic currents are estimated through surface altimetry and are represented by arrows. Sampling locations in different water types are indicated with different shapes. IS – inner shelf, CCE – cold core eddy, WCE – warm core eddy. 17

Figure 2.2 Mean temperature-salinity signatures (0 – 100m) for each water type: IS - inner shelf, CCE - cold core eddy and WCE - warm core eddy. Density contours are overlaid. 21

Figure 2.3 Bi-plot of mean (\pm SE) $\delta^{13}\text{C}$ (‰) vs. $\delta^{15}\text{N}$ (‰) values of each zooplankton species pooled for each water type. Abbreviated species names are displayed adjacent to data points, with corresponding names and feeding groups presented next to the graph. Bold names represent carnivorous (C) species. *Sapphirina augusta* is a parasitic (P) copepod. All remaining copepod and euphausiid species, and the salp *Thalia democratica*, are omnivorous (O). POM is particulate organic matter and represents the average across all water types (excluding WCEp). Feeding groups are based on references presented in Table 2.3. The inner groups have been enlarged (inset) for clarity (error bars not included). 22

Figure 2.4 a) $\delta^{13}\text{C}$ and b) $\delta^{15}\text{N}$ isotope values (mean \pm SE) of POM and zooplankton across water types in the Tasman Sea. $\delta^{13}\text{C}$ and $\delta^{15}\text{N}$ values were sorted in order of increasing trophic level (based on average $\delta^{15}\text{N}$). IS – inner shelf, CCE – cold core eddy, WCE – warm core eddy. 23

Figure 2.5 ^{15}N enrichment (Δ) for zooplankton taxa over POM (dashed line) across water types. IS – inner shelf, CCE – cold core eddy, WCE – warm core eddy. ^{15}N enrichment for the copepod species *Eucalanus elongatus* and the euphausiid species *Thysanoessa gregaria* are represented in their taxa groups for the CCE (+) and WCE (*). 28

Figure 2.6 $\delta^{13}\text{C}$ and $\delta^{15}\text{N}$ bi-plot for *Thysanoessa gregaria*, *Eucalanus elongatus* and *Thalia democratica*. Standard ellipse areas (SEA_B) are depicted with solid or dashed lines, with species labels displayed adjacent to ellipses. n – number of samples. 31

Figure 3.1 Schematic diagram of Heron and Benham's (1985) overwintering theory. During poor conditions (left pane) such as winter, *Thalia democratica* oozoids will release longer chains of blastozooid buds (buds per chain; BPC). However, slow growth will result in young being exposed to predation and competition for longer, resulting in fewer reaching maturity and smaller swarm sizes. When conditions improve (right pane) in spring, oozoids will release shorter chains (lower BPC) more quickly that will grow rapidly and form larger swarms. 42

Figure 3.2 Study area with satellite derived sea surface temperature (°C; A-C) and chlorophyll *a* ($\mu\text{g L}^{-1}$; D-F) overlaid. Images best represent conditions occurring on the first day of oceanographic sampling across the three years (Table 3.1). Due to cloud cover, satellite data represents an 8-day composite of sea surface conditions ending with the date given. Zooplankton sampling locations are represented by triangles. Black triangles denote stations

that were used for asexual reproduction analysis. Grey circle indicates location of the Port Hacking National Reference Station. Black line refers to 200 m isobath.....	45
Figure 3.3 Three chains of <i>Thalia democratica</i> buds in an oozoid individual. Buds in first and second chains are clearly segmented and distinguished from other chains (S1: first separation, S2: second separation). Buds from the third chain are still segmenting along the stolon. Only the first chain was considered for asexual reproduction analysis.	52
Figure 3.4 a) Mean (+SD) monthly abundance (ind. m ⁻³) for <i>Thalia democratica</i> at Port Hacking from 2002 - 2011. Black line represents long-term mean. Scale is log ₁₀ -transformed. b) Proportion of non-zero <i>T. democratica</i> hauls per month from 2002 - 2011 c) Seasonal abundances (ind. m ⁻³) of <i>T. democratica</i> from 2002 - 2011. ND - no data. Scale is log ₁₀ -transformed.....	58
Figure 3.5 Ordination of phytoplankton community structure using principal coordinates analysis, with year superimposed. Vectors overlaid are multiple correlations of a) phytoplankton species groupings: diatoms (Diat), prymnesiophytes (Prym) and prokaryotes (Prok) and b) phytoplankton size structure: picoplankton <2 μm (Pico), nanoplankton 2 - 20 μm (Nano) and microplankton >20 μm (Micro).	60
Figure 3.6 a) Mean (± SD) <i>Thalia democratica</i> abundance across three years of sampling (<i>Southern Surveyor</i> voyages) and for corresponding Port Hacking NRS hauls. b) Mean (± SD) asexual reproduction (buds per chain) across the three years from <i>Southern Surveyor</i> voyages. Letters denote significant differences at $p < 0.05$	61
Figure 3.7 Scatter plot showing relationship between log ₁₀ -transformed <i>Thalia democratica</i> abundance and asexual reproduction (buds per chain; $R^2 = 0.61$, $F_{1,22} = 33.83$, $p < 0.01$).	63
Figure 3.8 Fitted smoother value for proportional non-salp zooplankton abundance as obtained through generalised additive mixed modelling analysis illustrating the non-linear relationship with <i>Thalia democratica</i> abundance. Tick marks on the x-axis are observed data points. The y-axis represents fitted values. Dotted lines represent 95% confidence intervals.....	66
Figure 4.1 Life cycle of <i>Thalia democratica</i> showing four life history stages used in the models: females, males, juvenile oozoids and post-release oozoids. For life-history roles see Table 4.1. Modified from Fig. 1 in Henschke et al. (2011).....	79
Figure 4.2 Model schematic showing interactions between the environmental variables (ovals), input variables (white boxes) and the model outputs (grey boxes). Model equations are represented graphically in Figure 4.3. Juv – juvenile, PR – post-release.	82
Figure 4.3 Illustrations of the equations used in the salp population model. Numbers in brackets are the equation number.	91
Figure 4.4 The elasticity, or proportional sensitivity of population growth (λ) to changes in survival within the same stage (black bars), survival while transitioning to the next stage (grey bars) or fecundity (white bars). Because the elasticities of these matrix elements sum to 1, they can be compared directly in terms of their contribution to the population growth rate. Males are not included in the graph as λ was not sensitive to variation in male survival.	95
Figure 4.5 Standard model simulation showing one year of simulated <i>Thalia democratica</i> abundances for a) females, b) males, c) juvenile oozoids and d) post-release oozoids, as well as e) chlorophyll <i>a</i> biomass.	97

Figure 4.6 Results of sensitivity analysis for a sub-optimal temperature run (19°C). The bars represent the significant coefficients of model parameters signifying their influence on a) generation time, b) total salp biomass, c) blastozoid-to-oozoid ratio, d) female abundance, e) male abundance, f) juvenile oozoid abundance and g) post-release oozoid abundance. Parameter abbreviations are displayed in the plot. * indicates which parameters were excluded from the final analysis.....	99
Figure 4.7 a) Location map showing areas along the New South Wales coast that were input in the time-series simulation. The locations are Coffs Harbour (red), Sydney (blue) and Eden (black). Long-term (2003 – 2012) averaged satellite derived sea surface temperature (b) and chlorophyll <i>a</i> biomass (c) showed variation across locations, and seasonality in oceanographic conditions.	100
Figure 4.8. Time-series simulation showing <i>Thalia democratica</i> population abundance (ind. m ⁻³) at Coffs Harbour (a), Sydney (b) and Eden (c). Values are superimposed onto one 12-month axis, with colours representing different years (2003 – 2012).	102
Figure 4.9. Proportional seasonal abundance of <i>Thalia democratica</i> (left-hand axis; bars) and mean seasonal generation time (right-hand axis; lines) derived from the time-series simulation for Coffs Harbour (black), Sydney (grey) and Eden (white). Note the right-hand axis is broken at 25 - 85 days.	104
Figure 5.1 a) Survey area in the southern Tasman Sea and southwestern Pacific Ocean east of New Zealand showing trawl stations and benthic sampling stations. b-c) Density distribution based on video footage/camera stills of <i>Thetys vagina</i> (ind. 1000 m ⁻²) at different stations in b) Bass Canon and on the c) Challenger Plateau. Depth contours are displayed in metres.	119
Figure 5.2 Sea floor photographs from the Tasman Sea. Scale bars refer to 10 cm. a) <i>Thetys vagina</i> carcasses at 1565 m depth taken in Bass Canyon. b) <i>Platymaia maora</i> feeding on <i>T. vagina</i> carcass at 482 m in Challenger Plateau.	124
Figure 5.3 a) Maximum yearly biomass (bars, t km ⁻³ WW) for salps and pyrosomes (dark bars; New Zealand fisheries database) from 1981 - 2011, and <i>Thetys vagina</i> (light bars; trans-Tasman pelagic trawls) in 2008, 2009 and 2011. Yearly mean (+SD) is represented by the solid line. Number of trawls per year are indicated above each bar. Station locations are presented in Figure 5.1. b) Mean (+SD) monthly biomass (t km ⁻³ WW) of salps and pyrosomes from 1981 – 2011. Number of trawls per month are indicated above each bar.	126
Figure 5.4 Relationship between mean (± SD) energetic content (kJ g ⁻¹ dry weight) and mean (± SD) C:N ratio as an indicator of quality of different marine organisms as a food item. Values for <i>Thetys vagina</i> obtained from this study. Other values obtained from previous studies: phytoplankton (Platt and Irwin, 1973), copepods (Donnelly et al., 1994; Ikeda et al., 2006), cnidarians and ctenophores (Clarke et al., 1992) and fish (Childress and Nygaard, 1973).	128

List of Tables

Table 2.1 Mean characteristics (\pm SD) over the top 50 m of the water column. The surface mixed layer depth is calculated from the minimum depth at which $T < T(10\text{ m}) - 0.4^\circ\text{C}$ or $S > S(10\text{ m}) + 0.03$ following Condie & Dunn (2006). Values in parentheses correspond to ranges. n - number of stations; IS - inner shelf; CCE - cold core eddy; WCE - warm core eddy; WCEp - warm core eddy preliminary POM transect.	24
Table 2.2 POM and zooplankton isotope values of $\delta^{13}\text{C}$ and $\delta^{15}\text{N}$ (mean \pm SD; ‰). n - sample size. Δ - ^{15}N enrichment relative to POM.....	25
Table 2.3 Copepod and euphausiid isotope values of $\delta^{13}\text{C}$ and $\delta^{15}\text{N}$ (mean \pm SD; ‰) separated by feeding group. n - sample size. References are indicated in brackets. All omnivorous copepods are predominantly herbivorous, with the exception of the predominantly carnivorous <i>Undeuchaeta major</i> . Some species were sampled across more than one water type (*), however, for each species $\delta^{13}\text{C}$ and $\delta^{15}\text{N}$ values did not significantly differ across water types.....	27
Table 3.1 Hydrographic and zooplankton characteristics across the three years. Inner shelf water characteristics are depth averaged over the top 50 m of the water column. Values are mean \pm SD. Values in parentheses are ranges. Proportion of mature blastozoids is based on the percentage of population that is greater than 4 mm in length. n - number of stations.	46
Table 3.2 Stations for blastozoid growth experiments in October 2009. Time is in Australian Eastern Standard time. n - number of stations. Values in parentheses represent number of tanks allocated to each collection time: T0, T4 and T8 respectively.....	50
Table 3.3 Synopsis of the final additive mixed modelling analysis. Edf - estimated degrees of freedom.....	65
Table 4.1 Life-history stages of <i>Thalia democratica</i> included in the models and shown in Fig. 4.1.....	78
Table 4.2 Stage-class population matrix for <i>Thalia democratica</i> based on fecundity, growth and survival. Values were based on published data presented in the size-structured population model below.	80
Table 4.3 Parameter values used in the model simulation. Parameters used in the sensitivity analysis are in bold. Parameter values were estimated from the cited literature or inferred (see methods for details).	92
Table 4.4 Results of the long-term (2003 - 2012) seasonal analysis at Coffs Harbour, Sydney and Eden. Values are means (\pm SD). The result of Tukey's HSD test for abundance and generation time are indicated by letters (^{a,b,c}); seasons within each location not sharing a letter are significantly different ($p < 0.05$).	101
Table 5.1 Megafaunal taxa observed directly feeding on or close to (potential feeders) <i>Thetys vagina</i> carcasses on the Challenger Plateau. Footnotes denote previous records of taxa feeding on salps.....	125
Table 5.2 Biochemical and elemental composition of <i>Thetys vagina</i> expressed either as a percentage of total dry weight (DW) or measured values. All values are means \pm SD. Ranges are displayed in brackets. n - number of individuals measured.	127

Chapter 1

Introduction: Understanding process influencing salp swarms

1.1 Gelatinous zooplankton

The word “plankton” is derived from the Greek word “planktos”, which means to drift, and refers to the weak swimming ability of aquatic plant (phytoplankton) and animal (zooplankton) organisms (Hays et al., 2005). Zooplankton range in size from 20 μm up to 200 mm, and encompasses a diverse group of organisms including crustaceans such as copepods and krill and gelatinous organisms such as cnidarians (jellyfish), ctenophores and the pelagic tunicates (Hays et al., 2005). Zooplankton are important members of aquatic communities as they play a key link between primary producers (phytoplankton) and higher trophic levels such as fish (Johnson et al., 2011).

It has been suggested that the composition of the zooplankton community within the oceans is shifting towards gelatinous species due to anthropogenic changes such as overfishing or climate change (Richardson et al., 2009). Recent reviews of long-term changes in gelatinous zooplankton abundances have failed to reach a consensus on whether gelatinous zooplankton abundances are increasing worldwide, but these studies have highlighted the significant gaps in our understanding of the population dynamics of gelatinous zooplankton (Brotz et al., 2012; Condon et al., 2012; Condon et al., 2013). Each of these aforementioned reviews has grouped cnidarians, ctenophores and the pelagic tunicates (salps, doliolids and larvaceans) together as “jellyfish” in their assessment (Brotz et al., 2012; Condon et al., 2013). Although each of those organisms can form dense swarms, pelagic tunicates differ from cnidarians and ctenophores (traditional jellyfish) in several fundamental ways such as their morphology, life

history, ecology and ancestry (Gibbons and Richardson, 2013). In particular, pelagic tunicates are holoplanktonic, non-selective suspension feeders and are abundant in both the open ocean as well as coasts and estuaries (Gibbons and Richardson, 2013). Tunicates occur in our phylum, Chordata, making them the most closely related invertebrates to vertebrate chordates (Deibel and Lowen, 2012), and far removed from the cnidarians and ctenophores. Furthermore, their responses to environmental changes and the role they play in the marine ecosystem are likely to differ from that of cnidarians and ctenophores. With a changing environment, pelagic tunicate abundances are believed to increase in response only to changes in ocean warming and stratification, whereas cnidarians and ctenophores will also benefit from overfishing, eutrophication and hypoxia (Gibbons and Richardson, 2013).

1.2 Pelagic tunicates

The subphylum Tunicata is divided into three classes: the sessile Ascidiacea (sea squirts), the pelagic Thaliacea (salps, doliolids and pyrosomes) and the pelagic Appendicularia (larvaceans). The name “Tunicata” is derived from the cellulose-like polysaccharide “tunic” that encloses the body of an adult, a characteristic shared among all members of the subphylum (Deibel and Lowen, 2012). The pelagic tunicates have transparent gelatinous bodies, primarily made of acidic mucopolysaccharides (Godeaux, 1965), and have a high water content of up to 95% of wet weight (Acuña, 2001). They are highly abundant grazers that are ubiquitous throughout the world’s oceans and use mucous sheets, nets, or filters, to capture food (Alldredge and Madin, 1982). Generally, most species live in the open ocean where particle concentrations are lower, as their mucous filters have been found to clog in areas of high particulate matter (Harbison et al., 1986). However, many smaller species can inhabit the particle rich coastal waters

without affecting their filters (Deibel and Lowen, 2012). The main differences between thaliaceans and appendicularians are their physical shape and reproductive methods. Thaliaceans are barrel shaped compared to the tadpole-like appendicularians, and have a reproductive strategy that involves the alternation of asexual and sexual generations (Deibel and Lowen, 2012). Although understudied, salps are the most well-researched thaliacean, with little known on the life history characteristics of pyrosomes and doliolids (Deibel and Lowen, 2012).

1.3 The salp life cycle and swarm formation

The thaliacean life cycle allows populations to grow exponentially while maintaining genetic variability (Alldredge and Madin, 1982; Godeaux et al., 1998). The typical salp life cycle involves the obligatory alternation between two life history stages: the sexually reproducing blastozooids, and the asexually reproducing oozoids (Heron, 1972). In the blastozooid (aggregate) generation, the young blastozooid buds are female (A1; Fig. 1.1) and are immediately fertilized upon release by older male blastozooids (A3). These females grow a single internal embryo (A2), which is the beginning of the oozoid (solitary) generation (S1). Once the oozoid embryo is released, the female blastozooids develop testes and function as male, dying shortly after externally fertilising the new generation of blastozooid buds. The oozoid embryo grows to asexually produce up to three releases of genetically identical blastozooid buds (S2). Although blastozooids only produce one offspring per individual, oozoid fecundity is high relative to other zooplankton. For the fast growing *T. democratica*, the ratio of total blastozooids released per oozoid individual can reach 240:1 under “ideal” conditions (Heron 1972), whereas for the slower growing *Salpa thompsoni*, each oozoid can release up to 900 blastozooid buds (Foxton, 1966).

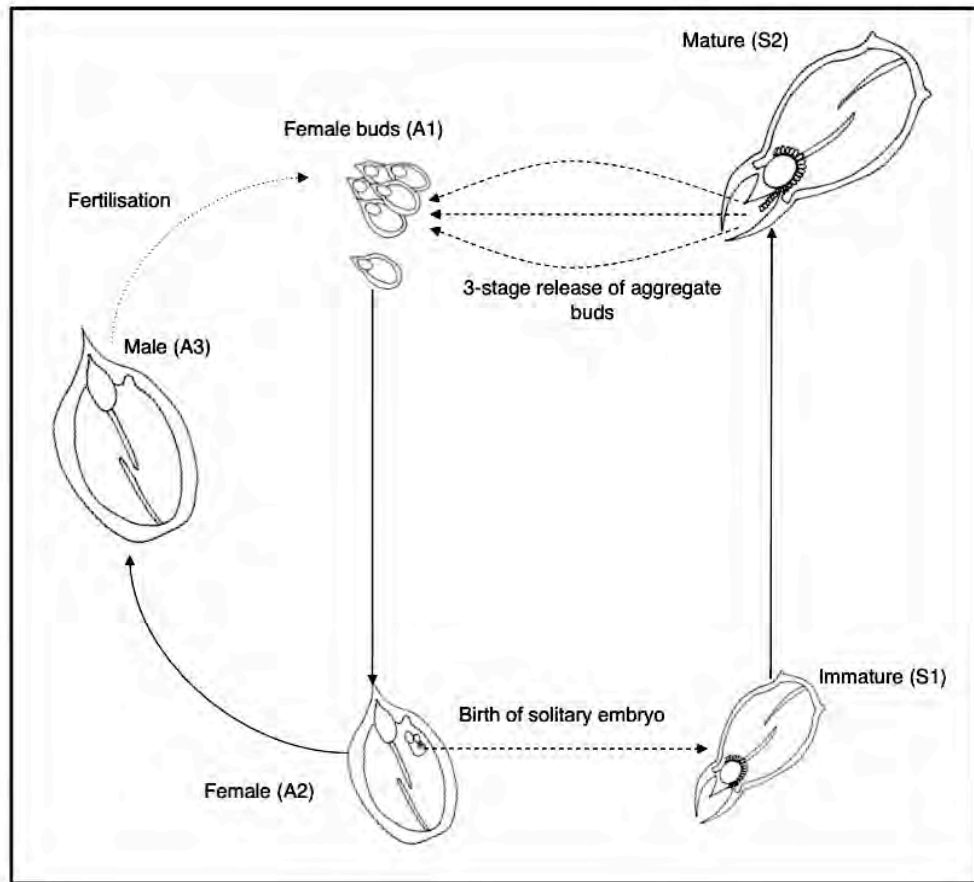


Figure 1.1 Life cycle of the salp *Thalia democratica*, demonstrating alternation between aggregated sexual (A1 to A3) and solitary asexual (S1 and S2) generations (Heron & Benham 1985). Blastozooid female buds (A1) are fertilised immediately upon release by mature male blastozooids (A3). These female buds then grow an embryo internally (A2). Once the embryo is released, the blastozooid female develops testes and functions as a male (A3). The embryo is the start of the oozoid generation. The immature oozoid (S1) develops up to 3 chains of between 20 and 80 blastozooid buds, released by mature oozoids (S2). Dashed lines represent the shift in generation. Dotted line represents external fertilization. Figure from Henschke et al. (2011).

Salp swarms periodically occur in continental shelf and slope areas all around the world, with abundances often exceeding 1000 individuals (ind.) m^{-3} (Andersen, 1998). Swarms are ephemeral, only lasting from weeks to a few months (Deibel and Paffenhofer, 2009). The presence of salp swarms have been related to intrusions of cool nutrient-rich water (Blackburn, 1979; Heron and Benham, 1984; Deibel and Paffenhofer, 2009), suggesting the salps are responding to increases in phytoplankton abundance. Not all salp species have the ability to form swarms, and this capability is restricted to those species which have life cycles typically shorter than 6 weeks (Madin and Deibel, 1998). Species that occur in higher latitudes, such as *Salpa thompsoni*, rarely form swarms, with highest recorded abundances of 5 ind m^{-3} (Park and Wormuth, 1993). They have slow growth from 0.07 - 0.4% length h^{-1} with generation times of 9 months, and it has been suggested that for large abundances to occur, optimal conditions must have occurred for one or more years prior (Loeb and Santora, 2012). Faster growing salps, on the other hand, such as *Thalia democratica* or *Salpa fusiformis*, can rapidly respond to environmental changes to form swarms (Andersen, 1998). Generation times for *T. democratica* range from 2 - 21 days (Braconnot, 1963; Heron, 1972; Deibel, 1982), and individual growth rates range from 0.3% length h^{-1} (Deibel, 1982) to 28% length h^{-1} (Le Borgne and Moll, 1986), making them one of the fastest growing metazoans on earth (Alldredge and Madin, 1982; Hopcroft and Roff, 1995). Salp growth rates have been found to vary depending on environmental conditions such as temperature and food availability (Heron, 1972; Deibel, 1982; Heron and Benham, 1984), however, “optimal” conditions promoting maximum growth are still unknown. High salp biomass can occur either behaviourally through mating aggregations, or as a consequence of rapid population increase from reproduction. Throughout this thesis

when referring to a salp “swarm” we consider salp populations of high abundance (> 50 ind. m^{-3}) that are a result of rapid population increase and not mating aggregations.

1.4 Feeding and trophic role of salps

Salps are highly efficient filter feeders, capable of rapidly filtering particles up to a rate of 100 mL min^{-1} (Harbison and Gilmer, 1976). Salp swarms can constitute 99% of the zooplankton biomass (Siegel and Harm, 1996) and their grazing pressure can exceed the total daily primary production in an area (Dubischar and Bathmann, 1997). Salps can transfer this matter to the sea floor in fast-sinking (up to 2700 m d^{-1}), carbon-rich (up to 37% dry weight) faecal pellets (Bruland and Silver, 1981; Perissinotto and Pakhomov, 1998) or salp carcasses (Henschke et al., 2013; Smith Jr et al., 2014). As a result, the influence of salp swarms on the biogeochemical cycle is substantial, contributing 10-fold more carbon to the seafloor than in areas without salp swarms (Fischer et al., 1988).

Unlike other zooplankton, salps can consume food over a wide size range, from $<1 \mu\text{m}$ to 1 mm in size (Vargas and Madin, 2004). Both copepods and krill can only consume particles greater than 5 to $10 \mu\text{m}$ (Bautista et al., 1992; Maciejewska, 1993), suggesting that competition for phytoplankton is likely to occur when abundances of salps are high. Alternatively, as salps can also ingest zooplankton eggs and nauplii, high abundances of salps will increase predatory pressure on juvenile zooplankton. Although no direct interaction between the proportion of krill and salp density has been observed (Kawaguchi et al., 1998), studies have shown an inverse relationship between copepod and salp abundance (Berner, 1957), with copepods being more scarce when high salp abundance occurs over an extended period of time (Fraser, 1962; Humphrey, 1963).

Recently, only a weak negative correlation was identified between *Thalia democratica* abundance and copepod abundance in the Tasman Sea, despite the dominance of *T. democratica* (59% of total zooplankton; Henschke et al., 2011). It has been suggested that comparing gelatinous and non gelatinous zooplankton by enumeration may be misrepresentative due to their morphological differences, such as size and water content (Henschke et al., 2011). Therefore, in order to understand the competitive and predatory relationships between salps and other zooplankton, studies focused on feeding dynamics and niche relationships may be more appropriate.

Due to their gelatinous body and high water content, salps are still believed to be of low nutritional value (Moline et al., 2004), particularly as fish can only partially assimilate their mucopolysaccharide tunic through digestion (Kashkina, 1986). As a result, salps could be described as a “trophic dead end”, consuming large quantities of carbon and not transferring it to higher trophic levels. However, salps are often found in the stomach of a variety of organisms. Predators include more than 47 fish species (Kashkina, 1986), crustaceans (Hopkins, 1985; Kawaguchi and Takahashi, 1996), echinoderms (Duggins, 1981; Domanski, 1984), corals (Hoeksema and Waheed, 2012) and birds (Ainley et al., 1991). With protein constituting up to 80% of their organic matter (Madin et al., 1981), and the salp nucleus being filled with nutrient rich phytoplankton for most of the time (Kashkina, 1986), salps may be valuable to predators. Fish have been observed avoiding salps when they occur in dense swarms ($>100 \text{ ind. m}^{-3}$), as they can potentially clog the fish gills (Kashkina, 1986). If fish are a major predator of salps, and avoid consuming salps when they are at swarm abundances, it is necessary to identify what happens to salp carcasses after the demise of a swarm, and how they contribute to the food web.

1.5 Salps in the Tasman Sea ecosystem

The Tasman Sea is dominated by the southward-flowing boundary current, the East Australian Current (EAC; Cresswell, 1994). The EAC originates in the Coral Sea, transporting warm, oligotrophic water southward along the Australian continental shelf until it separates from the coast between 30 to 34°S and flows eastward across the Tasman Sea (Godfrey et al., 1980). South of this separation zone, the area develops into a mesoscale eddy field, forming nutrient-rich cold core (CCE; cyclonic) and oligotrophic warm core (WCE; anticyclonic) eddies (Nilsson and Cresswell, 1981). The EAC is distinctive from the two other main water types in the Tasman Sea: inner shelf water and upwelled water (Cresswell, 1994; Henschke et al., 2011). Both inner shelf and upwelled water are typically cooler than the EAC. Upwelled water has been lifted from the continental slope and is generally higher in nutrients and chlorophyll *a* (Roughan & Middleton 2002). Inner shelf water in the Tasman Sea is generally more saline, with moderate chlorophyll *a* biomass and nutrient concentrations (Henschke et al., 2011). Due to the occurrence of several water types, the Tasman Sea is a dynamic ecosystem, rich in biological diversity (Baird et al., 2008).

Although the first observation of salp swarms in the Tasman Sea was in 1770 by the explorer Joseph Banks (Beaglehole, 1963), historical records of salps or even zooplankton within the Tasman Sea are scarce. The first and only comprehensive study of Tasman Sea pelagic tunicates was undertaken by Thompson and Kesteven (1942) from 1938 to 1942. After crustaceans, tunicates were the most abundant zooplankton group, with a total of 42 pelagic tunicate species identified within the Tasman Sea (Thompson and Kesteven, 1942). *Thalia democratica* was by far the most abundant

tunicate species in the Tasman Sea, forming swarms during spring (Thompson and Kesteven, 1942). Since then, the occurrence of salp swarms in the Tasman Sea had been mentioned in several papers, but not analysed to determine the causes (Sheard, 1949; Tranter, 1962; Young, 1989; Harris et al., 1991) until recently (Henschke et al., 2011). Higher abundances of *T. democratica* were found in inner shelf waters which were dominated by higher proportions of diatoms compared to EAC water (Henschke et al., 2011), and the highest recorded abundance of *T. democratica* to date was observed within a productive cold core eddy (5003 ind. m⁻³; Everett et al., 2011). Smaller salps tend to dominate the zooplankton in the Tasman Sea, although low abundances of large salps, such as *Thetys vagina*, are sometimes observed (Henschke et al., 2011). Very little is known of the ecology and impact of these large salps on the marine environment.

1.6 Aims and thesis objectives

The main objective of this thesis is to further understand the processes influencing salp swarms. In particular, this thesis focuses on the formation of salp swarms and their trophic influence on the marine ecosystem. Knowledge of pelagic tunicates in the Tasman Sea is hindered by large intervals between datasets. This thesis provides the most comprehensive study of Tasman Sea salp ecology since 1942, and includes a 30-year time-series of salp abundance. It increases the understanding of salp swarm processes by investigating population demographics and by creating an environmentally-dependent population model. As salps are difficult to culture in the laboratory (Heron, 1972; Harbison et al., 1986; Raskoff et al., 2003), little is known about the temporal evolution of a salp swarm. A population model can be used to investigate how life history characteristics change as a swarm evolves. From these

results one can identify factors that cause variation in the magnitude and location of salp swarms. This thesis also examines the role of salps in the zooplankton trophic niche to investigate competition during a salp swarm. Finally, as the fate of salp carcasses in the marine ecosystem after the demise of a swarm is unknown, this thesis identifies the potential for large salp carcasses to play a major role as food fall to the benthos. Unlike the well-studied effects of salp faecal pellets (Perissinotto and Pakhomov, 1998) and appendicularian mucous sheets (Robison et al., 2005) on the carbon cycle, data on the export of carbon from moribund pelagic tunicates are scarce. Results from this study provide new evidence for the importance of gelatinous carbon incorporation to the detrital food web and sediments.

The specific objectives of this thesis were to:

- Investigate the role of the small salp *Thalia democratica* in the zooplankton food web using a stable isotope perspective (Chapter 2);
- Examine the population demographics and interannual variability of swarms of *Thalia democratica* (Chapter 3);
- Develop a *Thalia democratica* population model to simulate seasonal and long-term trends in salp abundance (Chapter 4); and
- Quantify the biomass and energetic input of carcasses of the large salp, *Thetys vagina*, on the sea floor (Chapter 5).

1.7 Thesis chapters

Chapter 2 examines the stable isotope composition of the Tasman Sea zooplankton community and the role that the salp *Thalia democratica* plays within the zooplankton community. Communities across different water types are compared to examine the role

of changing phytoplankton conditions in trophic niche width. I also compare the trophic niche of three co-existing zooplankton species, a salp, a copepod and a krill to investigate niche use.

Chapter 3 investigates demographic characteristics such as asexual reproduction and growth rate across three *Thalia democratica* swarms in the spring of 2008, 2009, and 2010 in the Tasman Sea. Asexual reproduction rate (buds per chain) was negatively related to the salp swarm abundance. The relationship between swarm abundance and demographics with environmental variables, such as phytoplankton community composition and zooplankton abundance, is described. Chapter 3 has been published in *Marine Biology*:

Henschke N, Everett JD, Doblin MA, Pitt KA, Richardson AJ, Suthers IM (2014) Demography and interannual variability of salp swarms (*Thalia democratica*). *Marine Biology* 161: 149-163.

Chapter 4 presents a size-structured numerical model of *Thalia democratica* population dynamics. It considers both life history parameters (fecundity, growth rates and mortality) as well as environmental parameters (temperature, salinity, phytoplankton abundance) to simulate the formation of *T. democratica* swarms at three locations along the south-east Australian coast. The most important variables affecting salp swarm abundance were ingestion rate and phytoplankton abundance. A modified version of Chapter 4 has been published in *Journal of Plankton Research*:

Henschke N, Everett JD, Smith JA, Suthers IM (in press) Population drivers of a *Thalia*

democratica swarm: insights from population modelling. Journal of Plankton Research.

Chapter 5 examines the fate of *Thetys vagina* individuals after the collapse of a swarm. It presents the first long-term (30 y) dataset of large salp abundance in the Tasman Sea. It identifies the potential for salp carcasses to be a major food-fall contributor to the benthic ecosystem and quantifies the energetic and carbon input that is deposited within the Tasman Sea by salp carcasses on a yearly scale. Chapter 5 has been published in *Marine Ecology Progress Series*:

Henschke N, Bowden DA, Everett JD, Holmes SP, Kloster RJ, Lee RW, Suthers IM (2013) Salp-falls in the Tasman Sea: a major food input to deep sea benthos. *Marine Ecology Progress Series* 491: 165-175.

Chapter 6 summarises the main findings and implications of the research presented in this thesis. It discusses both the significance and limitations of this research and proposes avenues for future research.

The main chapters are written as four stand-alone manuscripts (Chapters 2 to 5) in anticipation for publication in peer-reviewed journals. Each chapter is self-contained and subsequently, there will be some repetition. The two published chapters are included in the appendices.

Chapter 2

The zooplankton trophic niche across different water types: a stable isotope analysis

Abstract

The trophic relationships of 21 species from an oceanic zooplankton community were studied using stable isotopes of carbon and nitrogen. Zooplankton and suspended particulate organic matter (POM) were sampled in three different water types: inner shelf (IS), a cold core eddy (CCE) and a warm core eddy (WCE). The zooplankton niche within this study was large, with $\delta^{15}\text{N}$ values ranging from 3.87‰ for the parasitic copepod *Sapphirina augusta* to 10.15‰ for the euphausiid, *Euphausia spinifera*. $\delta^{13}\text{C}$ varied from -22.59 to -19.41‰ as a result of the copepod *Euchirella curticauda* and *E. spinifera*. The isotopic composition of POM varied significantly among the three water types; as did the trophic enrichment of zooplankton over POM, with the lowest enrichment in the recently upwelled IS water type (0.53‰) compared to the warm core eddy (1.64‰) and cold core eddy (2.74‰). The WCE was an oligotrophic environment and was associated with an increased trophic level for omnivorous zooplankton (copepods and euphausiids) to a similar level as carnivorous zooplankton (chaetognaths). Trophic niche width comparisons across three zooplankton species indicated that both niche partitioning and competition occurs within the zooplankton community. The trophic relationships among the zooplankton are dynamic and respond to different water types.

2.1 Introduction

Zooplankton are an essential component of marine food webs and changes in zooplankton assemblages can have cascading effects for the fish that feed on them (Johnson et al., 2011), through to top-predators and fisheries (Frederiksen et al., 2006). Within the zooplankton food web are many diverse and interacting taxa (Thompson and Kesteven, 1942; Voronina, 1998) creating a challenge to understand their trophic relationships. Knowledge of the trophic niche of various zooplankton is necessary to evaluate their response to different oceanographic conditions, as zooplankton provide bottom-up regulation of marine food webs.

A species' trophic niche is the sum of all interactions that link it to other species within an ecosystem (Elton, 1927), representing both its habitat requirements and trophic role (Leibold, 1995). Stable isotope analysis is a common tool for characterizing the trophic niche, by identifying trophic interactions (Peterson and Fry, 1987). The isotope ^{15}N can be used to estimate an organism's trophic position as stepwise enrichment between 1 - 5‰ (average 3.4‰) generally occurs between prey and predators (Minagawa and Wada, 1984; Vander Zanden and Rasmussen, 1999; Post, 2002). The isotope ^{13}C shows much less trophic enrichment (average 0.4‰), and is used for identifying dietary sources (Post, 2002). Trophic niche width is often calculated using the variation in the isotopic signature of organisms (typically in $\delta^{13}\text{C}$ - $\delta^{15}\text{N}$ isotope space; Bearhop et al., 2004; Layman et al., 2007a). By comparing the trophic niche of an organism through time or during different oceanographic conditions, the changes in dietary behaviour can be identified (Layman et al., 2007b). A reduction in prey diversity, for example, can affect the consumer niche, manifested as decreased trophic niche width (for grey snapper; Layman et al., 2007b) or increased carnivory (for copepods; Landry, 1981).

Suspended particulate organic matter (POM) is often used in stable isotope analysis as a proxy for phytoplankton, and hence can be used as a baseline for marine food webs (Post, 2002). The $\delta^{13}\text{C}$ and $\delta^{15}\text{N}$ stable isotope signature of POM has been found to vary across water types in relation to different oceanographic conditions (Stowasser et al., 2012). Off south-east Australia, the western Tasman Sea has several different water types including cyclonic cold core eddies (CCE), anti-cyclonic warm core (WCE) eddies (Nilsson and Cresswell, 1981) and nutrient-rich inner shelf (IS) water (Henschke et al., 2011). CCEs may entrain IS water (Mullaney and Suthers, 2013), resulting in a 16% increase in chlorophyll *a* compared to surrounding waters (Everett et al., 2012). As well as enhanced primary production, coastal CCEs have been shown to promote zooplankton production (Kimura et al., 2000), and aid in the recruitment and survival of larval fish (Kasai et al., 2002). In comparison, WCEs have on average 28% less surface chlorophyll *a* compared to surrounding waters (Everett et al., 2012). As a result, the ecosystems that develop within a WCE are generally composed of smaller phytoplankton cells and lower zooplankton biomass (Waite et al., 2007b). Therefore, the different oceanographic conditions in IS, CCE and WCE water types should be reflected in the POM isotopic signature and subsequently the zooplankton isotopic signature.

The aim of this study was to quantify the zooplankton food web of the western Tasman Sea using stable isotope analysis. The trophic niche characteristics of zooplankton relative to POM were compared across water types to determine the trophic outcomes of different oceanographic conditions. To investigate specific niche use, the trophic niches of three co-existing species were compared: the salp *Thalia democratica*, the copepod *Eucalanus elongatus* and the euphausiid *Thysanoessa gregaria*.

2.2 Methods

2.2.1 Field sampling

Zooplankton and phytoplankton samples were collected from a 2010 austral spring voyage (September – October) onboard the *RV Southern Surveyor* off south-eastern Australia in the Tasman Sea (Fig. 2.1a). Sampling stations were chosen based on water type characteristics using daily Moderate Resolution Imaging Spectroradiometer (MODIS) satellite imagery. The sampling area extended southward from Stockton Bight (32°43' S, 152°13' E) to Jervis Bay (35°03' S, 150°43' E). Three water types were sampled: inner shelf water (IS; $n = 4$), a cold core eddy (CCE; $n = 5$) and a warm core eddy (WCE). The WCE was sampled initially only for POM (WCEp; $n = 4$) and then 10 days later was sampled for both POM and zooplankton (WCE; $n = 4$) to compare changing POM communities.

At each sampling station, a Seabird SBE911-plus Conductivity-Temperature-Depth (CTD) probe equipped with a Chelsea AquaTracker Mk3 fluorometer was used to profile salinity, temperature and fluorescence. Bulk POM samples for stable isotope analysis were collected from the surface and the chlorophyll *a* maximum. Between 2 and 6 L of seawater was filtered onto pre-combusted GF/F filter papers under low vacuum pressure (30 - 40 mm Hg). The POM samples were stored frozen until later analysis.

Zooplankton collection was subsequently performed at each station. A Multiple Opening/Closing Net and Environmental Sensing System (MOCNESS) was used for depth-stratified sampling of the entire zooplankton community. For this study, only samples collected from 0 - 100 m depth were used. Immediately after collection, the

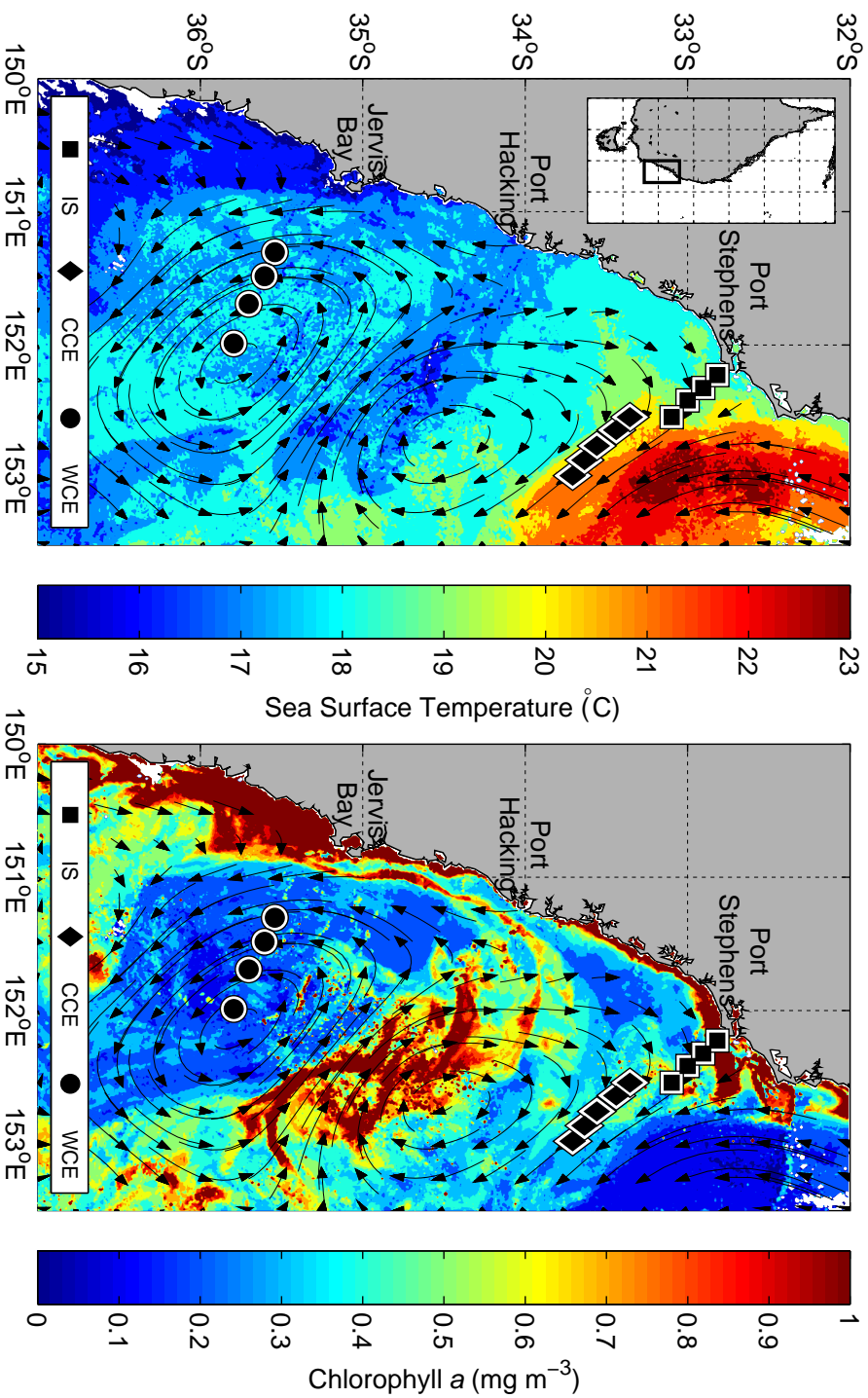


Figure 2.1 Location plot with satellite-derived sea surface temperature ($^{\circ}\text{C}$); left) and chlorophyll a ($\mu\text{g L}^{-1}$; right) overlaid on best representing conditions occurring during sampling (Table 2.1). Geostrophic currents are estimated through surface altimetry and are represented by arrows. Sampling locations in different water types are indicated with different shapes. IS – inner shelf, CCE – cold core eddy, WCE – warm core eddy.

main representatives of the zooplankton community were identified to species and frozen. Once returned to the laboratory, these specimens were freeze-dried and homogenized, and loaded into tin capsules for stable isotope analysis. Multiple individuals were homogenised in each sample in order to meet the necessary weight requirements needed for stable isotope analyses (1 – 2.5 mg dry weight). As zooplankton guts were not evacuated before analysis the results will include recent ingestion (if regurgitation did not occur during capture) as well as time-averaged ingestion.

2.2.2 Stable isotope analysis

In order to keep data comparable with previous stable isotope research in the Tasman Sea (Davenport and Bax, 2002; Revill et al., 2009), data were not corrected for lipid content. Both Davenport and Bax (2002) and Revill et al. (2009) deemed lipid removal to be unwarranted due to the low oil content (~1%) of most Australian fish and crustaceans (Nichols et al., 1998).

Analysis of stable isotope samples were done at the IsoEnvironmental Laboratory (<http://www.isoenviron.co.za/>), Rhodes University, South Africa, with a Europa Scientific 20-20 isotope ratio mass spectrometer (IRMS) linked to a preparation unit (ANCA SL). Beet sugar, ammonium sulphate and casein were used as internal standards and calibrated against the International Atomic Energy Agency (IAEA) standards CH-6 and N-1. Standards of Vienna Pee Dee Belemnite (VPDB) for ^{13}C and atmospheric nitrogen for ^{15}N were used to express delta values (δ). Repeated measurements of an internal standard indicated measurement precision of $\pm 0.09\%$ and $\pm 0.19\%$ for $\delta^{13}\text{C}$ and $\delta^{15}\text{N}$ respectively.

2.2.3 Statistical analyses

A one-way analysis of variance (ANOVA) was used to test the null hypothesis of no significant difference in $\delta^{13}\text{C}$ or $\delta^{15}\text{N}$ values among IS, CCE and WCE water types separately for each taxon. Tukey's HSD test was used for *a posteriori* pairwise comparisons between factor levels for all ANOVAs. ^{15}N enrichment relative to POM (Δ) was calculated as the difference between mean ^{15}N for the species group and mean ^{15}N for POM at each water type.

Trophic niche widths were quantified using Bayesian ellipses (Jackson et al., 2011), using the R package SIAR (Parnell et al., 2010). This method generates standard ellipse areas (SEA_B ; bivariate equivalents to standard deviations), and can be used to compare populations with variation in sample size as well as correct for small sample sizes (Jackson et al., 2011). There were no significant differences in $\delta^{13}\text{C}$ or $\delta^{15}\text{N}$ values for *Eucalanus elongatus* (CCE and WCE), *Thysanoessa gregaria* (CCE and WCE) and *Thalia democratica* (IS, CCE and WCE) across water types for each species, so samples were pooled for between species comparisons. To compare trophic niche widths among species, 15 random SEA_B values for each species were tested using a one-way ANOVA. Tukey's analysis was used for *a posteriori* pairwise comparisons between factor levels for all ANOVAs. All analyses were performed in R v. 3.0.3 (R Development Core Team 2012).

2.3 Results

2.3.1 Water type characterisation

During sampling, the East Australian Current (EAC) was approximately 22°C and separated from the coast at 33°S and a large WCE was evident off Jervis Bay (34°S; Fig. 2.1a). When the WCE was first sampled (WCE prior; WCEp), it was deeply mixed (283 ± 60 m) and chlorophyll *a* concentrations were low (0.75 µg L⁻¹; Table 2.1). For the second sampling (WCE), the eddy began to encroach on the shelf and mix with inner shelf water, resulting in higher chlorophyll *a* concentrations (1.03 µg L⁻¹; Table 2.1) and a lower mixed layer with higher variability (137 ± 114 m; Table 2.1). A CCE was sampled at 32.5°S and the adjacent inner shelf region at 32°S. From observations of satellite imagery, upwelling occurred during sampling of the inner shelf water type (Fig. 2.1b), however this had not yet translated into the chlorophyll *a* signature (1.16 µg L⁻¹; Table 2.1). As well as satellite imagery, water types were further distinguished based on temperature-salinity profiles from the surface to 100 m depth (Fig. 2.2).

2.3.2 Particulate organic matter

$\delta^{13}\text{C}$ values for POM ranged from -24.07 to -18.02‰, and $\delta^{15}\text{N}$ values ranged from 3.06 to 8.69‰ (Fig. 2.3). Mean $\delta^{13}\text{C}$ (± SD) values for POM differed significantly across water types ($F_{2,24} = 4.79$, $p = 0.02$; Table 2.2, Fig. 2.4a). $\delta^{13}\text{C}$ was lowest in the CCE (-23.40 ± 0.65) and significantly higher in the IS (-21.70 ± 1.71). $\delta^{13}\text{C}$ in the WCE did not differ significantly from any other water type. Mean (± SD) $\delta^{15}\text{N}$ values for POM followed a similar trend (Table 2.2, Fig. 2.4b). $\delta^{15}\text{N}$ was significantly lower in the CCE (4.52 ± 1.10) and WCE (5.16 ± 0.90) than in the IS water type (7.08 ± 1.00; $F_{2,24} = 16.12$, $p < 0.01$). The WCEp was significantly more depleted in both ^{13}C (-24.77 ± 0.56) and ^{15}N (1.66 ± 0.57) than the WCE ($F_{1,14} = 23.96$, $p < 0.01$; $F_{1,14} = 85.44$, $p <$

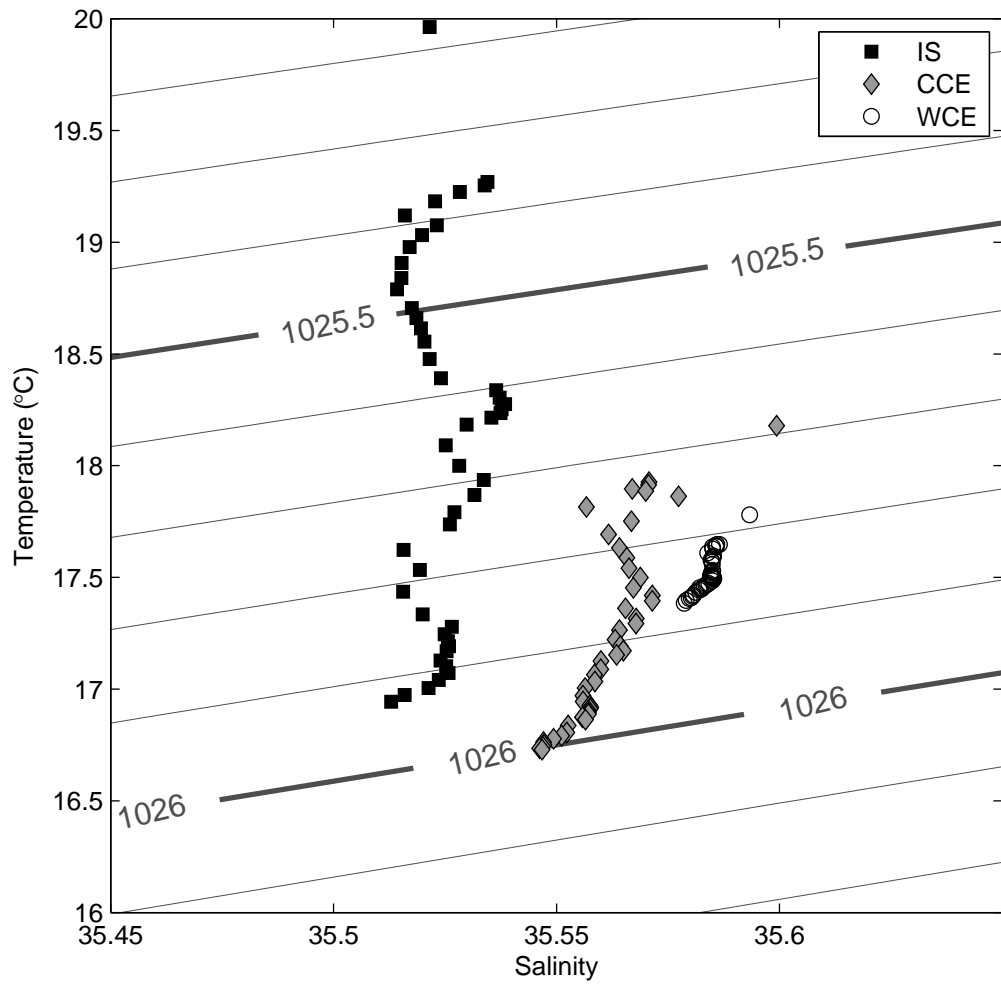


Figure 2.2 Mean temperature-salinity signatures (0 – 100m) for each water type: IS - inner shelf, CCE - cold core eddy and WCE - warm core eddy. Density contours are overlaid.

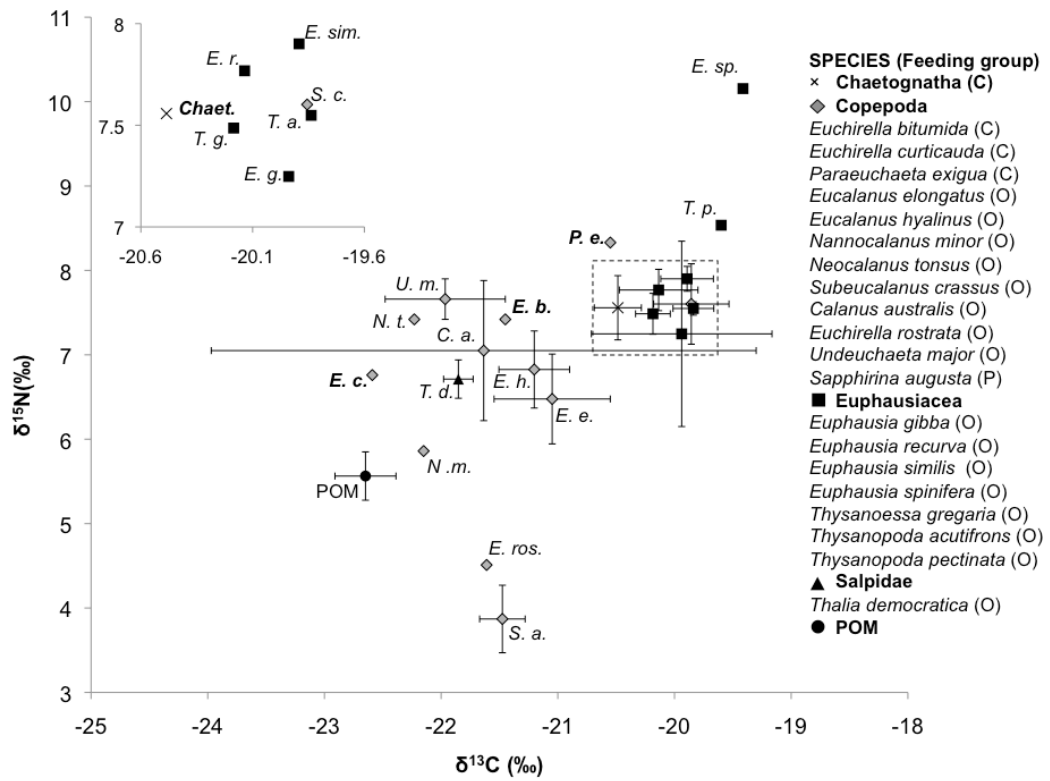


Figure 2.3 Bi-plot of mean (\pm SE) $\delta^{13}\text{C}$ (‰) vs. $\delta^{15}\text{N}$ (‰) values of each zooplankton species pooled for each water type. Abbreviated species names are displayed adjacent to data points, with corresponding names and feeding groups presented next to the graph. Bold names represent carnivorous (C) species. *Sapphirina augusta* is a parasitic (P) copepod. All remaining copepod and euphausiid species, and the salp *Thalia democratica*, are omnivorous (O). POM is particulate organic matter and represents the average across all water types (excluding WCEp). Feeding groups are based on references presented in Table 2.3. The inner groups have been enlarged (inset) for clarity (error bars not included).

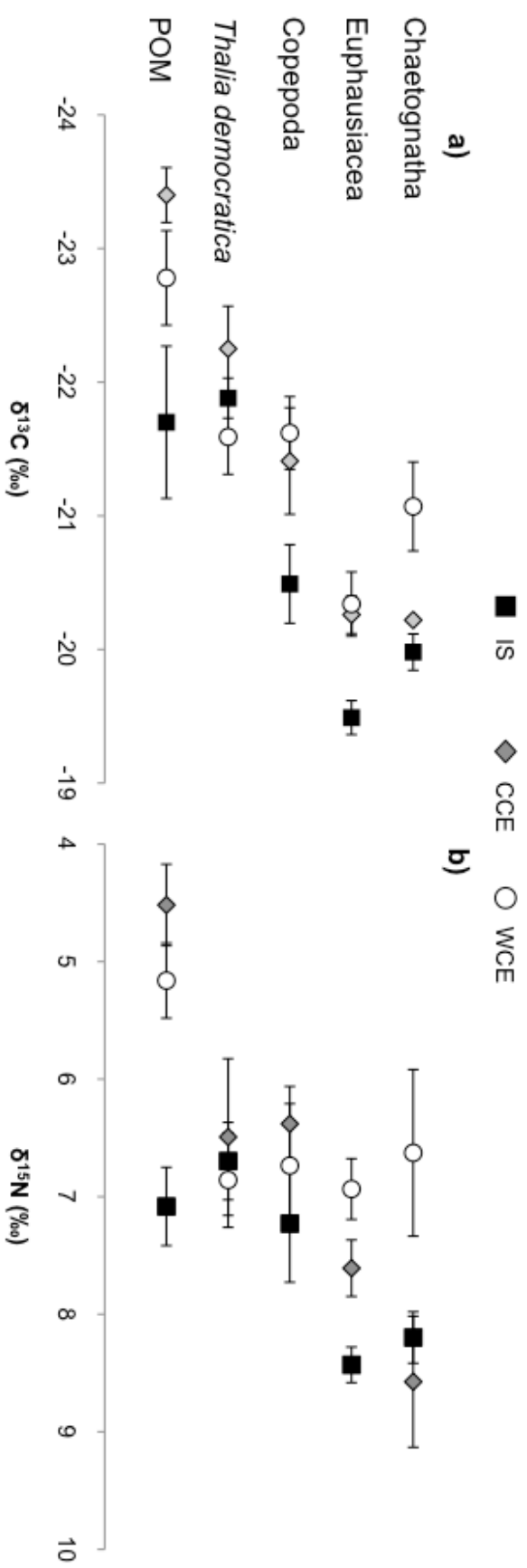


Figure 2.4 a) $\delta^{13}\text{C}$ and b) $\delta^{15}\text{N}$ isotope values (mean \pm SE) of POM and zooplankton across water types in the Tasman Sea. $\delta^{13}\text{C}$ and $\delta^{15}\text{N}$ values were sorted in order of increasing trophic level (based on average $\delta^{15}\text{N}$). IS – inner shelf, CCE – cold core eddy, WCE – warm core eddy.

Table 2.1 Mean characteristics (\pm SD) over the top 50 m of the water column. The surface mixed layer depth is calculated from the minimum depth at which $T < T(10\text{ m}) - 0.4^\circ\text{C}$ or $S > S(10\text{ m}) + 0.03$ following Condie & Dunn (2006). Values in parentheses correspond to ranges. n - number of stations; IS - inner shelf; CCE - cold core eddy; WCE - warm core eddy; WCep - warm core eddy preliminary POM transect.

Water type	n	Temperature ($^\circ\text{C}$)	Salinity	Nitrate+Nitrite ($\mu\text{mol m}^{-3}$)	Chlorophyll a ($\mu\text{g L}^{-1}$)	Mixed layer depth (m)
IS (27 Sept.)	4	18.07 \pm 0.37 (17.54 – 18.37)	35.52 \pm 0.03 (35.48 – 35.56)	2.25 \pm 0.58 (1.64 – 2.86)	1.16 \pm 0.19 (1.01 – 1.42)	13.40 \pm 12.62 (2.98 – 29.79)
CCE (26 Sept.)	5	17.21 \pm 0.58 (16.54 – 17.70)	35.56 \pm 0.02 (35.53 – 35.59)	2.12 \pm 0.24 (1.89 – 2.33)	1.42 \pm 0.22 (1.18 – 1.71)	17.62 \pm 9.29 (3.97 – 350.13)
WCE (3 Oct.)	4	17.51 \pm 0.57 (16.76 – 17.99)	35.58 \pm 0.02 (35.56 – 35.60)	1.68 \pm 0.75 (0.75 – 2.58)	1.03 \pm 0.33 (0.62 – 1.39)	137.17 \pm 113.67 (20.85 – 274.80)
WCep (23 Sept.)	4	18.03 \pm 0.09 (17.91 – 18.11)	35.60 \pm 0.00 (35.60 – 35.60)	2.45 \pm 0.07 (2.35 – 2.53)	0.75 \pm 0.34 (0.41 – 1.09)	282.97 \pm 60.00 (215.31 – 350.13)

Table 2.2 POM and zooplankton isotope values of $\delta^{13}\text{C}$ and $\delta^{15}\text{N}$ (mean \pm SD; ‰). n - sample size. Δ - ^{15}N enrichment relative to POM.

Water type	Species	n	$\delta^{13}\text{C}$	$\delta^{15}\text{N}$	Δ
IS	POM	9	-21.70 \pm 1.71	7.08 \pm 1.00	-
	<i>Thalia democratica</i>	9	-21.88 \pm 0.45	6.70 \pm 0.99	-0.38
	Copepoda (Parasite)	1	-21.67	3.47	-3.61
	Copepoda (Omnivore)	8	-20.33 \pm 0.93	7.56 \pm 0.94	0.48
	Copepoda (Carnivore)	1	-22.55	8.33	1.25
	Euphausiacea	12	-19.49 \pm 0.44	8.32 \pm 0.36	1.26
CCE	Chaetognatha	7	-19.98 \pm 0.36	8.20 \pm 0.58	1.12
	POM	10	-23.40 \pm 0.65	4.52 \pm 1.10	-
	<i>Thalia democratica</i>	2	-22.25 \pm 0.45	6.49 \pm 0.94	1.97
	Copepoda (Parasite)	1	-21.28	4.27	-0.25
	Copepoda (Herbivore)	1	-22.15	5.86	1.34
	Copepoda (Omnivore)	8	-22.78 \pm 1.62	5.16 \pm 1.02	0.64
	Copepoda (Carnivore)	2	-21.59 \pm 0.81	6.86 \pm 0.47	2.34
	Euphausiacea	18	-20.26 \pm 0.60	7.61 \pm 1.02	3.09
WCE	Chaetognatha	2	-20.22 \pm 0.03	8.57 \pm 0.79	4.05
	POM	8	-22.78 \pm 1.00	5.16 \pm 0.90	-
	<i>Thalia democratica</i>	4	-21.59 \pm 0.56	6.86 \pm 0.81	1.70
	Copepoda (Omnivore)	7	-21.62 \pm 0.72	6.74 \pm 1.40	1.58
	Euphausiacea	8	-20.34 \pm 0.68	6.97 \pm 0.78	1.81
WCEp	Chaetognatha	7	-21.07 \pm 0.88	6.63 \pm 1.87	1.47
	POM	8	-24.77 \pm 0.56	1.66 \pm 0.57	-

0.01). There are no large river systems near the sampling locations, and no large rainfall events prior to sampling which suggests that it is unlikely that terrestrial source materials could be present in the POM.

2.3.3 Zooplankton isotope analysis

$\delta^{15}\text{N}$ values ranged from 3.87‰ for the parasitic copepod *Sapphirina augusta* to 10.15‰ for the euphausiid, *Euphausia spinifera*, whereas $\delta^{13}\text{C}$ ranged from -22.59 to -19.41‰ as a result of the copepod *Euchirella curticauda* and *E. spinifera* (Fig. 2.3). Mean (\pm SD) ^{15}N trophic enrichment over POM for all zooplankton overall was 1.64 ± 1.16 ‰, however, this varied across water types. Trophic enrichment over POM for zooplankton was lowest in the IS water type (0.53‰) compared to the CCE (2.74‰) and WCE (1.64‰).

Mean $\delta^{13}\text{C}$ and $\delta^{15}\text{N}$ values for *Thalia democratica* ranged from -22.56 to -21.03‰ and 6.49 to 6.86‰ respectively, and did not differ significantly across water types (Table 2.2, Fig. 2.4). Generally, *T. democratica* was the least enriched across all water types (Table 2.2; Fig. 2.5), with trophic enrichment varying from -0.38 to 1.97‰. In the IS, *T. democratica* samples were actually ^{15}N depleted compared to POM. There was no significant correlation between *T. democratica* and POM in $\delta^{13}\text{C}$ ($r = 0.2$, $p = 0.47$) or $\delta^{15}\text{N}$ ($r = 0.02$, $p = 0.93$).

Copepods had the largest $\delta^{13}\text{C}$ and $\delta^{15}\text{N}$ range compared to other zooplankton overall and $\delta^{13}\text{C}$ and $\delta^{15}\text{N}$ values did not significantly differ across water types (Table 2.2, Fig. 2.4). Mean (\pm SD) $\delta^{13}\text{C}$ values ranged from -22.59‰ for the carnivore *Euchirella curticauda* to -19.86 ± 0.72 ‰ for *Subeucalanus crassus*, an omnivore (Table 2.3; Fig.

Table 2.3 Copepod and euphausiid isotope values of $\delta^{13}\text{C}$ and $\delta^{15}\text{N}$ (mean \pm SD; ‰) separated by feeding group. n - sample size. References are indicated in brackets. All omnivorous copepods are predominantly herbivorous, with the exception of the predominantly carnivorous *Undeuchaeta major*. Some species were sampled across more than one water type (*), however, for each species $\delta^{13}\text{C}$ and $\delta^{15}\text{N}$ values did not significantly differ across water types.

Species	Feeding group	n	$\delta^{13}\text{C}$	$\delta^{15}\text{N}$
Copepoda				
<i>Sapphirina augusta</i> *	Parasite (1)	2	-21.48 \pm 0.28	3.87 \pm 0.57
<i>Nannocalanus minor</i>	Herbivore (2)	1	-22.15	5.86
<i>Euchirella rostrata</i>	Omnivore (2)	1	-21.61	4.51
<i>Calanus australis</i> *	Omnivore (3)	2	-21.64 \pm 3.30	7.05 \pm 1.17
<i>Eucalanus elongatus</i> *	Omnivore (4)	6	-21.05 \pm 1.22	6.48 \pm 1.30
<i>Eucalanus hyalinus</i> *	Omnivore (5)	5	-21.20 \pm 0.68	6.83 \pm 1.02
<i>Neocalanus tonsus</i>	Omnivore (6)	1	-22.23	7.42
<i>Subeucalanus crassus</i> *	Omnivore (5)	5	-19.86 \pm 0.72	7.60 \pm 1.07
<i>Undeuchaeta major</i>	Omnivore (7)	2	-21.97 \pm 0.73	7.66 \pm 0.34
<i>Euchirella bitumida</i>	Carnivore (8)	1	-21.45	7.42
<i>Euchirella curticauda</i>	Carnivore (8)	1	-22.59	6.76
<i>Paraeuchaeta exigua</i>	Carnivore (9)	1	-20.55	8.33
Euphausiacea				
<i>Euphausia gibba</i>	Omnivore (10)	2	-19.94 \pm 1.09	7.25 \pm 1.55
<i>Euphausia recurva</i> *	Omnivore (10)	5	-20.14 \pm 0.75	7.77 \pm 0.55
<i>Euphausia similis</i> *	Omnivore (10)	8	-19.82 \pm 0.59	7.87 \pm 0.37
<i>Euphausia spinifera</i>	Omnivore (10)	1	-19.41	10.15
<i>Thysanoessa gregaria</i> *	Omnivore (10)	18	-20.35 \pm 0.65	7.49 \pm 1.03
<i>Thysanopoda acutifrons</i>	Omnivore (10)	2	-19.84 \pm 0.25	7.55 \pm 0.11
<i>Thysanopoda pectinata</i>	Omnivore (10)	1	-19.60	8.54

1. Wickstead (1962); 2. Kouwenberg (1994); 3. Peterson et al. (1990); 4. Timonin (1971); 5. Paffenhofer and Lewis (1989); 6. Zeldis et al. (2002); 7. Sano et al. (2013); 8. von Vaupel Klein (1998); 9. Park (1994); 10. Pillar et al. (1992).

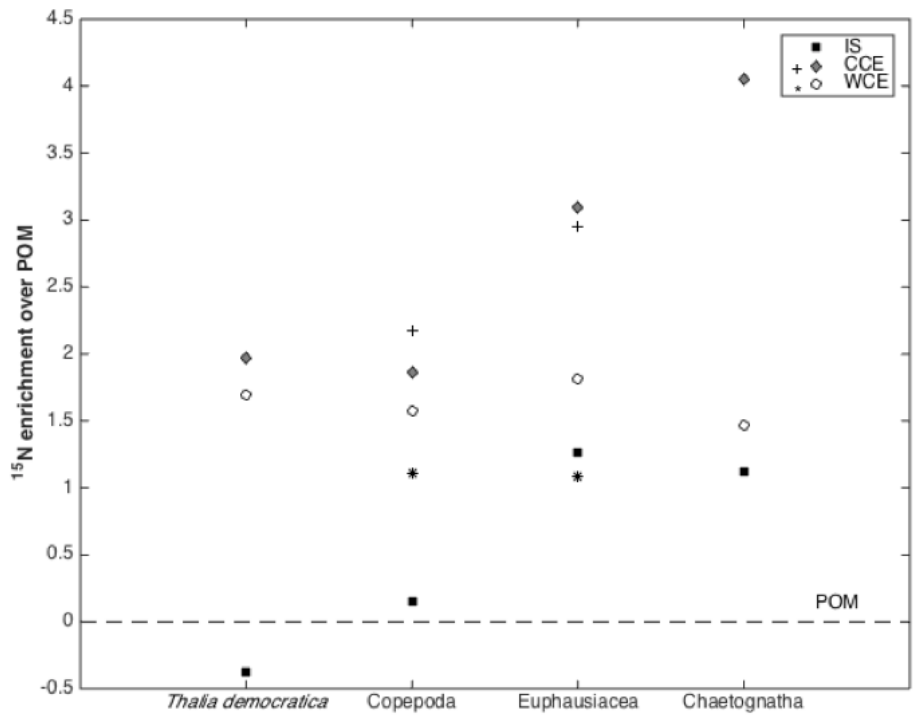


Figure 2.5 ¹⁵N enrichment (Δ) for zooplankton taxa over POM (dashed line) across water types. IS – inner shelf, CCE – cold core eddy, WCE – warm core eddy. ¹⁵N enrichment for the copepod species *Eucalanus elongatus* and the euphausiid species *Thysanoessa gregaria* are represented in their taxa groups for the CCE (+) and WCE (*).

2.3). *Sapphirina augusta* was the most ^{15}N depleted ($3.87 \pm 0.57\text{‰}$) compared to the more ^{15}N enriched carnivore *Paraeuchaeta exigua* (8.33‰ ; Table 2.3; Fig. 2.3).

Trophic enrichment over POM for the copepods ranged from 0.15‰ in the IS to 1.86‰ in the CCE (Table 2.2, Fig. 2.5).

Mean (\pm SD) $\delta^{13}\text{C}$ and $\delta^{15}\text{N}$ values for euphausiids differed significantly across the water types, with the most depleted values in the WCE and CCE and increasing in enrichment in the IS ($F_{2,35} = 7.79$, $p = 0.002$; $F_{2,35} = 8.03$, $p < 0.01$; Table 2.2, Fig. 2.4). All euphausiid species identified were omnivorous (Table 2.3; Fig. 2.3). $\delta^{13}\text{C}$ and $\delta^{15}\text{N}$ did not differ significantly across species and values ranged from -19.94 and 7.25‰ for *Euphausia gibba* to -20.69 and 10.15‰ for *E. spinifera*.

Chaetognaths also had significantly lower $\delta^{13}\text{C}$ in the WCE compared to the IS ($F_{2,13} = 5.19$, $p = 0.02$), however, $\delta^{15}\text{N}$ values did not significantly differ across water types (Table 2.2, Fig. 2.4). In the IS and CCE, euphausiids (3.09‰ CCE) and chaetognaths (4.05‰ CCE) occupied a higher trophic level than copepods (1.86‰ CCE) and *T. democratica* (1.97‰ CCE), however, trophic enrichment for both euphausiids (1.26‰ IS) and chaetognaths (1.12‰ IS) were also lower than expected in the IS (Table 2.2, Fig. 2.5). In the WCE, ^{15}N trophic enrichment for copepods (1.6‰ for all copepods; 1.1‰ for *E. elongatus*) was similar to euphausiids (1.8‰ for all euphausiids; 1.1‰ for *T. gregaria*) and chaetognaths (1.5‰), suggesting that in the WCE they belong to a similar trophic level (Table 2.2; Fig 2.5).

2.3.4 Trophic niche widths across species

The copepod *Eucalanus elongatus* had a significantly larger trophic niche width (mean $SEA_B = 5.27$; 95% Bayesian credible interval (BCI) = 2.00 - 9.86) than *T. democratica* (mean $SEA_B = 1.81$; 95% BCI = 1.03 - 2.79) and the euphausiid *Thysanoessa gregaria* (mean $SEA_B = 2.06$; 95% BCI = 1.23 - 3.06; $F_{2,42} = 53.66$, $p < 0.01$; Fig. 2.6). Mean (\pm SD) $\delta^{13}C$ values for *T. gregaria* (-20.19 ± 0.63) was significantly different from both *T. democratica* (-21.85 ± 0.49) and *E. elongatus* (-21.05 ± 1.22 ; $F_{2,36} = 23.36$, $p < 0.01$).

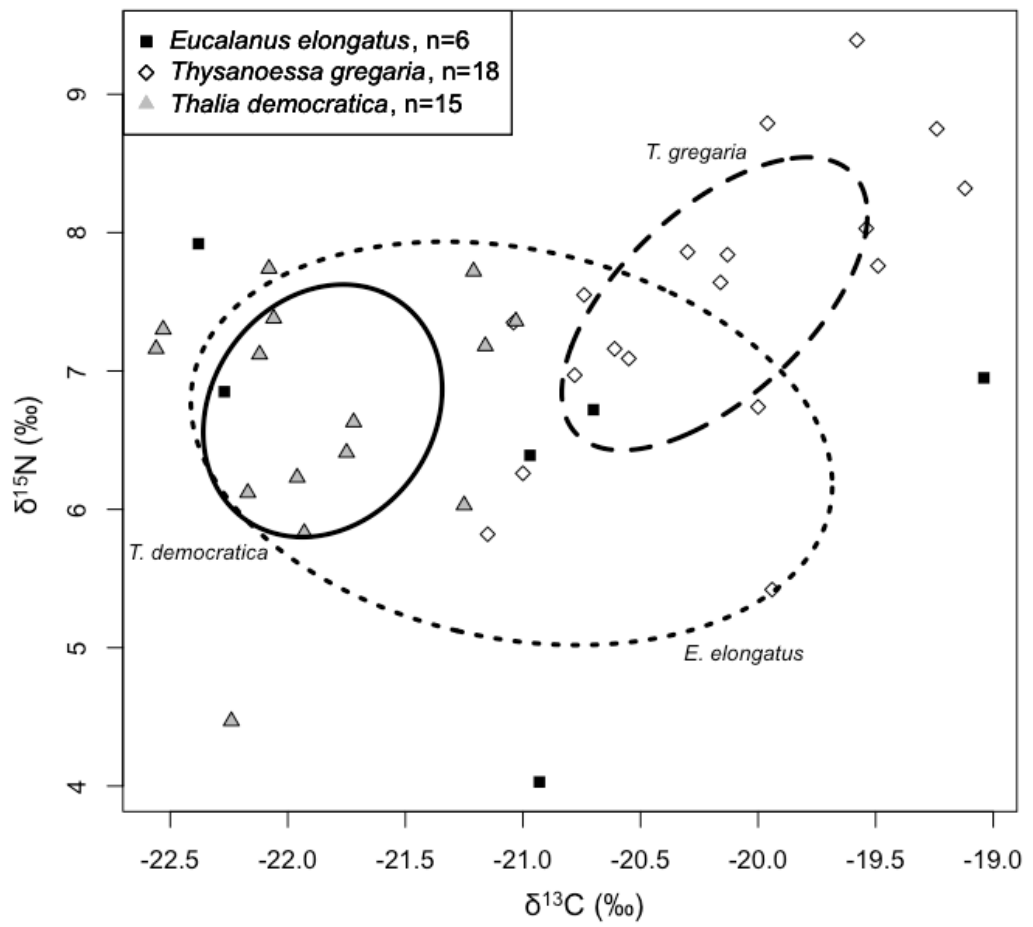


Figure 2.6 $\delta^{13}\text{C}$ and $\delta^{15}\text{N}$ bi-plot for *Thysanoessa gregaria*, *Eucalanus elongatus* and *Thalia democratica*. Standard ellipse areas (SEA_B) are depicted with solid or dashed lines, with species labels displayed adjacent to ellipses. n – number of samples.

2.4 Discussion

This study quantified the POM and zooplankton food web across three water types of the western Tasman Sea using stable isotope analysis of 21 species. We also examine the potential for competition between three omnivorous zooplankton using a novel Bayesian ellipse analysis. The variation between water types was evident in the isotopic values of POM, and was transferred to the zooplankton. Relative trophic level for the majority of the 21 species of zooplankton sampled were consistent with previously established feeding groups. Some euphausiids were more enriched in ^{15}N than expected, and chaetognaths were less enriched in ^{15}N than expected. Within species, diets were surprisingly robust across disparate ocean conditions. The lack of distinct enrichment differences between trophic levels suggests that there was a high degree of omnivory occurring in the zooplankton. There is also evidence that the diet of omnivorous zooplankton can vary in response to local conditions, with zooplankton becoming more carnivorous when chlorophyll *a* concentrations were low, such as in the WCE. A detailed niche width analysis of three co-existing zooplankton species provides evidence for food competition (between *Eucalanus elongatus* and *Thalia democratica*), but also for niche partitioning (between *Thysanoessa gregaria* and the other two species). Water type is likely to have a large impact on the niche of the resident zooplankton, but careful sampling of numerous elements of the food web through time is needed to distinguish dietary changes from baseline isotopic changes driven by oceanographic events such as upwelling.

2.4.1 Particulate organic matter

The isotopic values for POM in this study were within the range for temperate marine phytoplankton (-18 to -28‰ $\delta^{13}\text{C}$; Goericke et al., 1994) and within the range

previously found in the Tasman Sea ($-21.5\text{‰ } \delta^{13}\text{C}$, $2.3 - 8.4\text{‰ } \delta^{15}\text{N}$; Davenport and Bax, 2002). Both $\delta^{13}\text{C}$ and $\delta^{15}\text{N}$ values for POM were significantly enriched in the IS compared to the CCE and WCE. Several factors can alter the $\delta^{13}\text{C}$ and $\delta^{15}\text{N}$ values of POM including differences between phytoplankton species (Wong and Sackett, 1978) and differences in species cell size (Rau et al., 1990) and differences in nutrient sources and concentrations which may result in different growth conditions for phytoplankton (Altabet and Francois, 1994). The IS water type was sampled off Stockton Bight (Fig. 2.1a), an area known to be enriched in nutrients (Suthers et al., 2011) and chlorophyll *a* (Everett et al., 2014). Satellite images also indicated persistent upwelling occurring in the area prior to sampling. Correspondingly, high abundances of the dinoflagellate *Noctiluca scintillans* were observed in the IS water type (Henschke, unpublished data), which has been associated with upwelling events (Dela-Cruz et al., 2008). As diatoms tend to dominate in recently upwelled water (Ragueneau et al., 2000), this suggests that higher quantities of diatoms enriched the IS POM values compared to the CCE and WCE (Rau et al., 1990; Fry and Wainright, 1991). Depleted ^{13}C and ^{15}N values in the WCEp coupled with low chlorophyll *a* concentrations ($0.75 \pm 0.34 \mu\text{g L}^{-1}$), suggest that smaller phytoplankton species were abundant (Rau et al., 1990), and that the phytoplankton community within the WCEp was characteristic of an oligotrophic environment (Waite et al., 2007b). For the second sampling of the WCE, cooler water had been brought to the surface as a result of the eddy encroaching on the shelf promoting a phytoplankton bloom (chlorophyll *a*: $1.03 \pm 0.33 \mu\text{g L}^{-1}$). This mechanism most likely resulted in the more enriched ^{13}C and ^{15}N values in the POM compared to the previous sample.

2.4.2 Isotopic enrichment of Tasman Sea zooplankton

In this study, average enrichment in ^{15}N of zooplankton above POM across all water masses was 1.64‰. Previous studies in the Tasman Sea found trophic enrichment levels of ~1.5‰ for zooplankton (Davenport and Bax, 2002), and a meta-analysis has identified a mean ^{15}N enrichment of 2.08‰ for invertebrates, significantly lower than vertebrates (2.88‰; Vanderklift and Ponsard, 2003). Therefore less ^{15}N trophic enrichment than the generally accepted 3.4‰ (Minagawa and Wada, 1984) may be a characteristic of some zooplankton taxa. This is likely due to differences in the synthesis and excretion of nitrogenous waste across taxa, as ammonotelic invertebrates were found to have significantly lower ^{15}N enrichment than ammonotelic vertebrates (Vanderklift and Ponsard, 2003). All taxa exhibited ^{13}C enrichment over POM ranging from 0.63 – 3.18‰, with the exception of *Thalia democratica* in the IS (-0.18‰). This level of trophic enrichment agrees with previously reported ranges of ^{13}C enrichment between 0.8 - 2.7‰ over POM for marine zooplankton (del Giorgio and France, 1996).

Thalia democratica had the lowest $\delta^{15}\text{N}$ values across all water types (Table 2.2). ^{15}N enrichment relative to POM ranged from 0.83 to 1.97‰ across both the WCE and CCE. In the IS, however, *T. democratica* was ^{15}N depleted compared to POM (-0.38‰). Generally low nitrogen enrichment or depletion (around $\pm 1\%$) of salps relative to POM has been seen for *Salpa thompsoni* and *S. maxima* (Richoux and Froneman, 2009; Fanelli et al., 2011; Stowasser et al., 2012). Although POM is used as an approximation for phytoplankton, it also contains a mixture of bacteria, detritus, heterotrophs and sometimes zooplankton (Richoux and Froneman, 2009), indicating that its isotopic values will be enriched relative to pure phytoplankton. As a result, selective grazing and/or selective digestion can result in ^{15}N values for zooplankton that are depleted

relative to POM (del Giorgio and France, 1996). Alternatively, if the POM in the IS water types was isotopically enriched due to a recent upwelling event as observed in this study, these shifts may not have transferred to grazers by the time of sampling (Rolf, 2000). Either of these mechanisms might explain why *T. democratica*, and other salps, can show low levels of trophic enrichment.

Copepods, euphausiids and chaetognaths are expected to occupy higher trophic levels than salps due to a higher level of carnivory. The majority of copepod species sampled were omnivorous (70%; Table 2.3), with only three carnivorous species sampled; *Euchirella bitumida*, *E. curticauda* and *Paraeuchaeta exigua*. With the exception of *Sapphirina augusta*, relative $\delta^{15}\text{N}$ values for both copepod and euphausiid species were consistent with their previously established feeding groups (Table 2.3). Copepod $\delta^{13}\text{C}$ values were more variable than euphausiid values across all water types, indicating that copepods had a more diverse diet (Post, 2002). *S. augusta* was ^{15}N depleted compared to all other zooplankton species and POM. *Sapphirina* spp. sampled in the Leeuwin Current off Western Australia have also been observed depleted in ^{15}N compared to POM, which may be due to it feeding selectively on picoplankton (Waite et al., 2007a). More recently, suspended particulate nitrogen, such as marine snow, which is often depleted in ^{15}N (mean 0.2‰; Altabet, 1988), was associated with low $\delta^{15}\text{N}$ values for *Sapphirina ovatolanceolata-gemma* (Aberle et al., 2010). As there were high abundances of larvaceans during sampling (Chapter 3), *S. augusta* could be feeding on discarded larvacean houses, a major component of marine snow (Koski et al., 2007), or possibly on the faecal pellets of *T. democratica* (Suthers, pers. comm.). Unfortunately, the diet of species of *Sapphirina* remains uncertain (Wickstead, 1962).

In the CCE, $\delta^{15}\text{N}$ enrichment over POM for euphausiids (3.09‰) and chaetognaths (4.05‰) was consistent with their omnivorous and obligate carnivorous (Terazaki, 1998) feeding modes. Copepods in general were only enriched by 1.86‰, suggesting that they were more herbivorous compared to euphausiids. Considering their partial or complete carnivory, levels of ^{15}N enrichment over POM for copepods (0.15 - 1.53‰), euphausiids (1.25 - 1.96‰) and chaetognaths (1.12‰) were lower than expected in the IS water type (Table 2.1). Similar to the reasons for the isotopic signature of *Thalia democratica*, the POM may have been enriched by a recent upwelling event, but with sampling of the IS water occurring before this enrichment had entered the copepods, euphausiids and chaetognaths.

Similar levels of ^{15}N enrichment among copepods, euphausiids and chaetognaths were observed in the WCE, indicating that the copepods and euphausiids were more carnivorous than in the CCE. POM isotopic variation and food biomass (chlorophyll *a*) was low in the WCEp, suggesting that a prior limitation of phytoplankton forced the increased carnivory observed for the WCE zooplankton. This trend has been experimentally shown in the omnivorous copepod *Calanus pacificus*, which increased carnivory in response to a decrease in phytoplankton density (Landry, 1981), and in euphausiids in low phytoplankton areas of the Southern Ocean (Richoux and Froneman, 2009).

2.4.3 Species-specific trophic niche width

Zooplankton may exhibit niche differentiation or partitioning to avoid competition and promote the coexistence of species in the same area (Chase and Leibold, 2003). To explore this, the trophic niche widths for three co-existing omnivorous species were

compared: *Thysanoessa gregaria*, *Eucalanus elongatus*, and *Thalia democratica*. Each species occurs in the top 100 m of the water column and do not show diel vertical migration (Longhurst, 1985; Barange, 1990; Gibbons, 1997), suggesting that they will be competing for phytoplankton and/or zooplankton in the same volume of water. As *T. democratica* can consume phytoplankton particles (<1 μm - 1 mm) more efficiently than other zooplankton (Vargas and Madin, 2004), niche differentiation and an omnivorous feeding pattern is one way for both *E. elongatus* and *T. gregaria* to avoid competition. Niche differentiation can be clearly seen for *T. gregaria*, which was feeding on items more enriched in ^{13}C . This could be a result of *T. gregaria* feeding on different source materials, or feeding in different source waters. For example, one method of niche differentiation is to be separated from potential competitors in the vertical dimension. Similar patterns have been seen in three *Neocalanus* species, where trophic niche partitioning promoted their coexistence in the same region (Doi et al., 2010). A significantly larger trophic niche width (SEA_B) for *E. elongatus* suggests it is feeding on greater diversity than both *T. gregaria* and *T. democratica* (Fig. 2.6). Although this could be a result of a much lower sample size for *E. elongatus* ($n = 6$ compared to $n = 15$ and $n = 18$), as the ellipse based analysis used can be sensitive to sample size (Jackson et al., 2011), random resampling for $n = 6$ across all species still results in a significantly larger trophic niche for *E. elongatus* ($F_{2,42} = 8.721$, $p < 0.01$). Despite the larger niche width, the lack of niche differentiation between *T. democratica* and *E. elongatus* suggests that these two species may compete for food (e.g. Henschke et al., 2011). However, as niche overlap does not necessarily confirm that organisms are competing for the same food source, instead that they could be consuming food sources with similar isotopic signatures, an investigation of diet composition and foraging

behaviour (such as spatial segregation) is needed to reveal the degree of competition that is occurring between these zooplankton species.

2.4.4 Concluding remarks

This study presents an analysis of the Tasman Sea zooplankton trophic structure across three water types and 21 different taxa. Water type was found to influence the zooplankton niche via the varying response of their phytoplankton prey and POM to oceanographic differences. However, oceanographic characteristics within a water type are not constant, and processes such as upwelling can create temporal mismatch between the isotopic signatures of POM and some zooplankton species. Some zooplankton species appear to adapt to changes in the marine environment. In less biologically productive water types, such as the WCE for example, zooplankton diets can shift from omnivory to carnivory. Similarly, some zooplankton species, such as *Thysanoessa gregaria*, may be able to avoid competition through niche differentiation, whereas some form of competition may be unavoidable, such as seen between *Thalia democratica* and *Eucalanus elongatus*.

Chapter 3

Demography and interannual variability of salp swarms (*Thalia democratica*)

Abstract

Swarms of the pelagic tunicate, *Thalia democratica*, form during spring, but the causes of the large interannual variability in the magnitude of salp swarms are unclear.

Changes in asexual reproduction (buds per chain) of *T. democratica* populations in the coastal waters of south-east Australia (32 – 35°S) were observed in three austral springs (October 2008 – 2010). *T. democratica* abundance was significantly higher in 2008 (1,312 individuals m⁻³) than 2009 and 2010 (210 and 92 individuals m⁻³, respectively).

There was a significant negative relationship ($R^2 = 0.61$, $F_{1,22} = 33.83$, $p < 0.01$) between abundance and asexual reproduction (buds per chain). Similarly, relative growth rates declined with decreasing abundance. Generalised additive mixed modelling showed that *T. democratica* abundance was significantly positively related to preferred food >2 μm in size ($p < 0.05$) and negatively related to the proportion of non-salp zooplankton ($p < 0.01$). Salp swarm magnitude, growth, and asexual reproduction may depend on the abundance of larger phytoplankton (prymnesiophytes and diatoms) and competition with other zooplankton.

3.1 Introduction

Dense swarms of salps, a pelagic tunicate, intermittently occur in oceans around the world as a result of favourable hydrographic conditions, such as intrusions of nutrient-rich water (Blackburn, 1979; Heron and Benham, 1984; Deibel and Paffenhofers, 2009). Recent studies have related the patches of salps to meteorological and oceanographic data (Deibel and Paffenhofers, 2009), and show that cool, inner shelf water types promoted denser populations of the small salp, *Thalia democratica* (Henschke et al., 2011). It is still unknown, however, why the magnitude of salp swarms in the ocean can vary dramatically from year to year in the same location. A long-term, 25-year study of *T. democratica* in the Mediterranean Sea found that interannual abundances vary over 3 orders of magnitude (Licandro et al., 2006). Similarly, a variability of 2 - 3 orders of magnitude in biomass was seen in consecutive spring seasons in the Californian Current (Lavaniegos and Ohman, 2003).

Abundances of salps in swarms can often exceed 1000 individuals (ind.) m⁻³ (Andersen, 1998; Everett et al., 2011; Henschke et al., 2011), constitute 99% of the zooplankton biomass (Siegel and Harm, 1996), and cover an area up to 100 000 km² (Madin et al., 2006). Salps are highly efficient filter feeders, feeding on a wide size range of particles (0.1 μm - 1 mm), from bacteria to nauplii (Vargas and Madin, 2004; Sutherland et al., 2010). The grazing pressure created by salp swarms can remove the daily primary production in an area (Dubischar and Bathmann, 1997) and transfer this matter relatively efficiently to the sea floor in fast-sinking, carbon-rich faecal pellets (Bruland and Silver, 1981). As a result, the influence of salp swarms on the biogeochemical cycle is substantial, playing a significant role in carbon fluxes (Chapter 5; Andersen, 1998). Understanding the processes affecting the magnitude of salp swarms will aid

understanding of their role in the biological carbon pump and support the development of reliable biogeochemical and ecosystem models.

The salp life cycle involves the alternation of aggregated sexual and solitary asexual reproduction to generate swarming (Alldredge and Madin, 1982). Solitaries (oozoids) asexually produce a chain of genetically identical individuals (buds). These aggregate (blastozoid) buds are female and immediately fertilised after release from the oozoid. Once they develop and release one embryo, blastozoids then develop testes and fertilize the next generation of recently released buds. The embryo is the start of the next oozoid generation (Heron and Benham, 1985; Fig. 1 in Henschke et al., 2011). Although sexual reproduction only results in one offspring per parent, *Thalia democratica* oozoids can asexually produce 1 - 3 separate releases of 20 - 80 buds (Heron, 1972). Combined with fast growth rates, this results in rapid population growth, as one oozoid individual can potentially produce 240 blastozoid offspring in a week (Heron, 1972). Swarms of salps tend to be ephemeral, only lasting from one week up to one month (Deibel and Paffenhofer, 2009). As this duration corresponds to generation times of *T. democratica* (Braconnot, 1963; Deibel, 1982), it suggests that one of the main drivers of swarm formation is asexual reproduction.

Thalia democratica regularly swarm after the spring phytoplankton bloom (Heron, 1972; Deibel and Paffenhofer, 2009) and it is likely that swarm magnitude may be more dependent upon phytoplankton composition and/or abundance than other variables such as temperature and salinity. Similarly, Heron and Benham's (1985) theory of "overwintering" *T. democratica* populations suggest that asexual reproduction varies

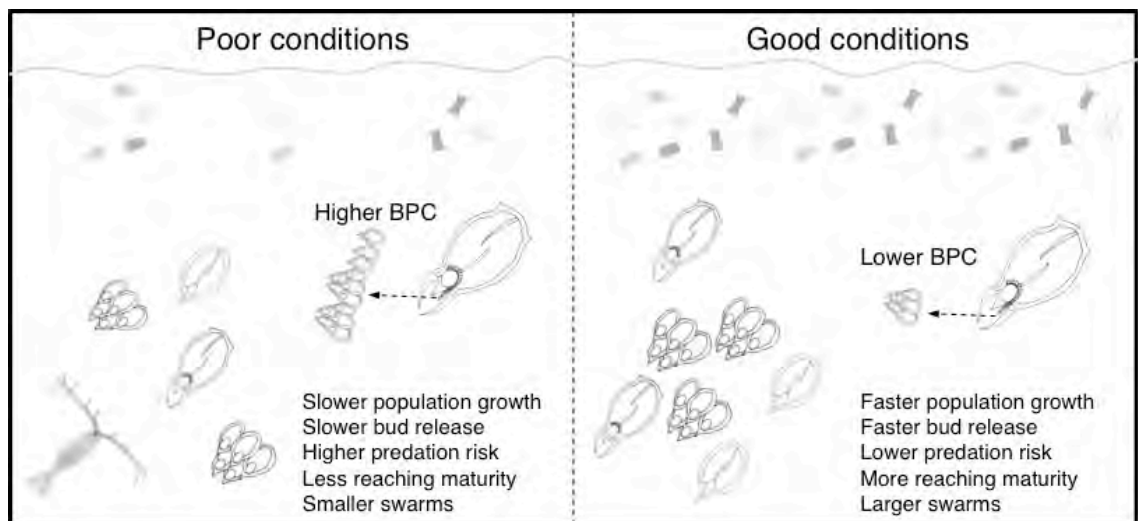


Figure 3.1 Schematic diagram of Heron and Benham's (1985) overwintering theory. During poor conditions (left pane) such as winter, *Thalia democratica* oozoids will release longer chains of blastozoid buds (buds per chain; BPC). However, slow growth will result in young being exposed to predation and competition for longer, resulting in fewer reaching maturity and smaller swarm sizes. When conditions improve (right pane) in spring, oozoids will release shorter chains (lower BPC) more quickly that will grow rapidly and form larger swarms.

depending on environmental conditions (Fig. 3.1). In poorer conditions, oozoids grow slowly, nursing longer chains of buds. Due to slower growth rates, the more vulnerable smaller stages (Heron et al., 1988) will be exposed to predation for longer, resulting in a lower percentage of young reaching maturity and smaller swarm sizes overall. On the other hand, when conditions are more suitable, the oozoid individuals have faster growth rates, produce shorter chains of buds more rapidly, and successfully reach maturity (Heron and Benham, 1985; Deibel and Lowen, 2012). Hence, asexual reproduction (buds per release) and population growth rates can be used as an indicator of nutritional status. Although “buds per release” may be a more accurate term as a measure of asexual reproduction, for the remainder of this chapter the term “buds per chain” is used to be consistent with existing literature. When referring to buds per chain

we are not describing the total reproductive output, but instead the buds released from a single chain release.

This study examines the magnitude and demography of *Thalia democratica* swarms during the austral spring (September - November) across three years. The first aim was to examine the annual salp swarms of three research voyages (2008 - 2010) in the context of a zooplankton monitoring station (2002 - 2010) off Sydney. To examine swarm demographics, asexual reproduction and growth rate for each swarm was calculated. In order to have a comparable measure of growth rate across the three swarms, growth rate was calculated from formalin-fixed *T. democratica* samples using methods by Heron and Benham (1985). This calculation is based on significant correlations between five life history stages and previously estimated growth rates (Heron and Benham, 1984; 1985). Heron and Benham's (1985) growth calculation generally results in faster growth rates when compared with laboratory experiments (Deibel, 1982; Le Borgne and Moll, 1986). The second aim, therefore, was to assess the validity of Heron and Benham's (1985) growth calculation as either a direct or relative measure, by comparing with growth rate experiments conducted on live specimens from the same population. The third aim was to identify links between environmental conditions, in particular the phytoplankton community composition, and *T. democratica* swarm demographics (asexual reproduction and growth rate) across three consecutive spring seasons.

3.2 Methods

3.2.1 Long-term *Thalia democratica* sampling

Zooplankton were sampled monthly from January 2002 to December 2012 at the Port Hacking National Reference Station (NRS; 100 m deep) off Sydney, Australia (34° 09' S, 151° 15' E; Fig. 3.2). A 20 cm diameter 100 μ m mesh net was used to sample from 2002 to January 2009. Since February 2009, a larger 60 cm diameter net has been used with the same mesh size. Nets were dropped at a rate of 1 ms⁻¹ to 100 m below the surface using a drop net (Heron, 1982). Samples were fixed in a 5% formalin solution and analysed by the Plankton Ecology Laboratory, CSIRO. Data presented in this paper are single values from each haul ($n = 94$) but averaged for monthly analysis. Data are freely available via the Integrated Marine Observing System (IMOS) data portal: <http://imos.aodn.org.au/>.

3.2.2 Oceanographic sampling procedure

Three austral spring (September - November) voyages aboard the R.V. *Southern Surveyor* were undertaken off south-east Australia in the Tasman Sea in 2008, 2009 and 2010 (Table 3.1). The study area extended from Diamond Head in the north (31° 30' S, 152° 30' E) to Jervis Bay in the south (35° 03' S, 150° 43' E; Fig. 3.2). Samples were collected along transects from the inner shelf water type (Cresswell, 1994; Henschke et al., 2011). Data included in this paper from 2008 was a random selection from inner shelf stations previously determined by Henschke et al. (2011). These locations were chosen with the aid of daily Moderate Resolution Imaging Spectroradiometer (MODIS) and Advanced Very High Resolution Radiometer (AVHRR) satellite imagery during the cruise. Transects had 5 - 12 equidistant stations. At stations along each sampling transect, a Seabird SBE911-plus Conductivity-Temperature-Depth (CTD) equipped

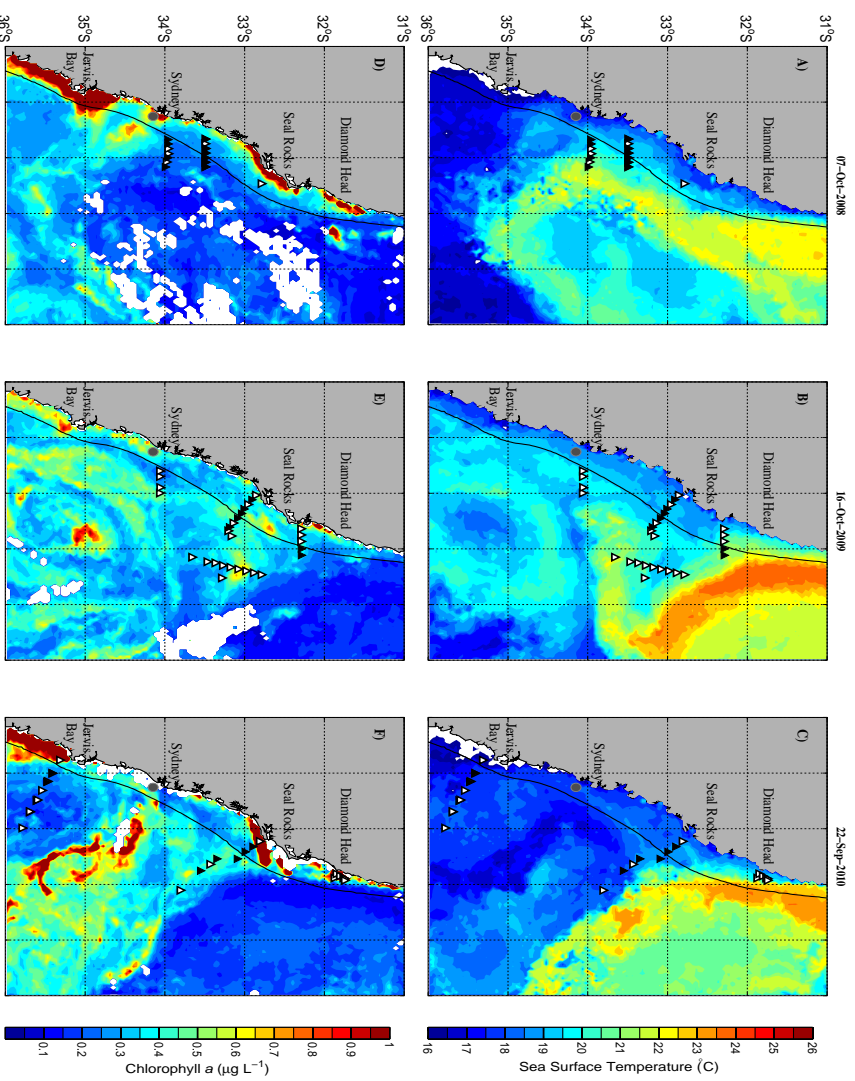


Figure 3.2 Study area with satellite derived sea surface temperature ($^{\circ}\text{C}$; A-C) and chlorophyll *a* ($\mu\text{g L}^{-1}$; D-F) overlaid. Images best represent conditions occurring on the first day of oceanographic sampling across the three years (Table 3.1). Due to cloud cover, satellite data represents an 8-day composite of sea surface conditions ending with the date given. Zooplankton sampling locations are represented by triangles. Black triangles denote stations that were used for asexual reproduction analysis. Grey circle indicates location of the Port Hacking National Reference Station. Black line refers to 200 m isobath.

Table 3.1 Hydrographic and zooplankton characteristics across the three years. Inner shelf water characteristics are depth averaged over the top 50 m of the water column. Values are mean \pm SD. Values in parentheses are ranges. Proportion of mature blastozoids is based on the percentage of population that is greater than 4 mm in length. n - number of stations.

	Year		
	2008	2009	2010
Sampling date	10/10/08 - 20/10/08	16/10/09 - 27/10/09	22/09/10 - 05/10/10 ^a
Hydrographic conditions (mean \pm SD)			
n	15	29	25
Temperature ($^{\circ}$ C)	19.25 \pm 0.96 (18.24 - 21.45)	19.45 \pm 0.88 (18.28 - 21.84)	18.29 \pm 0.89 (17.31 - 20.17)
Salinity	35.54 \pm 0.03 (35.46 - 35.57)	35.51 \pm 0.04 (35.43 - 35.57)	35.55 \pm 0.04 (35.48 - 35.60)
n	4	12	17
Chlorophyll a (μ g L ⁻¹)	0.74 \pm 0.38 (0.40 - 1.22)	0.70 \pm 0.18 (0.42 - 0.88)	0.45 \pm 0.63 (0.08 - 2.44)
Zooplankton abundance (mean \pm SD)			
n	14	27	24
<i>Thalassia demOCRatica</i>	1312.3 \pm 545.0 (679.1 - 2352.1)	210.2 \pm 264.9 (0.6 - 1113.6)	91.9 \pm 118.7 (0 - 423.3)
Crustaceans	251.2 \pm 170.8	399.3 \pm 239.6	3136.8 \pm 4705.7
Doliolids	45.4 \pm 50.8	36.2 \pm 91.9	304.5 \pm 439.7
Larvaceans	31.4 \pm 41.1	55.8 \pm 57.1	3441.3 \pm 4674.5
Chaetognaths	3.0 \pm 3.1	8.9 \pm 6.0	89.0 \pm 64.4
Other	41.2 \pm 25.0	84.0 \pm 47.4	229.8 \pm 154.5
Total non-salp zooplankton	372 \pm 238	584 \pm 298	7201 \pm 9311
<i>Thalassia demOCRatica</i> life history characteristics			
n	10	7	7
Asexual reproduction (BPC)	36.08 \pm 4.75 (31.8 - 48)	45.68 \pm 7.48 (36.4 - 60)	53.15 \pm 4.12 (47.9 - 58.5)
Blastozoid : Oozoid	11.2 \pm 6.1 (5.5 - 26)	9.5 \pm 3.9 (6.1 - 15.9)	8.8 \pm 4.8 (4.5 - 15.3)
Relative growth index (% length h ⁻¹)	16.5 \pm 3.2 (8.2 - 22.6)	14.9 \pm 2.1 (12.3 - 17.6)	11.5 \pm 3.8 (6.4 - 17.5)
r_{max} (d ⁻¹)	2.8 \pm 0.5 (1.4 - 3.2)	2.7 \pm 0.3 (2.2 - 3.1)	2.1 \pm 0.7 (1.2 - 3.2)
n	31	24	19
Proportion of mature blastozoids (%)	13.51 \pm 8.69 (0 - 41.2)	11.62 \pm 8.42 (0.8 - 32.8)	5.55 \pm 7.76 (0 - 26.6)

^aSecond voyage for phytoplankton collection conducted 14/10/10 - 31/10/10

with an AquaTracker Mk3 fluorometer (Chelsea, UK) was used to record salinity, temperature and fluorescence, respectively.

To investigate the vertical distribution of the phytoplankton community across the three years, water was collected from the surface and the depth of the chlorophyll *a* maximum (as determined by the down-cast fluorescence profile), and four other depths (i.e., nominally surface, 10, 25, 50, 75, 100 m). A minimum volume of 2.2 L was filtered under low vacuum (e.g. ≤ 100 mm Hg) onto 25 mm GF/F filters in low light ($< 10 \mu\text{mol photons m}^{-2} \text{s}^{-1}$). Filters were folded in half, blotted dry on absorbent paper, placed into screw-capped cryovials and stored in liquid nitrogen until pigment analysis in the laboratory.

Water for chlorophyll *a* and accessory pigment analyses in 2010 was opportunistically sampled a fortnight after zooplankton sampling on a second voyage as the required phytoplankton expertise was not available during the salp sampling voyage. From inspection of MODIS satellite imagery, there were similar oceanographic conditions between the two voyages in 2010, as Tasman Sea water still dominated the region with the EAC separation remaining around 33°S. This was later confirmed when comparing mean values for depth-integrated fluorescence across the two voyages (ANOVA, $F_{1,69} = 0.81$, $p = 0.37$).

Phytoplankton assemblages sampled separately during 2010 at the Port Hacking NRS were dominated by prymnesiophytes in both September and October and did not differ significantly between the two months (Paired t test, $t_{38} = 1.24$, $p = 0.22$; Data freely available from IMOS, <http://imos.aodn.org.au/>). As the hydrographic characteristics of

the NRS has been shown to significantly correlate to inner shelf water in the area (Oke and Sakov, 2012), this shows statistically that phytoplankton assemblages in 2010 did not differ during the two week delay between zooplankton and phytoplankton sampling.

3.2.3 Pigment analyses

Phytoplankton pigment concentrations were estimated using High Performance Liquid Chromatography (HPLC) using procedures outlined in Doblin et al. (2011). HPLC analysis has the advantage of including all members of photosynthetic assemblages $>0.7 \mu\text{m}$ (cell counts with a microscope typically resolve species $>10 \mu\text{m}$ in diameter). The HPLC system was calibrated using phytoplankton reference cultures (Australian National Algae Culture Collection) with known pigment composition (Mantoura and Llewellyn, 1983; Barlow et al., 1993; Jeffrey et al., 1997).

The approach of Uitz et al. (2008) was used to assess the taxonomic community composition of phytoplankton and yield information about its size structure. While this method may be subject to error because pigments are shared between different phytoplankton groups, or some groups may be spread across different sizes, this approach yields useful information, e.g., pico-, nano- and micro-phytoplankton mainly include prokaryotes, diatoms and prymnesiophytes (coccolithophorids), respectively.

3.2.4 Shipboard zooplankton sampling

At each CTD station, two replicate vertical hauls of a N70 net (Kemp and Hardy, 1929) were made to 50 m for the collection of zooplankton. Modified from the original silk design, the 70 cm diameter N70 net had 3 sections of differing mesh sizes: a 53 cm long, 4 mm mesh section near the mouth; a 97 cm long, $400 \mu\text{m}$ mesh section in the

middle; and a 135 cm long, 225 μm mesh section near the cod end. Samples from each net haul were concentrated to 100 mL in a 5% formalin solution using a 200 μm sieve. In the laboratory, two replicate 1 mL subsamples were taken with a wide-mouth pipette from each net sample and examined in a Bogorov tray. Organisms were classified into groups commonly known to occur in the Tasman Sea: salps, doliolids, crustaceans, larvaceans and chaetognaths (Thompson and Kesteven, 1942). Other zooplankton identified in low numbers include: molluscs, cnidarians, ctenophores and annelids. Total length of the first 60 *Thalia democratica* individuals within each net haul sample were measured as by Foxton (1966), from the oral opening to the posterior ridge of the gut.

3.2.5 Shipboard growth experiments

In 2009, an extra vertical haul was undertaken at three sites (Table 3.2) for the collection of live *Thalia democratica* individuals for growth experiments. Mature oozoid *T. democratica* were removed from the cod end of the net and carefully transferred to a large (50 L) tank filled with site water taken from the surface depth. Salps were acclimatised overnight in a constant temperature room, with a 16/8 hour light/dark cycle. The constant temperature room was maintained at the ambient temperature of the mixed layer (Table 3.2).

Lights were turned on at 0400 h, preceding twilight, and oozoids bearing unreleased chains were transferred to individual 2 L tanks. Tanks were randomly allocated to three collection times, corresponding to how long the buds were left in the tanks to grow-out following their release from the oozoid: T0 (buds collected immediately after release), T4 (buds collected 4 hours after release) and T8 (buds collected 8 hours after release) (Table 3.2). Salps were continually observed for the point of bud release and the time of

release was recorded for each individual. To reduce the risk of mortality, water was gently mixed if salps became stuck on the surface due to surface tension (Heron, 1972).

Blastozooid buds experience sudden increases in length as they are being released which may alter calculated growth rates (Heron, 1972), but all chains in this study were collected after being fully released by the parent to eliminate any birthing effect. Once buds were successfully released, the oozoid was removed from the tank and fixed in 5% formalin, followed by the buds in the T0 group. Buds that were not fully released from their oozoid parent were removed from the experiment and not included in the data analysis. Buds from the T4 and T8 groups were subsequently collected after 4 or 8 hours respectively and fixed in 5% formalin solution. After collection, total lengths of buds and their oozoid parents were measured to estimate growth rates.

Table 3.2 Stations for blastozooid growth experiments in October 2009. Time is in Australian Eastern Standard time. *n* - number of stations. Values in parentheses represent number of tanks allocated to each collection time: T0, T4 and T8 respectively.

Experiment	<i>n</i>	Collection time	Location	Ambient temp (°C)	Growth rate (% length h⁻¹)
1	12 (4,4,4)	19th, 1615 h	33.30°S 154.35°E	20	2.32
2	19 (8,6,6)	20th, 1530 h	33.25°S 152.67°E	21.5	1.83
3	26 (10,8,8)	21st, 1715 h	33.20°S 152.61°E	20.5	2.20

3.2.6 *Thalia democratica* demographic analyses

Stations for asexual reproduction analysis were chosen randomly from within inner shelf waters sampled during research voyages and ranged from 7 (2009, 2010) to 10 (2008) CTD stations across the three years. Asexual reproduction was measured by quantifying the number of buds produced from the oldest fully developed chain (buds per chain, BPC) of an oozoid individual. A chain was only considered fully developed if it was clearly distinguished from the stolon (Fig. 3.3). This approach reduced the potential error associated with a young chain having not yet finished segmenting at the time of capture. Asexual reproduction of 20 individuals was measured from each sample. Where 20 oozoid individuals could not be found, the maximum number within the sample was used (minimum = 4).

The relative growth index (RGI; % length h^{-1}) across the three years was calculated using life history stages of fixed salps (Heron and Benham, 1985):

$$RGI = 0.576 - 0.0876 \ln(BPC) - 0.0211 \ln(OP) \quad (1)$$

where *BPC* = buds per chain (asexual reproduction), *OP* = offspring to parent ratio (i.e. blastozoid to mature oozoid).

The standard error for Heron and Benham's (1985) growth index estimates ranged from 0.67 - 0.78% length h^{-1} . This growth rate estimation was based on significant correlations that they found between five life history stages and previously estimated growth rates (Heron and Benham, 1984; 1985). As these life history stages are not affected by shrinking as a result of fixing, this equation is robust for use after long periods of fixing (Heron and Benham, 1985).

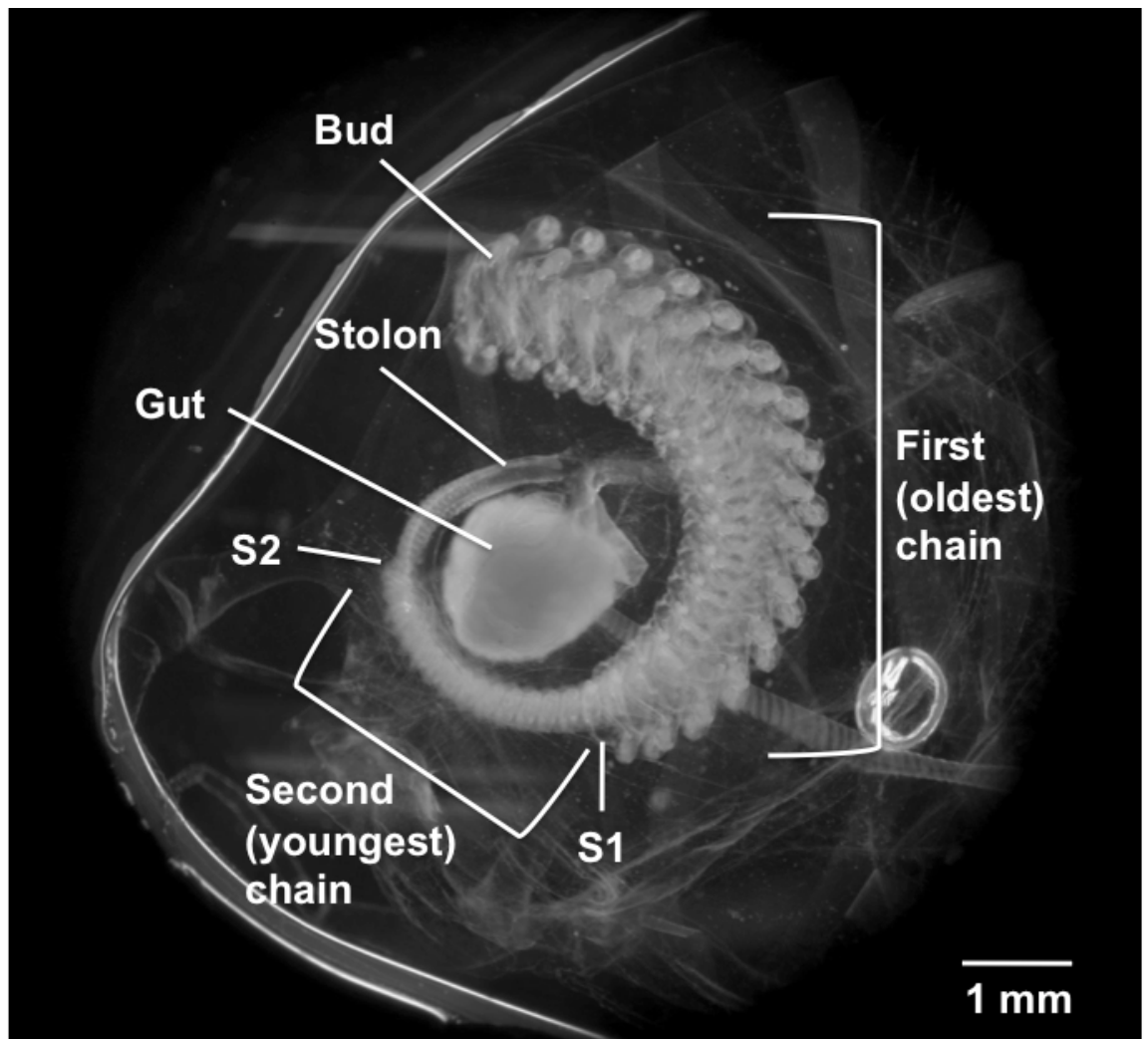


Figure 3.3 Three chains of *Thalia democratica* buds in an oozoid individual. Buds in first and second chains are clearly segmented and distinguished from other chains (S1: first separation, S2: second separation). Buds from the third chain are still segmenting along the stolon. Only the first chain was considered for asexual reproduction analysis.

Lifetime fitness ($r_{\max} \text{ d}^{-1}$) was calculated using the growth index (Equation 1) and asexual reproduction (BPC). Lifetime fitness refers to the maximum intrinsic rate of natural increase and is commonly used as a measure of adaption to different environmental conditions (Deibel and Lowen, 2012). As a result, increasing lifetime fitness reflects decreasing population turnover rate. The following equation from Troedsson et al. (2002) was used:

$$r_{\max} = \frac{\ln b}{T} \quad (2)$$

where b = lifetime egg production ($\text{BPC} \times 2.5$) and T = generation time in days.

Lifetime egg production was calculated assuming that the number of cohorts produced by each oozoid was 2.5, the median of most commonly observed chains released (Deibel and Lowen, 2012). Generation time was calculated as the time taken to complete one generation, assuming a standard maximum length of 15 mm for both blastozoid and oozoid individuals (Thompson, 1948) and using the calculated growth index (Equation 1).

3.2.7 Data analyses

An unbalanced one-way analysis of variance (ANOVA) was used to test the null hypothesis of no significant difference in each hydrographic condition (temperature, salinity and chlorophyll a) across the three ship-based sampling years. If the hydrographic data were not normally distributed within each year, a Mood's median test was undertaken to test the null hypothesis that the median values of each variable did not differ significantly across the years.

An unbalanced two-way ANOVA was used to test the null hypothesis of no significant difference in *Thalia democratica* abundance across years and seasons from the long-term NRS data. Unbalanced one-way ANOVAs were used to test the null hypotheses of no significant difference in oceanographic *T. democratica* abundance, asexual reproduction and abundance of non-salp zooplankton among years. Tukey's analysis was used for *a posteriori* pairwise comparisons between factor levels for all ANOVAs. Regression analyses were used to examine the relationship between *T. democratica* abundance and buds per chain ($n = 27$). An analysis of covariance (ANCOVA) was used to examine the relationship between growth rate and asexual reproduction (BPC). The two different growth methods, Heron and Benham's (1985) calculation and the laboratory experiments, were included as covariates. Where necessary, data were log-transformed to improve the assumptions of normality and homogeneity of variance, and to reduce the effect of outliers. All parametric tests were performed in R v. 2.15.2 (R Development Core Team, 2006).

Interannual variation in oceanographic phytoplankton assemblages was analysed using multivariate techniques. Bray-Curtis similarity matrices, based on log-transformed data, were constructed for both the phytoplankton community proxies (prymnesiophytes, diatoms and prokaryotes) as well as the size proxies (pico-, nano- and micro-phytoplankton). Principal coordinates analysis (PCO) was undertaken on these matrices to highlight relationships among phytoplankton communities across years. All multivariate non-parametric analyses were performed with PRIMER, Version 6 (Clarke and Warwick, 2001; Clarke et al., 2008).

To examine links between *Thalia democratica* swarm magnitude and environmental conditions, the relationship between abundance of *T. democratica* and environmental variables was analysed using a nonlinear generalised additive mixed-effects model (GAMM; Hastie and Tibshirani, 1990; Zuur et al., 2009). GAMMs extend traditional linear modelling by containing both random and fixed effects and applies a spline function to non-linear explanatory variables (Hastie and Tibshirani, 1990). A spline function creates a smoothed curve by sectioning the data into two or more segments and fitting polynomial curves to each segment (Zuur et al., 2009).

Prior to analysis, possible outliers or collinearity were identified through graphical analysis (boxplots and pair-wise scatter plots). No outliers were identified.

Phytoplankton size classes were considered for the model instead of species composition as *T. democratica* are opportunistic filter-feeders whose retention efficiency are only limited by size (Vargas and Madin, 2004). Food quality was grouped into two categories, preferred and non-preferred. Preferred included phytoplankton $>2 \mu\text{m}$ (i.e. nano- and microplankton) as *T. democratica* retention efficiency for these particles ranges from 80 - 100% (Vargas and Madin, 2004). Non-preferred included picoplankton ($<2 \mu\text{m}$) as retention efficiency on these particles is only 40 - 50% (Vargas and Madin 2004). As collinearity was observed between preferred and non-preferred food, preferred food was used as the main indicator of food quality. As well as preferred food the other explanatory variables that were used in the original model were: temperature, \log_{10} -chlorophyll *a* and proportion of non-salp zooplankton. Year was included as a random variable. As the relationship between salp abundance and proportion of non-salp zooplankton was non-independent, it was at risk of producing a spurious correlation (Brett, 2004). To determine if a spurious correlation did exist, the

procedure outlined by Brett (2004) was used, where the statistical significance of the correlation coefficient can be determined through Monte Carlo simulations. The variables: salp abundance, total zooplankton abundance and non-salp zooplankton abundance were randomly resampled using the same sample size as the original data ($n = 36$) and distribution pattern (mean and standard deviation). This was run 1000 times, and for each 1000 random sets, proportion of non-salp zooplankton was recalculated using the random sets of non-salp zooplankton abundance and total zooplankton abundance. All sets of salp abundance were then correlated with all sets of proportion of non-salp zooplankton, resulting in 1000 Pearson correlation coefficients that were all spurious. The mean Pearson correlation coefficient from these spurious data were then compared with the correlation coefficient of the original data to test the null-hypothesis of no significant difference from the spurious data.

A smoothing function was used only for the proportion of non-salp zooplankton, as all other explanatory variables had a linear relationship with \log_{10} -transformed salp abundance. Backward stepwise elimination was used to select significant parameters, and the most parsimonious model was chosen by comparing Akaike's Information Criterion (AIC) across models. An analysis of the model residuals suggested the model was robust. All analyses were performed using the mixed generalised additive model package "mgcv" in R (Wood, 2006) available at: cran.r-project.org. Modelling was performed in R v. 2.15.2 (R Development Core Team, 2006).

3.3 Results

3.3.1 Long-term *Thalia democratica* abundance

The long-term (2002 - 2010) abundance (ind. m⁻³, mean ± SD) of *Thalia democratica* at Port Hacking was 45.81 ± 140.40 ind. m⁻³ ($n = 93$; Fig. 3.4a). There was no significant difference in abundances across years ($F_{8,59} = 0.94$, $p = 0.49$), however, populations were significantly more abundant during the austral spring (September - November) when compared to autumn and winter ($F_{3,59} = 2.91$, $p = 0.04$; Fig. 3.4c). *Thalia democratica* abundance was generally low during most of the year and peaked in abundance in September (195.55 ± 325.54 ind. m⁻³) and October (233.10 ± 299.28 ind. m⁻³; Fig. 3.4a) during the spring. *T. democratica* were also present more frequently in samples from September and October (Fig. 3.4b). Interestingly, following peak abundances and presence of salps in September and October, November recorded the lowest presence of *T. democratica* in samples and mean abundances were an order of magnitude lower than previous months (Figs 3.4a and 3.4b). In the months of the spring voyages from this study, abundances of *T. democratica* were 637, 120 and 148 ind. m⁻³ (2008 - 2010 respectively; single tow values).

3.3.2 Hydrographic properties during the sampling period

The regional oceanography varied dramatically across the three years (Fig. 3.2). During 2008, the core of the East Australia Current (EAC) was 23°C and had penetrated as far south as Sydney (34°S), with a strong eastward retroflexion. During sampling, there was strong persistent upwelling off the coast at Seal Rocks (32° 27'S). In 2009, the EAC dominated the shelf off Sydney the month prior to sampling, but during sampling, a strong separation of the EAC from the Australian coast had formed at 32°S, with an average temperature of 23°C. In 2010, the EAC (22°C) had separated from the coast at

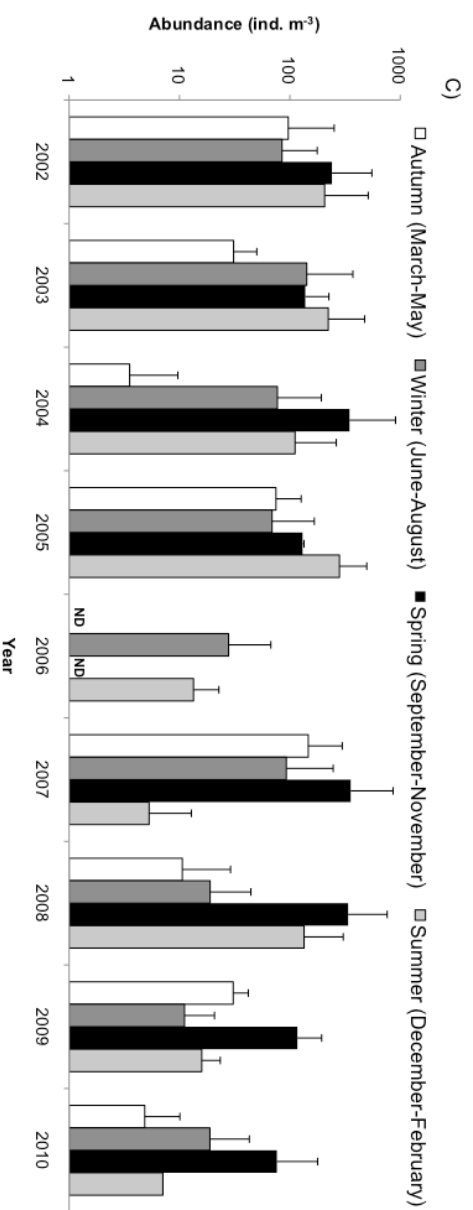
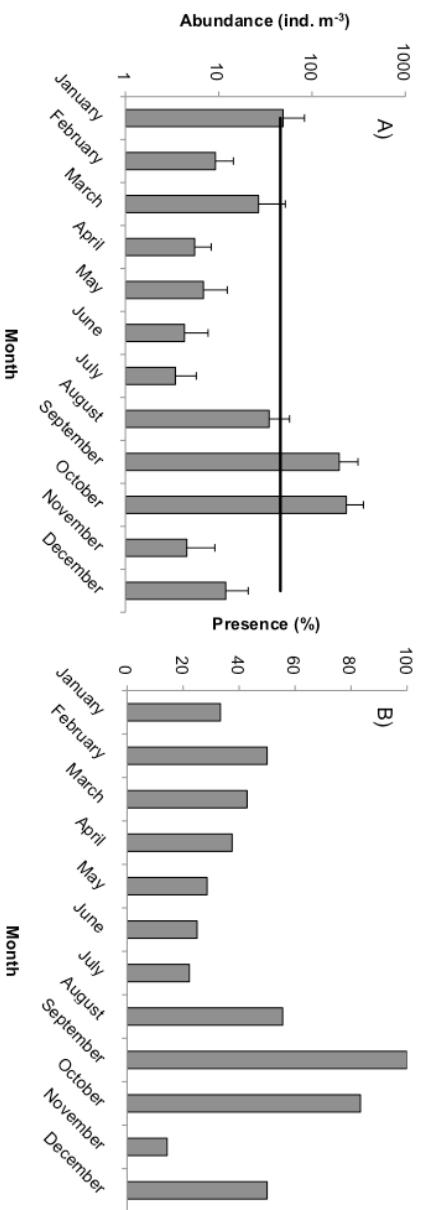


Figure 3.4 a) Mean (+SD) monthly abundance (ind. m⁻³) for *Thalassia demissa* at Port Hacking from 2002 - 2011. Black line represents long-term mean. Scale is log₁₀-transformed. b) Proportion of non-zero *T. demissa* hauls per month from 2002 - 2011 c) Seasonal abundances (ind. m⁻³) of *T. demissa* from 2002 - 2011. ND - no data. Scale is log₁₀-transformed.

33°S and Tasman Sea water dominated the region. In both 2009 and 2010 a large cyclonic eddy was evident off the coast at 33°S and upwelling off Seal Rocks was not observed in either year during sampling.

Hydrographic properties for inner shelf water (surface to 50 m) varied across the three years. In 2009, inner shelf water was less saline than in 2008 and 2010 (Table 3.1). Inner shelf water in 2010 was significantly cooler ($F_{2,21} = 7.52, p = 0.003$) and mean (\pm SD) chlorophyll *a* concentration was lower ($0.45 \pm 0.63 \mu\text{g m}^{-3}$, median = $0.23 \mu\text{g m}^{-3}$) than 2008 and 2009 ($0.74 \pm 0.38 \mu\text{g m}^{-3}$, median = $0.66 \mu\text{g m}^{-3}$; and $0.70 \pm 0.18 \mu\text{g m}^{-3}$, median = $0.77 \mu\text{g m}^{-3}$). Mood's median test confirmed that chlorophyll *a* levels were significantly lower in 2010 ($\chi^2_2 = 0.44, p < 0.01$). HPLC analysis identified that the phytoplankton communities in the inner shelf water differed across the three years. PCO analysis on pigments identified that prymnesiophytes (containing 19'hexanoyloxyfucoxanthin) dominated the phytoplankton community in 2008, prokaryotic picoplankton (containing zeaxanthin and divinyl-chl-*a*) in 2009, and there was a mix of both prymnesiophytes and microplankton diatoms in 2010 (Figs 3.5a and 3.5b).

3.3.3 *Thalia democratica* life history characteristics from ocean voyages

Thalia democratica was the dominant salp species sampled across the voyages, however, at a few stations *Salpa fusiformis*, *T. orientalis* and *Thetys vagina* occurred in low abundances ($<5 \text{ ind. m}^{-3}$). *T. democratica* abundance varied significantly across years. Mean abundances (\pm SD) of *T. democratica* decreased significantly from $1312.3 \pm 545.0 \text{ ind. m}^{-3}$ in 2008 to $210.2 \pm 264.9 \text{ ind. m}^{-3}$ in 2009, and were lowest in 2010 ($91.9 \pm 118.7 \text{ ind. m}^{-3}$; $F_{2,62} = 76.9, p < 0.01$; Table 3.1, Fig. 3.6a).

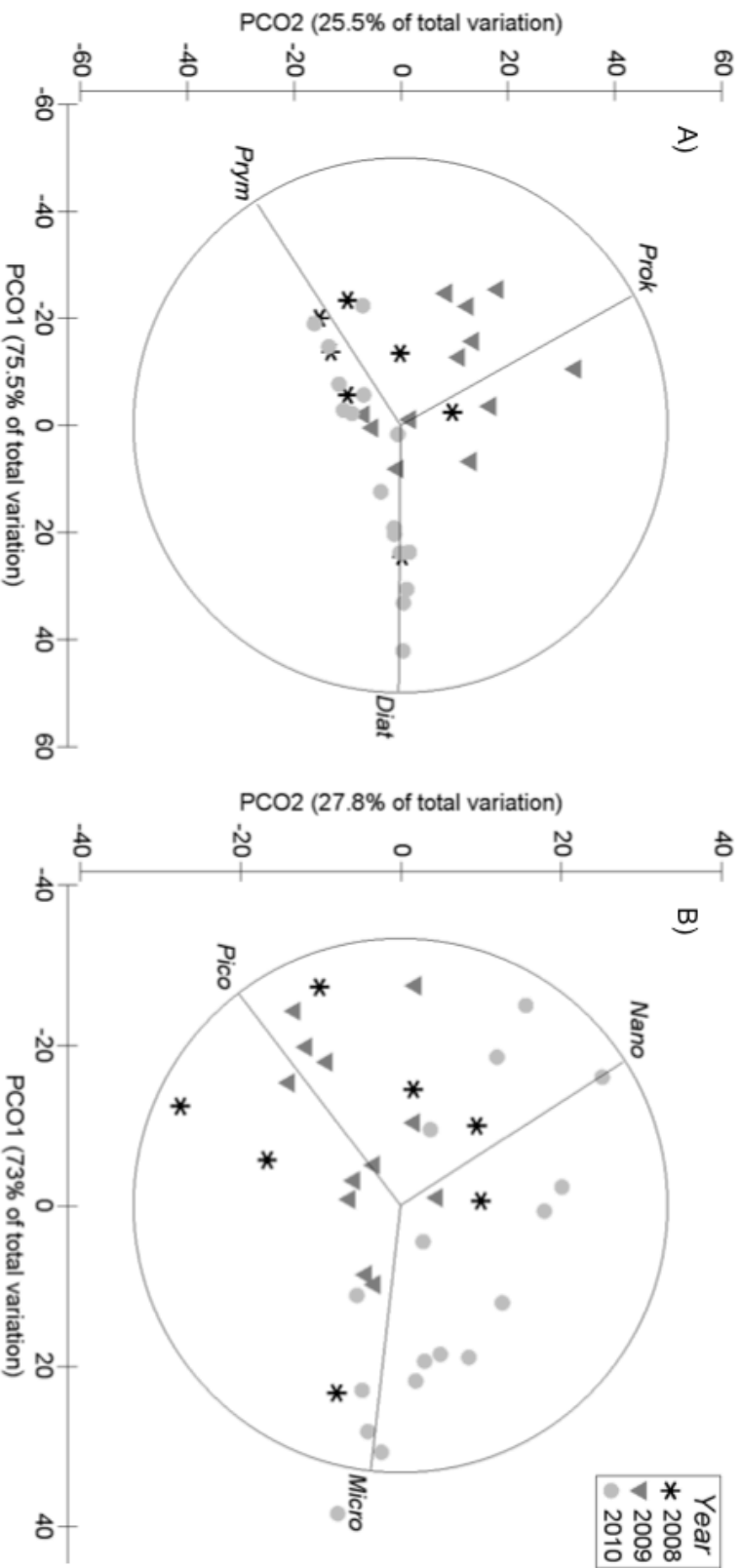


Figure 3.5 Ordination of phytoplankton community structure using principal coordinates analysis, with year superimposed. Vectors overlaid are multiple correlations of a) phytoplankton species groupings: diatoms (Diat), prymnesiophytes (Pym) and prokaryotes (Prok) and b) phytoplankton size structure: picoplankton <math>< 2 \mu\text{m}</math> (Pico), nanoplankton 2 - 20

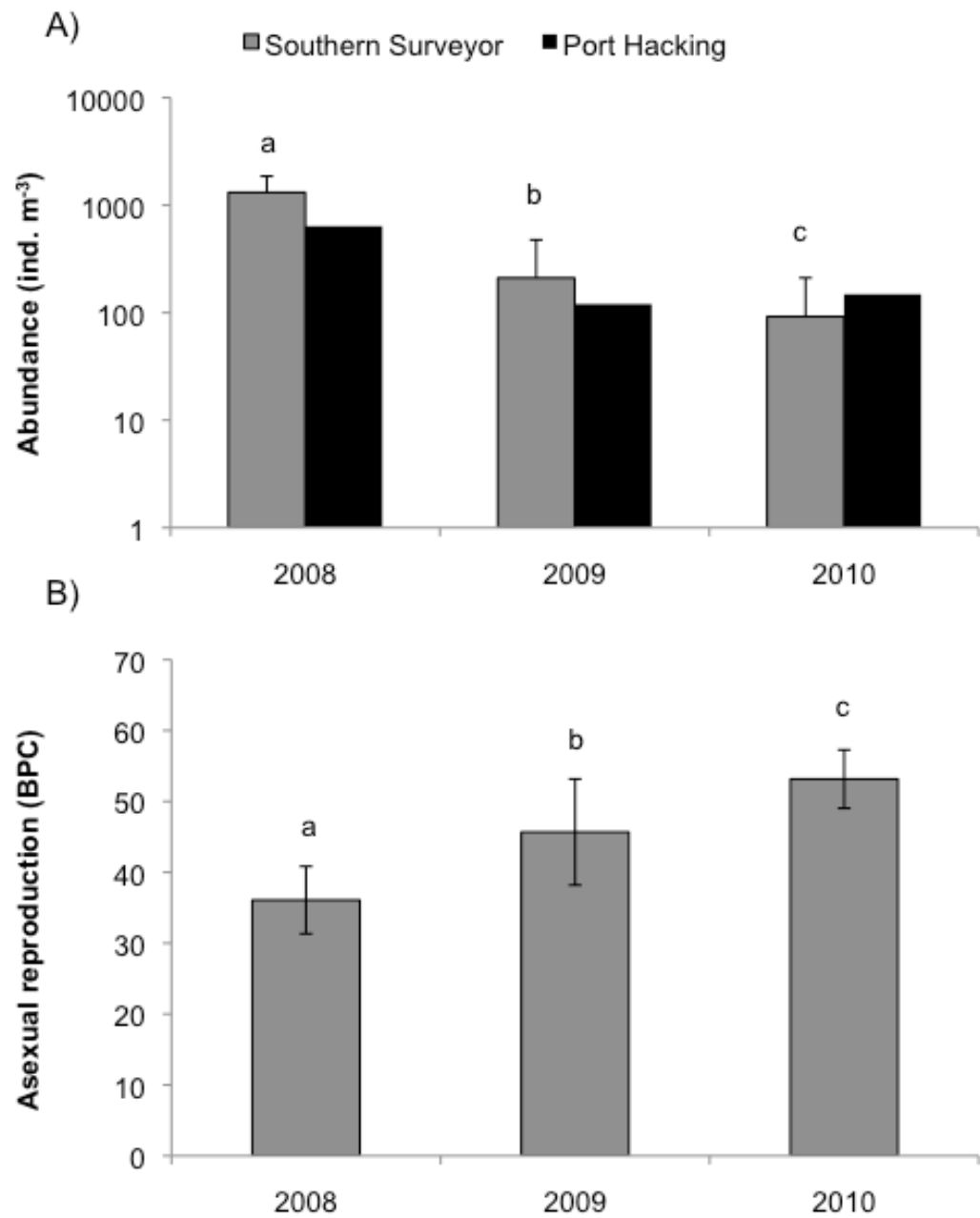


Figure 3.6 a) Mean (\pm SD) *Thalia democratica* abundance across three years of sampling (*Southern Surveyor* voyages) and for corresponding Port Hacking NRS hauls. b) Mean (\pm SD) asexual reproduction (buds per chain) across the three years from *Southern Surveyor* voyages. Letters denote significant differences at $p < 0.05$.

The proportion of blastozooids reaching maturity were significantly lower in 2010 (5.55 ± 7.76) than 2008 (13.51 ± 8.69) and 2009 (11.62 ± 8.42 ; $F_{2,71} = 5.47$, $p = 0.006$; Table 3.1). Although the blastozooid-to-oozoid ratio decreased throughout the years, this trend was non-significant ($F_{2,21} = 0.49$, $p = 0.62$).

Asexual reproduction (BPC) varied across years, significantly increasing each year from 2008 to 2010 ($F_{2,23} = 20.18$, $p < 0.01$; Fig. 3.6b). The relative growth index was significantly higher in 2008 ($16.5 \pm 3.2\%$ length h^{-1}) than in 2010 ($11.5 \pm 3.8\%$ length h^{-1} ; $F_{2,21} = 5.43$, $p = 0.01$; Table 3.1). Lifetime fitness rates also declined across the years, from 2.7 - 2.8 d^{-1} in 2008 and 2009 to 2.1 d^{-1} in 2010 (Table 3.1), however, this trend was not significant ($F_{2,21} = 3.41$, $p = 0.05$). Regression analysis identified a significant negative relationship between *T. democratica* abundance and asexual reproduction ($R^2 = 0.61$, $F_{1,22} = 33.83$, $p < 0.01$; Fig. 3.7).

3.3.4 Zooplankton community composition

In 2008 and 2009, mean (\pm SD) abundances of zooplankton excluding salps were 372 ± 238 and 584 ± 298 ind. m^{-3} respectively (Table 3.1). Copepods were the dominant group, comprising ~70% of the non-salp fraction of zooplankton. Non-salp zooplankton were significantly more abundant in 2010 than 2008 and 2009, with a mean abundance of 7201 ± 9311 ind. m^{-3} ($F_{2,62} = 12.34$, $p < 0.01$). The non-salp zooplankton community composition also shifted, with copepods and larvaceans constituting ~90% of the total zooplankton abundance in 2010.

3.3.5 Laboratory growth experiments

Blastozooid chains were released between 0330 and 0700 h AEST, with 85% of all chains released at 0530 h regardless of time of capture. Experimental growth rates ranged from 1.83 - 2.32% length h⁻¹ (Table 3.2). Growth rates did not vary significantly during the two time periods, with initial growth rates (0 - 4 hours) of 2.82% length h⁻¹, being similar to later growth rates (4 - 8 hours) of 2.12% length h⁻¹. Experimental growth rates were significantly lower (2.12 ± 0.26 ; $F_{1,8} = 101.84$, $p < 0.01$) than the relative growth index for the corresponding 2009 spring voyage (14.9 ± 2.1). There was no significant difference between the mean (\pm SD) asexual reproduction (BPC) calculated from the experiments (42.35 ± 10.43) and the mean asexual reproduction calculated from the 2009 voyage (45.68 ± 7.48 ; $F_{1,59} = 0.66$, $p = 0.42$). There was no significant interaction between method of growth calculation (growth experiment or growth index) and growth rate ($F_{1,23} = 0.25$, $p = 0.63$), however, there was a significant main effect for both factors (growth experiment, $F_{1,23} = 45.06$, $p < 0.01$ and growth index, $F_{1,23} = 4.97$, $p = 0.04$). This suggests that the slope of regression between growth rate and asexual reproduction was similar for both growth methods. Lifetime fitness values calculated from these laboratory determined growth rates found mean (\pm SD) values of 0.38 ± 0.01 , significantly lower than values calculated with the growth index ($F_{1,12} = 318.39$, $p < 0.01$).

3.3.6 Relationship between *Thalia democratica* abundance and the environment

Generalised additive mixed modelling (GAMM) identified a significant relationship between *Thalia democratica* and select environmental variables. This confirms that the relationship between salp abundance and proportion of non-salp zooplankton was not due to spurious correlations using a randomised resampling approach (Brett, 2004).

Average r for the correlation between salp abundance and proportion of non-salp zooplankton when the variables were randomly resampled was 0.003 (SD = 0.17, 95% confidence interval: -0.008 to 0.01). As the correlation coefficient of the original data ($r = -0.47$) exists outside of the distribution of the randomised data, this indicates that the relationship was not spurious.

The GAMM originally included four explanatory variables: temperature, \log_{10} -chlorophyll a , proportion of non-salp zooplankton and preferred food ($>2 \mu\text{m}$). Variables which were sequentially removed from the model were temperature followed by \log_{10} -chlorophyll a . The most parsimonious model included two significant terms: proportion of non-salp zooplankton and preferred food (Table 3.3). \log_{10} -transformed salp abundance was positively related to preferred food ($p < 0.05$, Table 3.3). As the relationship was non-linear, a smoother plot was used to illustrate the effect of proportion of non-salp zooplankton on *T. democratica* abundance. Increasing proportion of non-salp zooplankton has a significantly negative relationship with \log_{10} -transformed salp abundance ($p < 0.01$, Fig. 3.8).

Table 3.3 Synopsis of the final additive mixed modelling analysis. Edf - estimated degrees of freedom.

Parametric coefficients					Smooth term			
	Estimate	Standard error	t -value	p -value		Edf	F	p -value
Intercept	2.19	0.16	14.05	<0.01	Proportion of other zooplankton	2.92	15.2	<0.01
Preferred food	1.27	0.62	2.05	0.0489				
Model overview	R^2 adjusted: 0.56		AIC: 74.77					

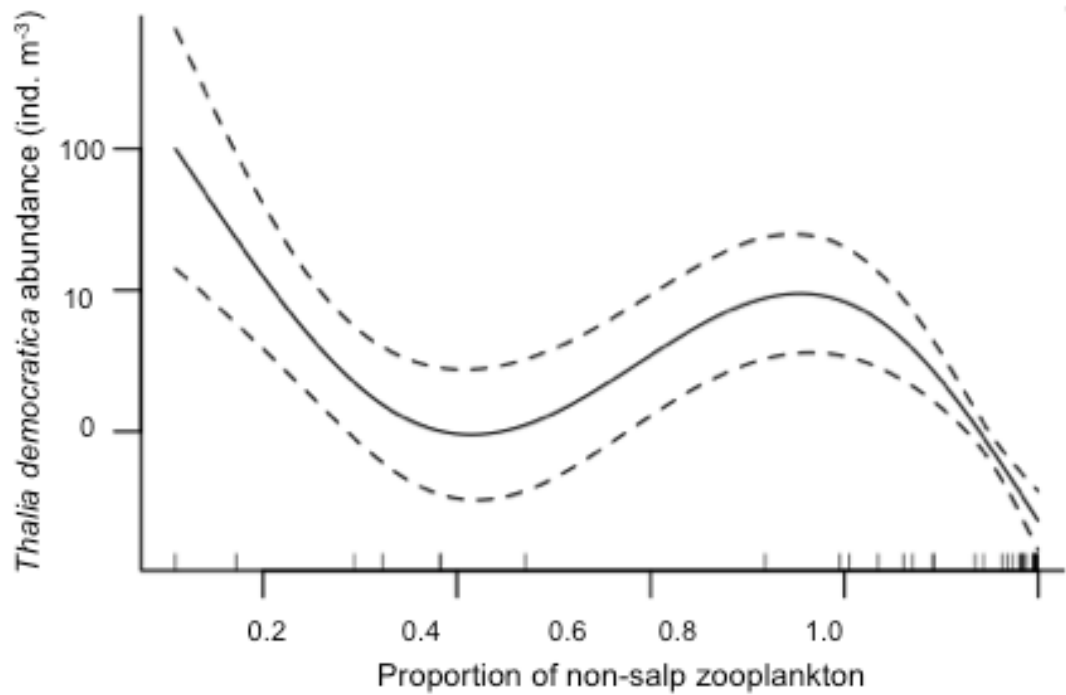


Figure 3.8 Fitted smoother value for proportional non-salp zooplankton abundance as obtained through generalised additive mixed modelling analysis illustrating the non-linear relationship with *Thalia democratica* abundance. Tick marks on the x-axis are observed data points. The y-axis represents fitted values. Dotted lines represent 95% confidence intervals.

3.4 Discussion

Long-term *Thalia democratica* abundances in this study confirms previous work that identifies spring as the most productive season (eg. Tranter, 1962; Licandro et al., 2006). This is most likely a result of high phytoplankton abundances after the spring bloom providing food for a developing salp swarm. However, there was significant variability in *T. democratica* abundances sampled during austral spring (September - November) voyages from 2008 - 2010. A ten-fold difference in salp swarm size across three voyages indicates the highly variable nature of salp swarms, even during optimal conditions. Considering Heron and Benham's (1985) theory of overwintering (Fig. 3.1), variations in swarm magnitude may reflect changes in *T. democratica* condition. Measures of *T. democratica* condition, such as growth and asexual reproduction, would therefore also represent a measure of the nutrition received. This growth-fecundity trade-off is also seen in other organisms, such as nematodes and fruit flies, where dietary restriction results in reduced fecundity (Partridge et al., 2005). However, that the opposite trend is seen in salps, where some form of dietary restriction (varied phytoplankton communities) results in increased asexual reproduction, most likely as a result of longer development time needed for reproductive effort (Lewontin, 1965).

3.4.1 Long-term monitoring

The context and seasonality for these three voyages is provided by the long-term monthly observations at Port Hacking, showing swarm formation during the spring. Similar trends in *Thalia democratica* abundance were observed between the long-term monitoring at Port Hacking and in the three spring voyages. Direct comparisons between sampling months show that *T. democratica* abundances sampled at Port Hacking and during the voyages were of similar magnitude (Fig. 3.6a), however

statistical comparisons could not be undertaken due to only one haul being performed at Port Hacking. *T. democratica* swarm abundance from the 2008 voyage was greater than the long-term October average obtained from Port Hacking. This was also the highest recorded abundance of *T. democratica* to date (Andersen, 1998; Henschke et al., 2011). Higher than average abundances of *T. democratica* during spring blooms have previously been recorded near Port Hacking in 1940 - 41 (Thompson and Kesteven, 1942) and 1960 (Tranter, 1962). Further sampling will be needed to indicate whether these high magnitude swarms are a reoccurring trend. Despite large variability in *T. democratica* abundance across the long-term survey, similar relative abundances to the spring voyages suggests that salp swarms at the Port Hacking station may be broadly representative of conditions for the surrounding shelf. This is consistent with oceanographic modelling observations (Oke and Sakov, 2012). Due to the patchy nature of salps, more extensive comparisons between the Port Hacking and other Australian National Reference Stations could be made using the recently commissioned Continuous Plankton Recorder program, and with zooplankton sampled in surrounding shelf areas.

3.4.2 Experimental growth comparison

Experimental growth rates of *Thalia democratica* measured in this study (1.83 - 2.32% length h^{-1} ; Table 3.2) fall within the range of previously observed growth rates; from 0.3% length h^{-1} (Deibel, 1982) to 28% length h^{-1} (Le Borgne and Moll, 1986). It should be noted however that laboratory experiments (Heron 1972; Deibel 1982) resulted in the slowest growth rates of only 0.3 - 3% length h^{-1} , whereas cohort tracking in the field and Heron and Benham's (1985) growth index resulted in the highest growth rates (Heron, 1972; Le Borgne and Moll, 1986; Tsuda and Nemoto, 1992). Growth rates from 0.3 -

0.9% length h^{-1} were obtained in laboratory experiments under low food concentrations (0.1 - 0.6 μg chlorophyll $a L^{-1}$; Deibel, 1982). Growth rates in this study were faster than those obtained by Deibel (1982), despite experiments being performed at similar temperatures (20°C). This variation was likely due to the experiments in this study being performed at higher food concentrations ($\sim 1.1 \mu g$ chlorophyll $a L^{-1}$) that are more likely to happen during swarm formation. Similarly, Heron (1972) found growth rates of small individuals could vary from 1% length h^{-1} when less food is available, to as high as 21% length h^{-1} when food conditions are “optimal”. Such fast growth rates in the laboratory, however, only occurred for embryos and “when extraordinary care was taken in collection and handling” (Heron, 1972). The growth rates decreasing rapidly after birth to a maximum of 3% length h^{-1} (Heron, 1972), similar to after birth growth rates found in this study (1.83 - 2.32% length h^{-1}).

Timing of blastozoid chain release was between 0300 to 0800 h and other studies agree with this observation (Miller and Cosson, 1997; Heron and Benham, 1984), suggesting that individuals used in these experiments were not adversely affected by capture. Predictable release times demonstrate that care must be taken when collecting samples for biomass and population demographic estimates during these spawning times, as swarm magnitude will be elevated as a result of mating aggregations at dawn (Heron, 1972). Faster growth rates of *Thalia democratica* ($>8\%$ length h^{-1}) were obtained from cohort tracking in the field (Heron, 1972; Tsuda and Nemoto, 1992). As sampling times were not mentioned in either study, to determine if higher growth rates were a result of natural conditions or swarming aggregations, future cohort studies should take into account time-of-day effects. For the purpose of this study, zooplankton samples for

abundance and biomass estimates during dawn and dusk were not incorporated in the results.

Measured growth rates in this study were less than the relative growth index by approximately an order of magnitude. Other studies that have applied Heron and Benham's (1985) growth index also calculated high growth rates similar to the range presented in this study, from 25 - 28% length h^{-1} (Le Borgne and Moll, 1986). As the relative growth index is based on growth rates obtained through cohort tracking (Heron and Benham, 1985), values are expected to be higher than growth rates obtained through laboratory experiments. Despite the growth rate experiments being performed on small individuals (~1.5 mm) who have been known to grow the fastest (Heron, 1972), experimental values were not comparable to the growth index. No laboratory study has been able to replicate high growth rates observed by cohort tracking or Heron's (1972) "optimal" experimental techniques. The experimental results presented here offer a good indication of growth rate, and suggest care must be taken when considering high growth rates obtained by cohort tracking or the relative growth index. Similar slopes for the growth index and the experimental growth rates with asexual reproduction suggest that the relative change in growth rate identified by the growth index may be correct. It is recommended that in future studies the relative growth index should be presented as a unitless measurement, as it combines important demographic qualities known to influence swarm magnitude (asexual reproduction and offspring to parent ratio).

3.4.3 *Thalia democratica* demography

Life history characteristics of the *Thalia democratica* swarms differed among the three voyages, in relation to declining swarm magnitudes. There was a significant increase in asexual reproduction (BPC) from 2008 to 2010 (Fig. 3.6b), and the proportion of blastozooids reaching maturity decreased. *T. democratica* swarms in 2008 had the highest abundance and fastest relative growth. Low asexual reproduction (BPC) indicates that in 2008 conditions were more suitable for the formation of large swarms, while declining abundance and relative growth in 2009 and 2010 indicates extrinsic conditions were less suitable than in 2008. A similar trend was seen in Heron and Benham's (1985) samples across spring, summer and winter where highest abundances and lowest buds per chain occurred in spring. Therefore, Heron and Benham's (1985) overwintering theory could also be an explanation for interannual variation in swarm magnitude.

3.4.4 Oceanographic influence on salp swarm magnitude

Temperature and salinity conditions in inner shelf water across the three sampling years all fell within tolerable ranges for *Thalia democratica* (11.5 – 25.6°C; Thompson, 1948). The largest environmental differences among years were evident in phytoplankton communities prior to and at the time of sampling. The influence of the EAC prior to sampling in the region in 2009 can be seen through the dominance of smaller prokaryotes in the phytoplankton that are typical of EAC water (Goericke and Repeta, 1992) compared to the larger prymnesiophytes that dominated in 2008 (Fig. 3.5a). Despite being non-selective filter feeders, *T. democratica* has different retention efficiency for different particle sizes, with greater than 80% efficiency on large particles such as prymnesiophytes and diatoms, and only 40 - 50% on particles <2 μm (Vargas

and Madin, 2004) such as the prokaryotes dominant in the EAC. Correspondingly, the generalised additive modelling revealed that *T. democratica* abundance was positively related to preferred food ($>2 \mu\text{m}$; Table 3.3). Although food abundance (as estimated by chlorophyll *a* concentration) was similar in 2008 and 2009, a dominance of smaller phytoplankton in 2009 ($<2 \mu\text{m}$) may have limited the ability of *T. democratica* populations to grow as fast or large as they did in 2008. Laboratory studies monitoring the effects of changing phytoplankton type on *T. democratica* growth and asexual reproduction are necessary to further elucidate this theory.

In 2010, phytoplankton communities were dominated by preferred food sizes (prymnesiophytes and diatoms), however, slower relative growth for the *Thalia democratica* swarm was observed. Corresponding to an observed ten-fold increase in total zooplankton biomass excluding salps in 2010, additive modelling identified a negative relationship between *T. democratica* and non-salp zooplankton abundance (Fig. 3.8). A much lower percentage of *T. democratica* young reaching maturity in 2010 (Table 3.1) suggests that additional non-salp zooplankton abundance may have increased predation on younger individuals as well as competition for food. Smaller stages of *T. democratica* are generally more nutritious, similar to crustaceans (Heron et al., 1988), and have been shown to be prey items for carnivorous copepods and fish (Pakhomov et al., 2002).

Another scenario to consider is the timing of the *Thalia democratica* swarm development. In 2008, the *T. democratica* swarm may have begun forming soon after the phytoplankton bloom, resulting in an earlier dominance over the food abundance. A later development in 2010 may have resulted in a large pre-existing competitive and

predatory zooplankton environment for the *T. democratica* swarm to develop in. Time-series studies considering the time-lag between phytoplankton blooms, zooplankton abundances and *T. democratica* swarm development, will help to identify how important time of development is to the eventual swarm magnitude.

3.4.5 Concluding remarks

This study identifies that salp life history characteristics such as asexual reproduction and growth rate were associated with interannual variations in abundance, and thus may be major factors determining swarm magnitude. The negative relationship between asexual reproduction and abundance is consistent with Heron and Benham's (1985) overwintering theory. This relationship appears to be mainly influenced by nutritional availability, in particular phytoplankton type. Interannual variation in life history characteristics identified in this study confirms previous work that suggests *Thalia democratica* and other gelatinous species are effective indicators of changing oceanographic conditions (e.g., Thompson and Kesteven, 1942; Hay, 2006). Detailed laboratory studies could test the hypothesis that the prey field determines salp condition in order to determine causality for variation in salp swarm magnitudes. As *T. democratica* swarms are prevalent within other western boundary currents in the world (Deibel and Paffenhofer, 2009), these results are globally relevant. The ability to predict patches and magnitude of salp swarms will be important for management of the marine environment as a whole, but particularly for improving the understanding of the biogeochemical cycle due to the influential role of the mass depositions of carbon-rich faecal pellets and carcasses (Chapter 5) produced in salp swarms.

Chapter 4

Population drivers of a *Thalia democratica* swarm: Insights from population modelling

Abstract

Gelatinous zooplankton such as the small salp, *Thalia democratica*, regularly form dense swarms around the world, however, little is known about the physiological and oceanographic drivers that influence the magnitude and occurrence of these swarms. A discrete-time, size-structured, *T. democratica* population model was developed to determine whether food and temperature were sufficient to explain the observed dynamics of salps. The model tracks cohorts of four life stages and incorporates size-dependent reproduction and mortality. Growth is a function of temperature and food quantity (chlorophyll *a* biomass). The model is consistent with general traits of salp population dynamics and average generation time and mean abundances of each stage correspond well to previously reported values. Temperature, ingestion rate and doubling time of phytoplankton were the most important parameters influencing salp biomass. A 10-year time-series simulation identified that salp abundances are proportionally higher in winter and spring (up to 90%), consistent with previous studies showing that salp swarms occur more often in spring and after intrusions of phytoplankton rich water. Temperature and chlorophyll *a* are sufficient to explain observed traits of salp populations and to replicate large-scale patterns (seasonal and latitudinal effects). This model could reveal areas more likely to promote salp swarms based on satellite oceanographic data and improve the understanding of the impact of salp swarms in a changing marine environment.

4.1 Introduction

Salps are pelagic tunicates that potentially have a major role in marine ecosystems. They often form large swarms after the upwelling of cool, nutrient rich water promoting blooms of phytoplankton (Henschke et al., 2011). Salps can feed more efficiently on phytoplankton than other zooplankton (Harbison and Gilmer, 1976; Blackburn, 1979), consuming particles from $<1 \mu\text{m}$ to 1 mm in size (Vargas and Madin, 2004; Sutherland et al., 2010). They then rapidly transfer this energy out of the euphotic zone through fast-sinking carbon-rich faecal pellets (Bruland and Silver, 1981) and carcasses (Chapter 5; Lebrato et al., 2013; Smith Jr et al., 2014). When salps occur in large swarms (up to 5003 ind. m^{-3} ; Everett et al., 2011), the carbon flux from salp faecal pellets can be 10-fold greater than the average daily flux (Fischer et al., 1988). This shows the large input salp swarms can make to the biogeochemical cycle (Chapter 5).

Despite the ecological importance of salps, there is a lack of data on basic ecological traits such as growth and mortality rates – primarily due to the difficulty in culturing salps in the laboratory (Heron, 1972; Harbison et al., 1986; Raskoff et al., 2003). There is also little information on the temporal evolution of salp swarms or how demographic characteristics or population growth rates change with time and oceanographic conditions. Experimental studies have shown that both temperature and chlorophyll *a* concentration drive variation in growth rates (Chapter 3; Heron, 1972; Deibel, 1982), however the shape of these relationships and the conditions which provide “optimal” growth rates are unknown. There is strong seasonality to the occurrence of salp swarms by some species (Chapter 3; Licandro et al., 2006), which suggests that the optimal temperature and chlorophyll *a* conditions driving growth rates would occur during spring when salp abundance is highest (Chapter 3; Heron, 1972; Licandro et al., 2006).

Salp populations are characterised by alternating generations of sexually reproducing blastozoid and asexually reproducing oozoid life history stages (Heron, 1972). Population-level traits such as generation time, the blastozoid-to-oozoid ratio and the proportion of mature stages are important drivers of salp abundance (Chapter 3). The blastozoid-to-oozoid ratio has been used in several studies as a tool to determine what stage of swarm formation the salp population is in (Menard et al., 1994; Loeb and Santora, 2012). Generation time is calculated as the time taken from birth of a female blastozoid to birth of the next generation of female blastozoids, and is positively correlated with individual growth rates (Heron, 1972). Observational sampling of these life-history characteristics often only provides a snapshot of swarm demographics. By exploring the temporal resolution of a salp swarm using a numerical model, one can identify how these traits may vary during the creation of a swarm under different environmental conditions. For example, the blastozoid-to-oozoid ratio or generation time of a seed population may determine the success of future swarm development.

There are no continuous long-term zooplankton time-series along the south-east Australian coast (Hobday et al., 2006; Poloczanska et al., 2007), unlike other oceanic regions, such as off California where the California Cooperative Oceanic Fisheries Investigations (CalCOFI) has sampled zooplankton, including salps, since 1949 (Lavaniegos and Ohman, 2003). The most recent spatially comprehensive salp survey for the Tasman Sea was done 50 years ago (Tranter, 1962), with smaller scale sampling occurring from 2002 (Chapter 3; Henschke et al., 2011). At this stage, it is difficult to understand the dynamics of salp populations, or model their distributions, using observational data. One way to enhance and validate the understanding of salp population dynamics is through numerical modelling.

In this study two numerical models were used to explore the population dynamics of the ubiquitous small salp, *Thalia democratica*. *T. democratica* is the most abundant salp in the Tasman Sea (Thompson and Kesteven, 1942; Henschke et al., 2011), and has a life cycle that involves sexual and asexual generations (Heron, 1972). A Lefkovitch (1965) matrix model was used to identify the life history stage which has the greatest impact on increasing *T. democratica* population size. A discrete-time, size-structured population model was then developed to predict *T. democratica* abundance in response to environmental conditions. This included simulations using actual temperature and chlorophyll *a* data from three sites on the south-east Australian coast, to examine whether the model predicts likely responses. In particular, the aims of this study were: i) to identify the life history stage that is most influential to salp abundance; ii) to develop a numerical salp population model to better understand the dynamics of salp populations; and iii) to identify which parameters most strongly influence population abundance, generation time and blastozooid-to-oozoid ratio.

4.2 Methods

4.2.1 General approach

Two models were used to examine the temporal dynamics within a *Thalia democratica* population. The first was a Lefkovich (1965) stage-class matrix model, which was used to identify which life stage of *T. democratica* has the greatest influence on population growth. The second model was a discrete-time size-structured population model, incorporating both temperature and chlorophyll *a* dependent growth. Temperature and chlorophyll *a* concentration (phytoplankton abundance) were used as the external drivers in this model, given their known association with salp abundance (Heron, 1972; Licandro et al., 2006; Deibel and Paffenhofer, 2009; Henschke et al., 2011). In both models, *T. democratica* has four life history stages (Fig. 4.1; Table 4.1): 1) Females, which is the blastozoid life stage from birth (female buds) until release of a juvenile oozoid; 2) Males, which is the life stage formed from females that have released a juvenile oozoid; 3) Juvenile oozoids, which is the life stage of an oozoid until the release of female buds (at around 10mm length); and 4) Post-release oozoids, which is the life stage of oozoids after the release of the first chain of female buds.

Table 4.1 Life-history stages of *Thalia democratica* included in the models and shown in Fig. 4.1.

Generation	Life-history stage	Size (mm)	Notes
Blastozoid	Female	>1	Released from juvenile oozoids. Will develop one juvenile oozoid embryo per female. Size at which females give birth begins at 4 mm, with the majority giving birth at 8 mm.
Blastozoid	Male	>4	Formed from females that have given birth to a juvenile oozoid. Males fertilise females upon release from a juvenile oozoid.
Oozoid	Juvenile oozoid	3 - 10	Juvenile oozoids produce the next female generation, with a mean asexual fecundity (R_s) of 81.78. Females are released at 10 mm.
Oozoid	Post-release oozoid	>10	Post-release oozoids develop from juvenile oozoids after they have released females.

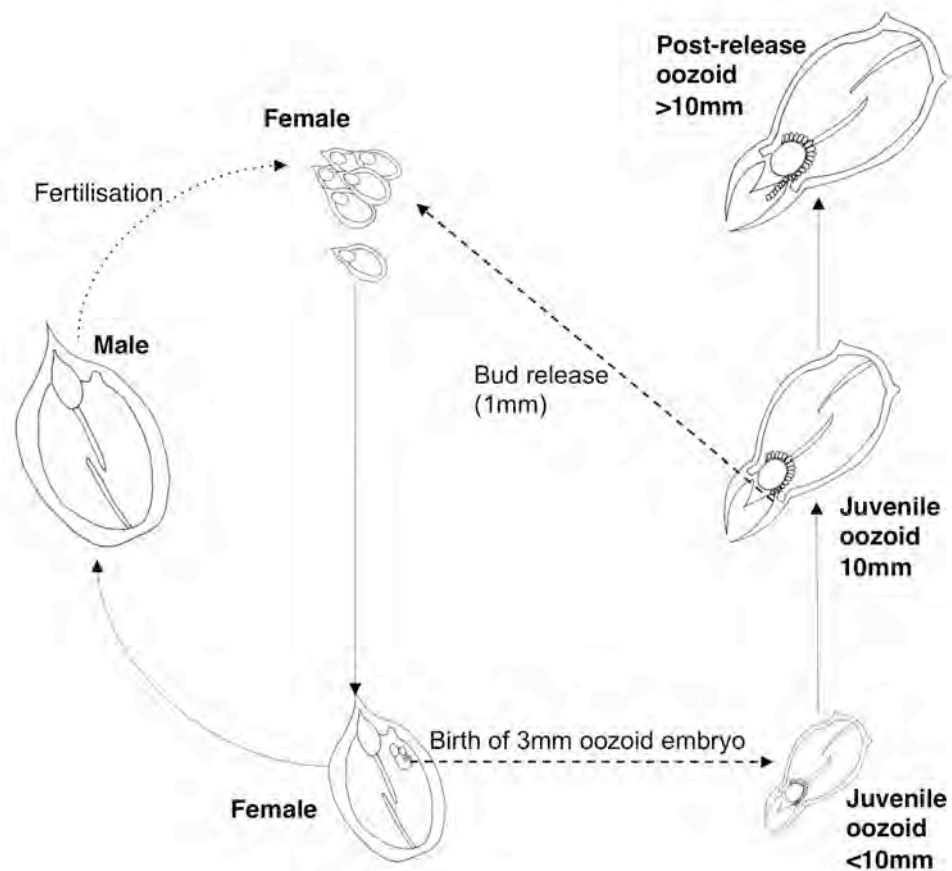


Figure 4.1 Life cycle of *Thalia democratica* showing four life history stages used in the models: females, males, juvenile oozoids and post-release oozoids. For life-history roles see Table 4.1. Modified from Fig. 1 in Henschke et al. (2011).

4.2.2 Lefkovitch matrix model

The Lefkovitch matrix (Lefkovitch, 1965) is a stage-structured model of population growth, and is used to forecast future population states. It assumes that the population will either grow or decline monotonically, and that each stage class will grow at the same rate. In a constant environment, the proportion of individuals in each stage class of a population tends toward a steady-state (stable-age) distribution (Lotka, 1925). As a result, the Lefkovitch matrix can be used to identify critical life history transitions. The Lefkovitch matrix for *Thalia democratica* takes the form of a population projection matrix (Table 4.2):

$$\begin{bmatrix} P_1 & 0 & 0 & F_4 \\ G_1 & P_2 & 0 & 0 \\ F_1 & 0 & P_3 & 0 \\ 0 & 0 & G_3 & P_4 \end{bmatrix} \begin{bmatrix} \text{Females} \\ \text{Males} \\ \text{Juvenile oozoids} \\ \text{Post - release oozoids} \end{bmatrix}$$

where F_i is the stage-specific fecundity (total lifetime reproductive output), P_i is the probability of surviving and remaining in the same stage and G_i is the probability of surviving and growing to the next i th stage (also known as the transition probability). Fecundity, survival and growth estimates are based on published data presented in the size-structured population model below.

Table 4.2 Stage-class population matrix for *Thalia democratica* based on fecundity, growth and survival. Values were based on published data presented in the size-structured population model below.

0.7939	0	0	4.233
0.1994	0.5500	0	0
0.2034	0	0.8162	0
0	0	0.1791	0.7458

4.2.3 Size-structured population model

The size-structured population model is a discrete-time model, following cohorts of each life history stage, at an hourly time step. It is size-structured because it uses size-dependent reproduction and mortality, where length (i.e. growth) is dependent on food consumption (chlorophyll *a* concentration) and temperature (Fig. 4.2).

Salp abundance

The abundance of salps at time t is given by:

$$N_t = \sum (Nf_{t,n} + Nm_{t,n} + Nj_{t,n} + Np_{t,n}) \quad (1)$$

where N_t is the total salp abundance (individuals m^{-3}), $Nf_{t,n}$ is the abundance of females, $Nm_{t,n}$ is the abundance of males, $Nj_{t,n}$ is the abundance of juvenile oozoids and $Np_{t,n}$ is the abundance of post-release oozoids from the n th generation at time t .

The abundance of females is calculated:

$$Nf_{t+1,n} = Nf_{t,n} \times e^{-Mf_t} - (Nf_{t,n} \times Rf_t) + (Rs_t \times Nj10_{t,n-1}) \quad (2)$$

where Mf_t is the instantaneous female mortality rate (h^{-1}), Rf_t is the actual female reproduction rate (oozoids female $^{-1} h^{-1}$), Rs_t is the oozoid reproduction rate (female buds oozoid $^{-1} h^{-1}$) and $Nj10_{t,n-1}$ is the abundance of juvenile oozoids (individuals m^{-3}) that are 10 mm long from the $n-1$ generation at time t . The term $Nf_{t,n} \times Rf_t$ represents the females that have recently reproduced and transitioned into males, and the term $Rs_t \times Nj10_{t,n-1}$ represents the number of female buds that were recently released from a juvenile oozoid.

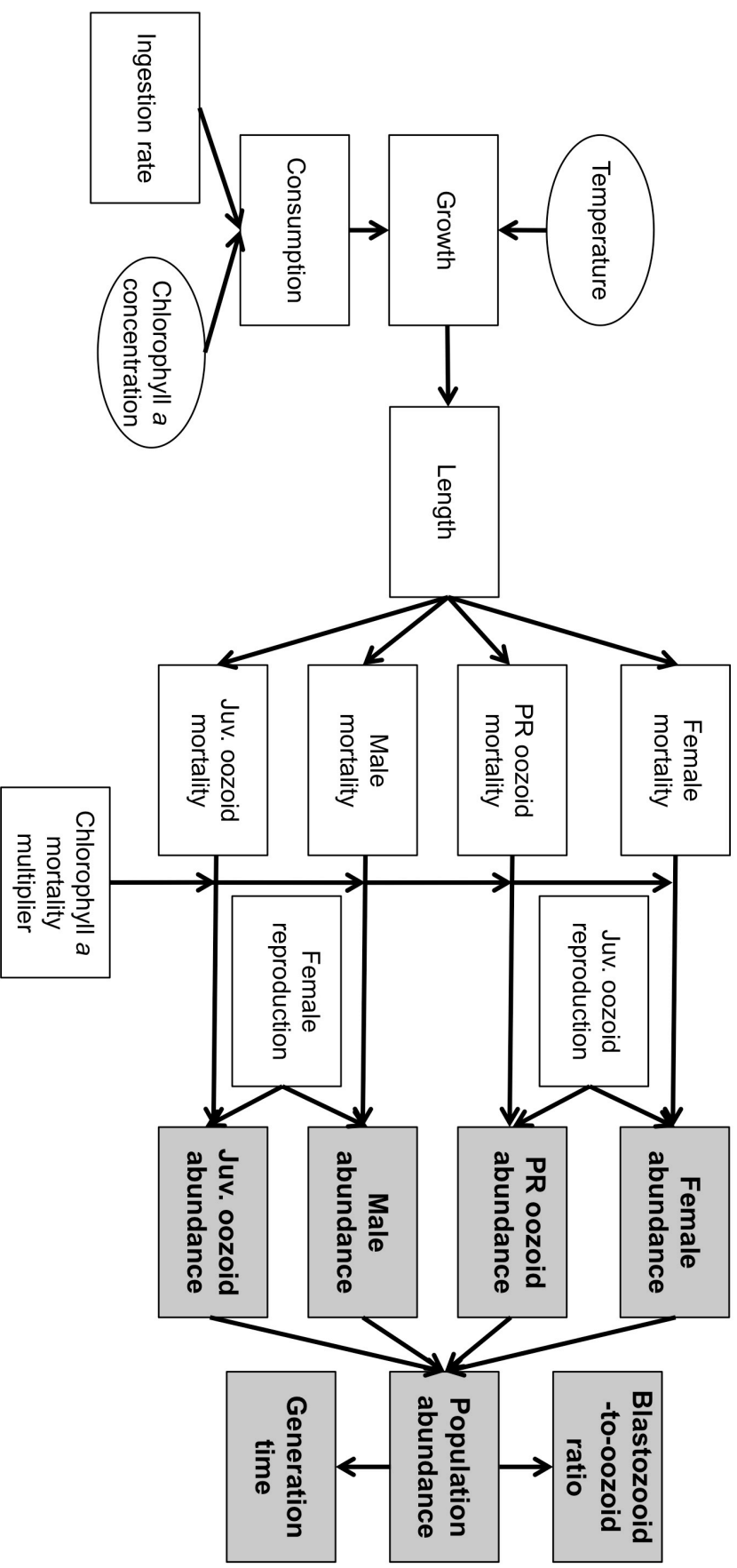


Figure 4.2 Model schematic showing interactions between the environmental variables (ovals), input variables (white boxes) and the model outputs (grey boxes). Model equations are represented graphically in Figure 4.3. Juv – juvenile, PR – post-release.

The abundance of males is calculated:

$$Nm_{t+1,n} = (Nm_{t,n} \times Mm) + (Nf_{t,n} \times Rf_t) \quad (3)$$

where Mm is the male mortality rate (h^{-1}).

The abundance of juvenile oozoids is calculated:

$$Nj_{t+1,n} = Nj_{t,n} \times e^{-Mj_t} + (Nf_{t,n} \times Rf_t) - Nj10_{t,n} \quad (4)$$

where Mj_t is the juvenile oozoid mortality rate (h^{-1}). $Nf_{t,n} \times Rf_t$ also refers to the abundance of juvenile oozoids released at time t as each female can only produce one offspring.

When juvenile oozoid length is greater than 10 mm (at $Nj10_{t,n}$; Heron, 1972), juvenile oozoids give birth to females and transition into post-release oozoids. Therefore within the same generation, the abundance of post-release oozoids is calculated:

$$Np_{t+1,n} = Np_{t,n} \times Mp_t + Nj10_{t,n} \quad (5)$$

where Mp_t is the post-release oozoid mortality rate (h^{-1}). The division between the two oozoid stages was done as a mathematical convenience, to ensure only one release of female buds per oozoid. Although an oozoid will have an average release of 2.5 chains in their lifetime (Deibel and Lowen, 2012), we have used a single release method to easily track cohorts in the model. As chain release generally occurs over a very short period of time (3-4 hrs) (Heron, 1972), it is unlikely that staggering chain release would alter the model results significantly. However, to incorporate lifetime fecundity, fecundity estimations used in the model was based on an average of 2.5 chain releases per individual.

Mortality rate

The length based instantaneous total mortality rate for females and juvenile oozoids are negative power curves (Fig. 4.3a). They are dependent on chlorophyll *a* concentration and are based on laboratory experiments performed by Deibel (1982):

$$Mf_t = a(Lf_t)^{-b} \times CM_t \quad (6)$$

where Mf_t is female mortality rate (h^{-1}), Lf_t is female length (mm) and CM_t is the chlorophyll *a* concentration mortality multiplier at time *t* (see equations 8 - 10); *a* and *b* are constants (Table 4.3). The same equation is used for juvenile oozoid mortality rate (Mj_t), where juvenile oozoid length (Lj_t) replaces female length (Lf_t) and the constants *c* and *d* replace *a* and *b*.

As males are known to die immediately after fertilization, irrespective of length (Miller and Cosson, 1997), their mortality rate includes a constant:

$$Mm_t = (1 - mm) \times CM_t \quad (7)$$

where Mm_t is male mortality rate (h^{-1}) at time *t* and mm (h^{-1}) is a constant. This constant (mm) was calculated assuming they have the same mortality rate as young females (Andersen and Nival, 1986), and is equal to the average mortality rate for a 1 – 2 mm female individual. Similarly, oozoids post-release are given a mortality rate (Mp_t) irrespective of length where mm is replaced by mp . As oozoids are generally found in much lower abundances than blastozooids (females and males; e.g. Chapter 3), it is assumed that after birth of females, post-release oozoids will have a mortality rate similar to, but not as high as, males.

The chlorophyll *a* concentration mortality multiplier (CM_t) increases salp mortality when biomass of chlorophyll *a* is low (Fig. 4.3b). This multiplier is necessary to

incorporate mortality due to starvation, as without it the only impact of low chlorophyll *a* concentrations on the salp population are reduced growth rates. Coefficients *f* and *g* are parameterized so that when chlorophyll *a* biomass is equal to 0.001 mg m⁻³, mortality is 10 times the normal rate. This was calculated based on Threlkeld (1976) who states that when zooplankton are starved, mortality will equal 100% after 5 days:

$$CM_t = f(Nc_t)^g \quad (8)$$

$$f = \frac{1}{\frac{-1}{K^{\log_{10}(K)+3}}} \quad (9)$$

$$g = \frac{-1}{\log_{10}(K) + 3} \quad (10)$$

where Nc_t is the concentration of chlorophyll *a* at time *t* (mg m⁻³) and *K* is the maximum value expected for chlorophyll *a* ('carrying capacity'; mg m⁻³). *K* was set at the maximum chlorophyll *a* concentration calculated from a 10-year time-series of data from the Sydney coast (2003 – 2012).

Length and growth rate

Female body length is calculated as:

$$Lf_{t+1} = Lf_t + (G_t \times Lf_t) \quad (11)$$

where Lf_t is the length of the female (mm) and G_t is the growth rate (mm mm⁻¹ h⁻¹) at time *t*. The same equation is used to calculate length for each life history stage, with Lf_t replaced by the respective length for each stage.

Growth is proportional to chlorophyll *a* concentration and temperature, and is calculated (Fig. 4.3c):

$$G_t = Gmax_t \times \frac{Nc_t}{C_t} \times Tvar_t \quad (12)$$

where G_t is the actual temperature and chlorophyll a dependent growth rate ($\text{mm mm}^{-1} \text{h}^{-1}$), $Gmax_t$ is the maximum length-dependent growth rate ($\text{mm mm}^{-1} \text{h}^{-1}$), C_t is salp consumption (mg m^{-3}) at time t and $Tvar_t$ is the deviation of the temperature (T_t ; °C) at time t from the optimal temperature (T_{opt} ; °C) at which $Gmax_t$ occurs. Growth (G_t) equals $Gmax_t$ when Nc_t and C_t both equal a specified chlorophyll a concentration Nc_{max} (0.4046 mg m^{-3}). Specifying Nc_{max} is necessary to avoid unrealistic slow growth at average chlorophyll a biomass (using K as the concentration of chlorophyll a at which $Gmax_t$ occurred created very slow growth, even with non-linear relationships between growth and consumption). Consumption for salps is a rate process, and the mass of phytoplankton ingested depends on their density in the water; thus, consumption (and hence growth) is reduced when: 1) $Nc_t < Nc_{max}$ (the concentration is too low to allow the ration required for $Gmax_t$ within the hourly time step); and 2) $C_t > Nc_{max}$ (salp consumption is large and depletes the phytoplankton before the ration required for $Gmax_t$ is achieved). Outside these conditions, Nc_t and C_t are both assumed to equal Nc_{max} for this equation. This means that more chlorophyll than Nc_{max} can be consumed, but G_t will not exceed $Gmax_t$. The value of Nc_{max} was chosen as the average spring chlorophyll a value. There are few data available to validate the structure of this consumption-based growth component, and future models may benefit from investigating the relationship between consumption and growth rate in more detail.

A normal distribution is used to describe the declining growth rate of salps on either side of T_{opt} , and $Tvar_t$ is found using the following normal probability density (Fig. 4.3d):

$$Tvar_t = \frac{f(T_t | T_{opt}, \sigma_T)}{f(T_{opt} | T_{opt}, \sigma_T)} \quad (13)$$

where σ_T is a parameter used to specify the range of temperatures at which *Thalia democratica* occurs (Thompson, 1948). This is the same for each stage.

Maximum length-dependent growth rate is the same for each stage is calculated from Heron (1972) using an exponential equation (Fig. 4.3e):

$$Gmax_t = he^{-jL_t} \quad (14)$$

where L_t is the stage-specific length (mm) at time t ; h and j are constants.

Consumption rate

Total salp population consumption (mg h^{-1}) is equal to the sum of stage specific consumption:

$$Ct = Nc_t \times (If_t \times Nf_t + Im_t \times Nm_t + Ij_t \times Nj_t + Ip_t \times Np_t) \quad (15)$$

where If_t is the female ingestion rate ($\text{mg salp}^{-1} \text{h}^{-1}$), Im_t the male ingestion rate, Ij_t is the juvenile oozoid ingestion rate, and Ip_t is the post-release oozoid ingestion rate at time t .

Thalia democratica ingestion rate assumes all particles filtered are consumed and is calculated from Mullin (1983) (Fig. 4.3f):

$$If_t = o(Lf_t)^p \quad (16)$$

where o and p are constants. The same equation is used for the other stages.

Chlorophyll a concentration

Chlorophyll a concentration (mg m^{-3}) is calculated as:

$$Nc_{t+1} = Nc_t + Gc_t - C_t \quad (17)$$

where Gc_t is the increase in chlorophyll a ($\text{mg m}^{-3} \text{h}^{-1}$) at time t .

Chlorophyll a increase was calculated using the Verhulst–Pearl logistic equation (Fig. 4.3g):

$$Gc_t = \frac{\ln(2)}{DT} \times Nc_t \times \frac{K - Nc_t}{K} \quad (18)$$

where DT is the doubling time of phytoplankton (h^{-1}). The logistic function was considered appropriate as chlorophyll a mass is an appropriate proxy of phytoplankton numeric abundance.

Reproduction

Female reproduction results in only one oozoid offspring per parent (Heron, 1972) and is calculated:

$$Rf_t = Rmax_t \times Rmf_t \quad (19)$$

where Rf_t is the average female reproduction rate (oozoids female⁻¹), $Rmax_t$ is the maximum average female reproduction rate (oozoids female⁻¹), and Rmf_t is the proportional reproduction success related to male density at time t .

As the size range of reproductive females varies (from 4 - 10 mm), a logistic curve was used to represent cumulative size-dependent female reproduction. It assumes that 50% of females will be reproducing at 8mm (Heron, 1972), and as they increase in size the likelihood of reproducing increases to a maximum average of one offspring per female.

Therefore maximum female reproduction is (Fig. 4.3h):

$$Rmax_t = \frac{1}{1 + e^{-(Lf_t - L_{50})}} \quad (20)$$

where the numerator is the maximum reproduction rate per individual female (1 oozoid female⁻¹) and L_{50} (mm) is the length at which 50% of the female population has reproduced.

As male fertilisation is necessary for the production of oozoids, actual reproduction rate will be dependent on the abundance of males. To incorporate male abundance into female reproduction rate the Beverton-Holt stock recruitment curve was used:

$$Rmf_t = \frac{MF_t}{MF_{50} + MF_t} \quad (21)$$

where MF_t is the male-to-female ratio at time t and MF_{50} is the ratio of males-to-females that gives 50% reproduction efficiency.

For oozoid reproduction, it was assumed that all chains of female buds will be released when an individual reached 10 mm (average size for female bud release; Heron, 1972). For each generation, the number of offspring released per oozoid was selected from a normal distribution (Fig. 4.3*i*):

$$Rj_t \sim N(\mu_{Rj}, \sigma_{Rj}) \quad (22)$$

where Rj_t is the oozoid reproduction rate (females oozoid⁻¹) at time t and μ_{Rj} and σ_{Rj} are the mean and standard deviation of the female offspring released per oozoid.

4.2.4 Standard simulation

A standard simulation of the size-structured population model was run to observe basic patterns and cycles within the salp population. The initial abundances of females and males to begin a simulation were derived from literature values (Chapter 3). The initial abundance of juvenile oozoids and post-release oozoids were set at zero in order to only

have one reproductive generation existing at a time. Model spin-up was one year and abundance values at the end of the simulation spin-up were used as initial conditions for the simulation from which output variables were recorded. Chlorophyll *a* carrying capacity and temperature were static and set at optimal conditions (i.e. 1.69 mg m⁻³ and 20.5 °C) to produce maximum salp growth rates. The standard simulation was run for a period of 10 years after the initial spin-up, by which time the model had reached a quasi steady-state. Output variables were averaged across the whole simulation (10 years). These variables were: stage-specific abundances; total salp biomass; generation time; and blastozooid-to-oozoid ratio. Salp biomass (mg C m⁻³) was calculated using a length-weight relationship for *Thalia democratica* individuals (Heron et al., 1988).

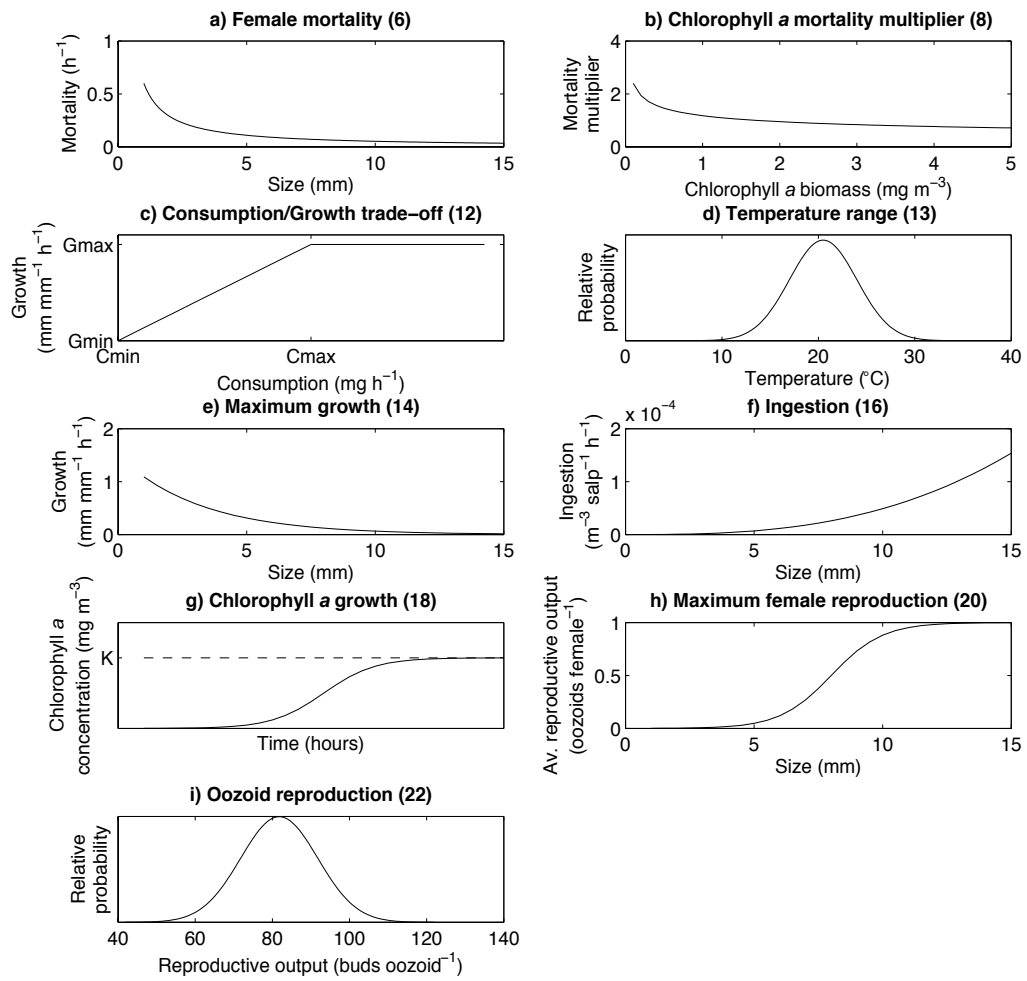


Figure 4.3 Illustrations of the equations used in the salp population model. Numbers in brackets are the equation number.

Table 4.3 Parameter values used in the model simulation. Parameters used in the sensitivity analysis are in bold. Parameter values were estimated from the cited literature or inferred (see methods for details).

Parameter	Equation	Description	Value	Units	Source
<i>a</i>	6	Female mortality coefficient	0.025	h ⁻¹	Inferred from Deibel (1982)
<i>b</i>	6	Female mortality exponent	1.06	-	Inferred from Deibel (1982)
<i>c</i>	6	Juvenile oozoid mortality coefficient	0.038	h ⁻¹	Inferred from Deibel (1982)
<i>d</i>	6	Juvenile oozoid mortality exponent	1.06	-	Inferred from Deibel (1982)
<i>mm</i>	7	Male mortality rate	0.03	h ⁻¹	Andersen and Nival (1986)
<i>mmp</i>	7	Post-release oozoid mortality rate	0.02	h ⁻¹	Best guess
<i>K</i>	9, 10, 23	Chl. <i>a</i> carrying capacity	1.69	mg m ⁻³	Maximum from 10 y Sydney time-series
<i>C_{max}</i>	12	Chl. <i>a</i> concentration for maximum salp growth	0.405	mg m ⁻³	Spring mean from 10 y Sydney time-series
<i>T_r</i>	13	Actual temperature	20.5	°C	Inferred from Thompson (1948)
<i>T_{opt}</i>	13	Optimal temperature	20.5	°C	Inferred from Thompson (1948)
<i>σ_T</i>	13	Temperature standard deviation	3.5	°C	Inferred from Thompson (1948)
<i>h</i>	14	Maximum growth coefficient	1.491	mm mm ⁻¹ h ⁻¹	Heron (1972)
<i>j</i>	14	Maximum growth exponent	0.313	mm ⁻¹	Heron (1972)
<i>o</i>	15	Ingestion rate coefficient	1.742×10 ⁻⁶	m ³ h ⁻¹	Mullin (1983)
<i>p</i>	15	Ingestion rate exponent	2.828	-	Mullin (1983)
<i>DT</i>	19	Chlorophyll <i>a</i> doubling time	0.042	h ⁻¹	Best guess
<i>L₅₀</i>	20	Female length at 50% reproducing	8	mm	Heron (1972)
<i>MF₅₀</i>	21	Male:female ratio for 50% reproduction success	0.025	-	Best guess
<i>μ_R</i>	22	Oozoid reproduction mean	81.78	ind. sol. ⁻¹	Deibel and Lowen (2012)
<i>σ_R</i>	22	Oozoid reproduction standard deviation	10	ind. sol. ⁻¹	Best guess

4.2.5 Sensitivity analysis

A sensitivity analysis was conducted on the model simulation as per Smith et al. (2012). This involved randomly varying a selection of input parameters over many iterations, followed by a model selection to discern which input variables are most influential to certain model outputs. Most parameters were included in the analysis, especially those with input values that were uncertain (e.g. the maximum growth coefficient, h), or if they were likely to vary biologically (e.g. temperature, T). Random sets of parameter values were created at either the assigned value or $\pm 10\%$ of the value. The model output variables that were tracked for the sensitivity analysis were population biomass, stage-specific salp abundance, blastozooid-to-oozoid ratio and generation time. For this analysis, the population model was run at sub-optimal temperatures ($T = 19^\circ\text{C}$) to better identify the sensitivity of model outputs to temperature. Random parameter values were varied across each simulation until the variance for the average model outputs stabilised (500 variations of random parameters). Parameter values were standardised according to Kleijnen (1997); and backwards step-wise regression analysis and Akaike's Information Criteria were used to determine the most influential input variables for each model output.

4.2.6 Time-series simulation

To compare model outputs with observational data, and to evaluate predicted seasonal and yearly variation in salp abundance, simulations were also done using a 10-year time-series (2003 - 2012) of satellite derived sea surface temperature ($^\circ\text{C}$) and surface chlorophyll a (mg m^{-3}). This differs from the standard simulation in that temperature now fluctuates over time (versus static temperature), and chlorophyll a concentration (N_c) is entered directly into equations 8 and 12, rather than calculated (equations 17,

18). Three locations were chosen along the New South Wales coast: Coffs Harbour (30.29°S, 153.16°E), Sydney (34°S, 151.15°E) and Eden (37.08°S, 149.96°E). The Coffs Harbour region is subtropical and dominated by the East Australian Current (EAC; Suthers et al., 2011). Both the Sydney and Eden regions are temperate and south of the EAC separation zone (Suthers et al., 2011). Daily observations of sea surface temperature and chlorophyll *a* data were obtained from the Moderate Resolution Imaging Spectroradiometer Aqua Satellite (MODIS) via the Integrated Marine Observing System (IMOS) Data Portal (<http://imos.aodn.org.au/imos/>) at 1 km resolution. To maximise data availability, 7-day running averages were calculated for both sea surface temperature and chlorophyll *a* concentration before data was interpolated into hourly increments to match the time step of the numerical model.

For each location, the time-series simulation was spun-up for 10 years to allow the model to reach a quasi steady-state before commencing the model simulations. The initial conditions of the spin-up were set from the 10-year average obtained from the standard-simulation. Temperature and phytoplankton biomass was derived from the 10-year MODIS archive (as above). Following the spin-up, the model-state from the final time-step was used to initialize the 10-year model simulation. Model outputs were averaged seasonally, and compared across years with a two-way analysis of variance (ANOVA). Differences in salp abundances across locations were compared using a one-way ANOVA. Tukey's HSD test was used for *a posteriori* pairwise comparisons between factor levels for all ANOVAs. All statistical tests were performed in R v.3.0.3 (R Development Core Team 2014).

4.3 Results

4.3.1 Lefkovitch matrix model

Based on the Lefkovitch matrix (Table 4.2) the *Thalia democratica* population stabilises and grows at a rate (λ) of 1.32 d^{-1} . The elasticity matrix (Fig. 4.4) shows the relative contributions of F_i , P_i and G_i to λ . λ was most sensitive to changes in survivorship (P_i). Juvenile oozoids appear to be the most important generation promoting population growth, with a 1% increase in the probability of juvenile oozoid survival resulting in a 0.29% increase in population growth.

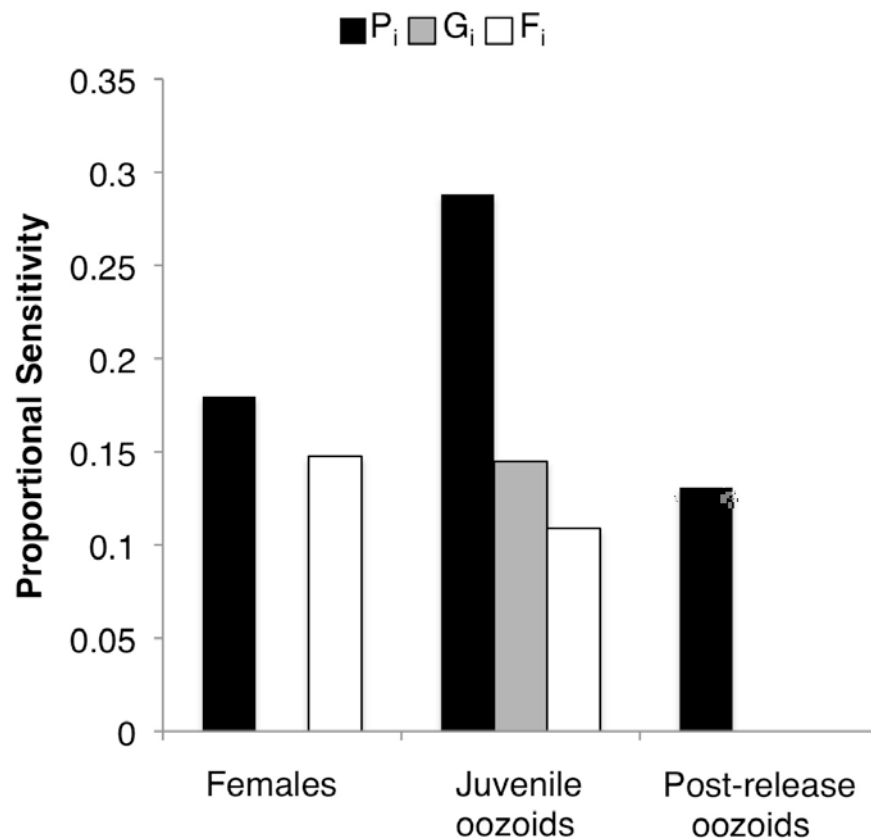


Figure 4.4 The elasticity, or proportional sensitivity of population growth (λ) to changes in survival within the same stage (black bars), survival while transitioning to the next stage (grey bars) or fecundity (white bars). Because the elasticities of these matrix elements sum to 1, they can be compared directly in terms of their contribution to the population growth rate. Males are not included in the graph as λ was not sensitive to variation in male survival.

4.3.2 Standard simulation

During the standard simulation (10 years), 308 generations of *Thalia democratica* females were released, with an average (\pm SD) generation time of 12 ± 5 days. The simulation shows the peaks of both female and oozoid births, with each appearing ~ 4 days apart (Fig. 4.5). Once oozoids are released, they dominate the *T. democratica* population until reproduction of the next generation of females. The average (\pm SD) blastozoid-to-oozoid ratio across the whole simulation is 9 ± 20 and ranged from less than 1 to 110 (at birth of female generation). Average (\pm SD) salp biomass across the whole simulation was $84.01 \pm 133.18 \text{ mg C m}^{-3}$, and the median salp abundance was $491.87 \text{ ind. m}^{-3}$. This biomass was dominated by the female ($1852.9 \pm 4854.4 \text{ ind. m}^{-3}$) and juvenile oozoid ($562.63 \pm 876.54 \text{ ind. m}^{-3}$) stages, with males ($165.99 \pm 386.11 \text{ ind. m}^{-3}$) and post-release oozoids ($21.67 \pm 60.10 \text{ ind. m}^{-3}$) occurring in lower abundances. Generations of large and small salp abundance cycle regularly (Fig. 4.5) due to variation in the abundance of juvenile oozoids available to reproduce. This is related to chlorophyll *a* concentration, as more female births generally occur after higher peaks of chlorophyll *a*, and less female births occur when biomass of chlorophyll *a* is increasing back towards *K*. There is also a varying offset between peaks of chlorophyll *a* concentration and salp abundance. When chlorophyll *a* biomass is high, salp abundance will peak after ~ 8 days, whereas when the biomass is low, the salp abundance will peak after ~ 14 days.

4.3.3 Sensitivity analysis

As the influence of temperature (T) within this model is proportional to ΔT , when ΔT approaches zero (i.e. $T_t = T_{opt}$), the sensitivity of each model output to temperature

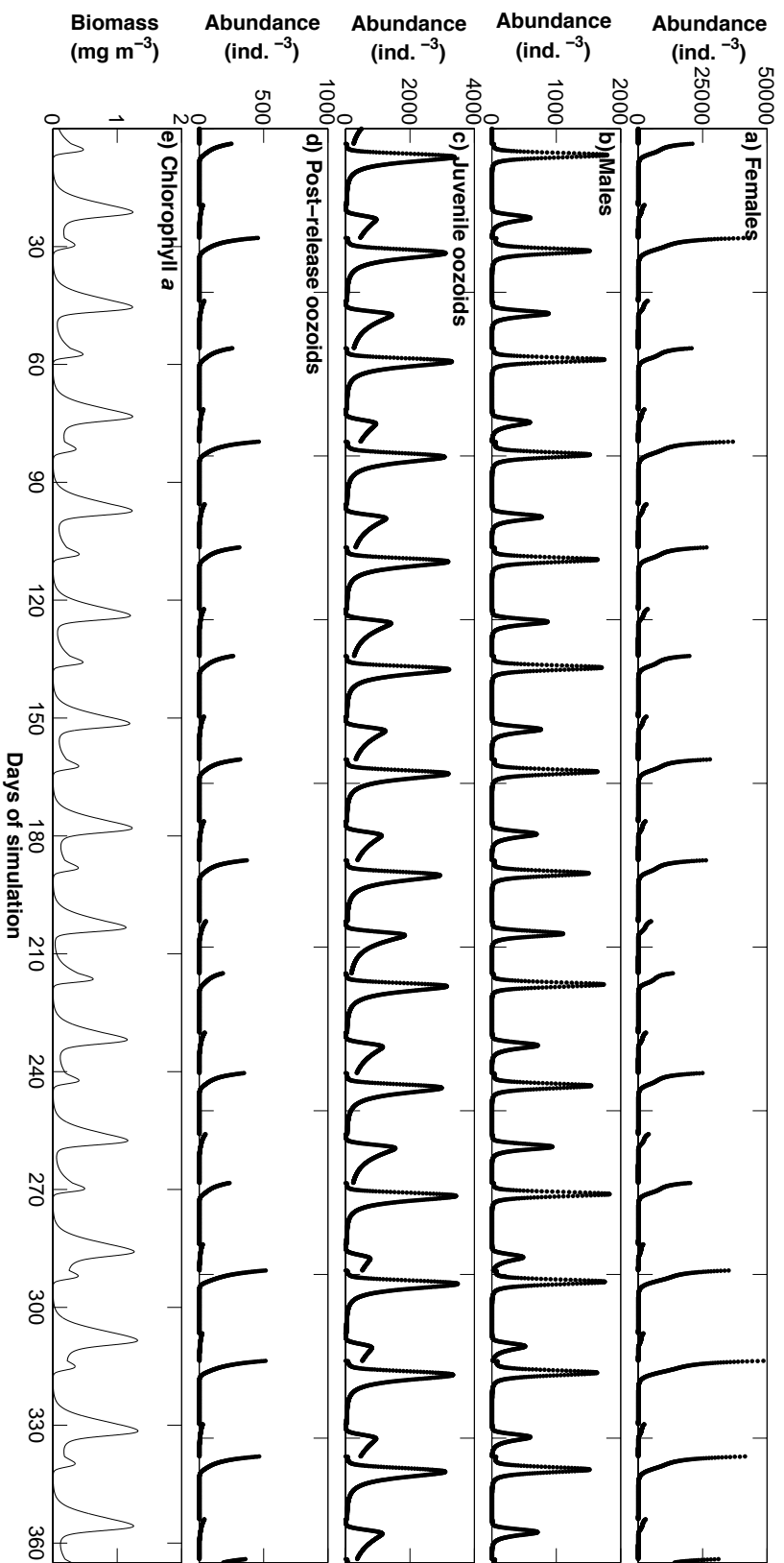


Figure 4.5 Standard model simulation showing one year of simulated *Thalia demouca* abundances for a) females, b) males, c) juvenile oozoids and d) post-release oozoids, as well as e) chlorophyll *a* biomass.

approaches zero. During sub-optimal temperature conditions (i.e. $\Delta T > 0$), the most parsimonious model explaining the variation of generation time contained nine parameters, and explained 82% of the variation ($F = 247.1$, $p < 0.01$; Fig. 4.6a). Temperature (T) and the juvenile oozoid mortality coefficient (c) were the parameters with the largest influence on generation time. The best model for *T. democratica* biomass consisted of 12 parameters (1 non-significant (a); $R^2 = 0.96$, $F = 1052$, $p < 0.01$; Fig. 4.6b). The doubling time of chlorophyll a (DT) and the *T. democratica* ingestion rate coefficient (o) had the largest influence on total salp biomass. The length at which 50% of females were reproducing (L_{50}) had by far the largest influence on the blastozooid-to-oozoid ratio ($R^2 = 0.97$, $F = 1511$, $p < 0.01$; Fig. 4.6c). DT , o , c and L_{50} played the largest influences on female ($R^2 = 0.84$, $F = 258.5$, $p < 0.01$; Fig. 4.6d), male ($R^2 = 0.98$, $F = 1820$, $p < 0.01$; Fig. 4.6e), juvenile oozoid ($R^2 = 0.97$, $F = 1444$, $p < 0.01$; Fig. 4.6f) and post-release oozoid abundances ($R^2 = 0.81$, $F = 192$, $p < 0.01$; Fig. 4.6g), but to different degrees.

4.3.4 Time-series simulation

Strong seasonal trends were observed in sea surface temperature (SST) and chlorophyll a biomass across all locations (Fig. 4.7). SST was significantly higher in Coffs Harbour compared to Sydney and was lowest overall in Eden ($F_{2,108} = 659.17$, $p < 0.01$). Across all locations, SST was higher in summer and autumn ($F_{3,108} = 423.75$, $p < 0.01$; Table 4.4). Warmer SST was associated with lower chlorophyll a biomass, with the highest chlorophyll a biomass occurring in winter and spring ($F_{3,108} = 66.96$, $p < 0.01$; Table 4.4), and the highest overall chlorophyll a biomass in Eden ($F_{2,108} = 65.77$, $p < 0.01$). Seasonal variation in salp abundances were observed in the time-series simulation, but there was no effect of year on total salp abundance across all locations (Fig. 4.8).

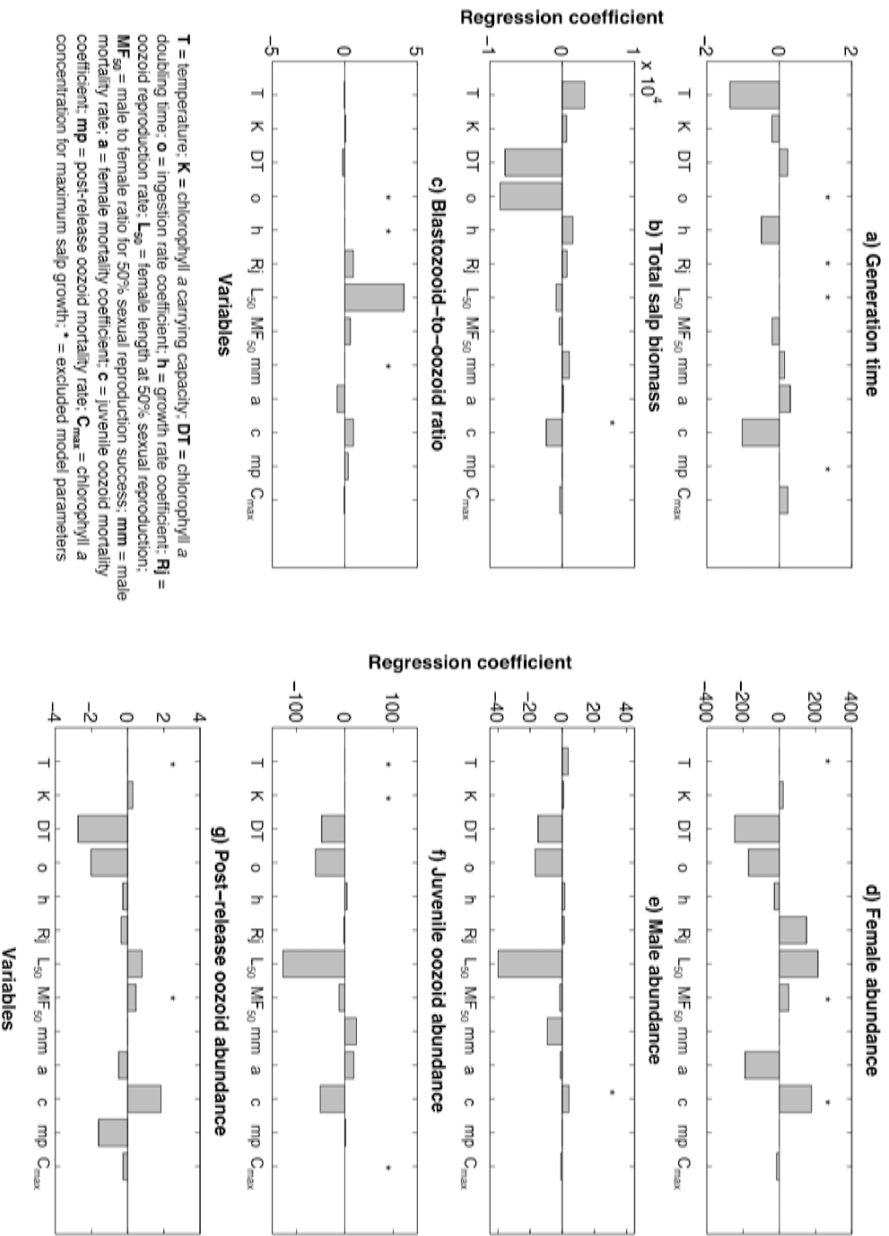


Figure 4.6 Results of sensitivity analysis for a sub-optimal temperature run (19°C). The bars represent the significant coefficients of model parameters signifying their influence on a) generation time, b) total salp biomass, c) blastozoid-to-oozoid ratio, d) female abundance, e) male abundance, f) juvenile oozoid abundance and g) post-release oozoid abundance. Parameter abbreviations are displayed in the plot. * indicates which parameters were excluded from the final analysis.

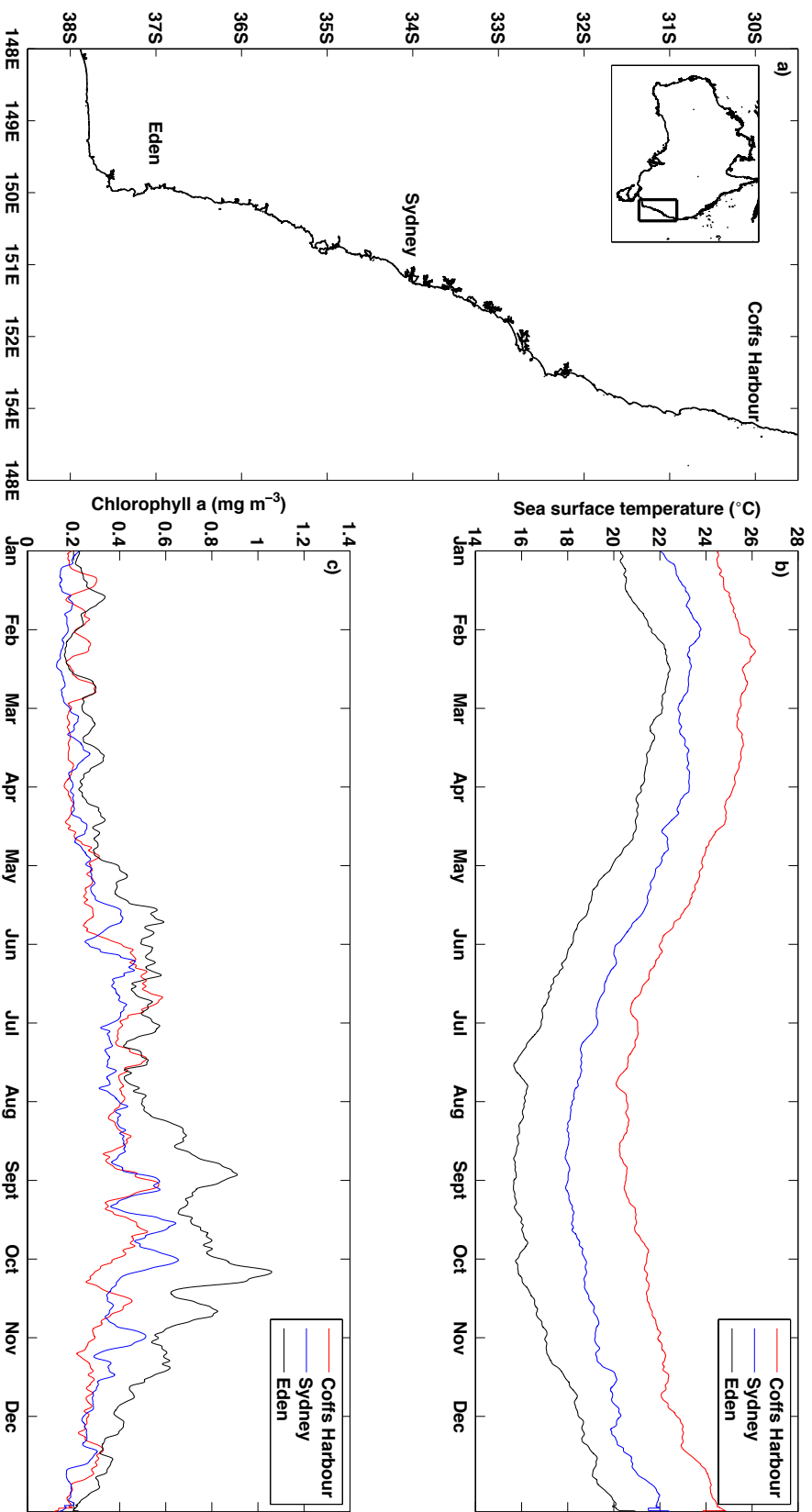


Figure 4.7 a) Location map showing areas along the New South Wales coast that were input in the time-series simulation. The locations are Coffs Harbour (red), Sydney (blue) and Eden (black). Long-term (2003 – 2012) averaged satellite derived sea surface temperature (b) and chlorophyll *a* biomass (c) showed variation across locations, and seasonality in oceanographic conditions.

Table 4.4 Results of the long-term (2003 - 2012) seasonal analysis at Coffs Harbour, Sydney and Eden. Values are means (\pm SD). The result of Tukey's HSD test for abundance and generation time are indicated by letters (^{a,b,c}); seasons within each location not sharing a letter are significantly different ($p < 0.05$).

Location	Season	Temperature (°C)	Chlorophyll <i>a</i> (mg m ⁻³)	<i>T. democratica</i> abundance (1000 ind. m ⁻³)	Generation time (days)
Coffs Harbour	Spring	21.75 \pm 0.49	0.33 \pm 0.09	70.47 \pm 80.67 ^a	19 \pm 3 ^a
	Summer	24.33 \pm 0.50	0.23 \pm 0.03	0.0008 \pm 0.003 ^b	94 \pm 1 ^b
	Autumn	24.33 \pm 0.50	0.23 \pm 0.03	0.0008 \pm 0.003 ^b	94 \pm 1 ^b
	Winter	20.78 \pm 0.37	0.44 \pm 0.09	28.47 \pm 41.36 ^c	13 \pm 4 ^c
Sydney	Spring	19.13 \pm 0.47	0.40 \pm 0.08	86.59 \pm 93.46 ^a	18 \pm 2 ^a
	Summer	22.26 \pm 0.58	0.25 \pm 0.06	10.29 \pm 25.05 ^b	17 \pm 4 ^a
	Autumn	22.26 \pm 0.58	0.25 \pm 0.06	10.29 \pm 25.05 ^b	17 \pm 4 ^a
	Winter	18.70 \pm 0.62	0.40 \pm 0.09	61.84 \pm 77.13 ^a	15 \pm 3 ^a
Eden	Spring	16.89 \pm 0.38	0.65 \pm 0.12	34.36 \pm 46.55 ^a	15 \pm 2 ^a
	Summer	20.41 \pm 0.52	0.35 \pm 0.05	58.72 \pm 66.41 ^a	15 \pm 2 ^a
	Autumn	20.41 \pm 0.52	0.35 \pm 0.05	58.72 \pm 66.41 ^a	15 \pm 2 ^a
	Winter	16.40 \pm 0.69	0.57 \pm 0.07	37.83 \pm 45.36 ^a	21 \pm 2 ^b

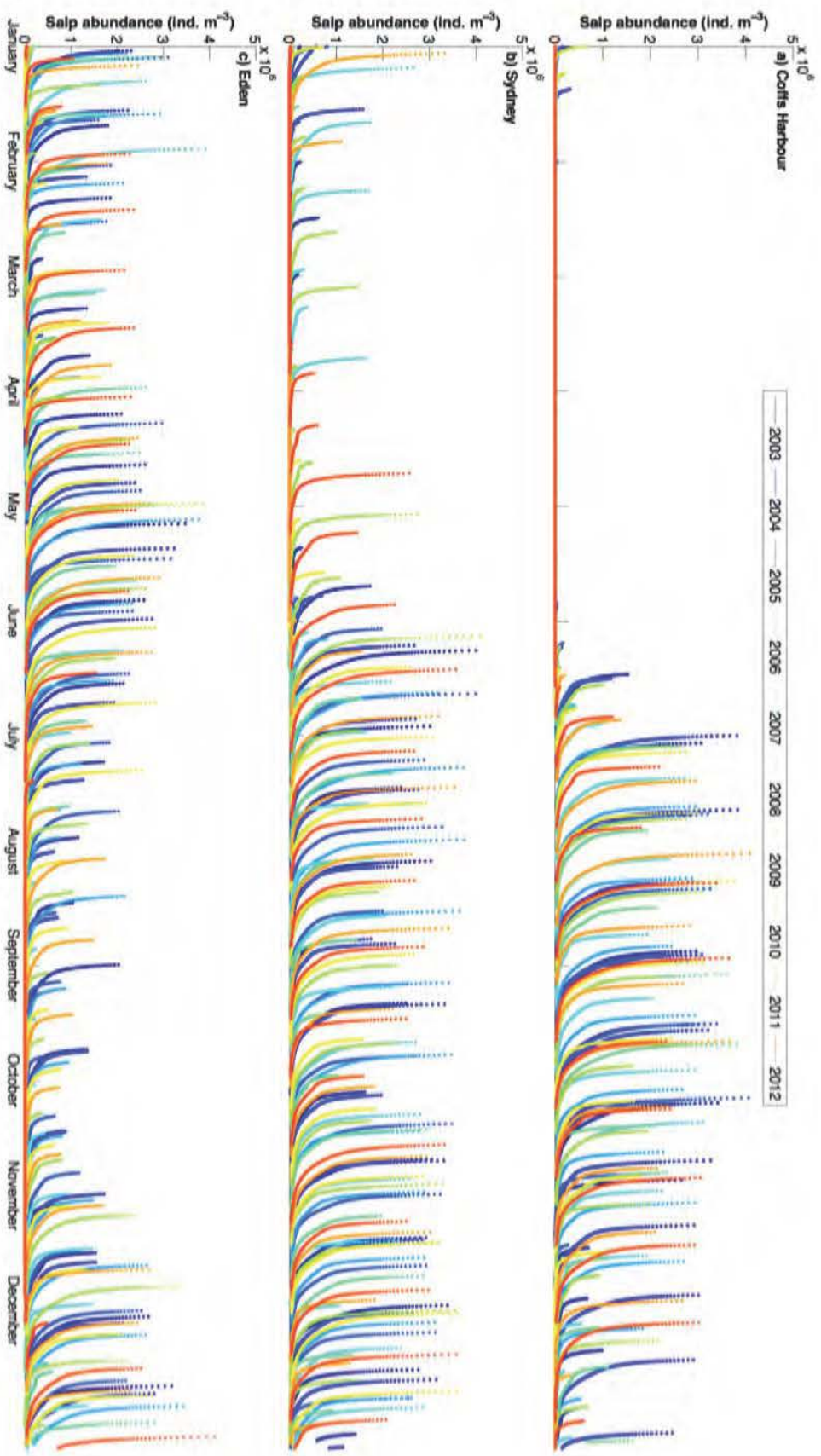


Figure 4.8. Time-series simulation showing *Thalia democraica* population abundance (ind. m⁻³) at Coffs Harbour (a), Sydney (b) and Eden (c). Values are superimposed onto one 12-month axis, with colours representing different years (2003 – 2012).

At Coffs Harbour and Sydney, salp abundances were significantly higher in spring and winter compared to autumn and summer (Coffs: $F_{3,152} = 21.257$, $p < 0.01$; Sydney: $F_{3,152} = 14.354$, $p < 0.01$; Fig. 4.9; Table 4.4). There was no difference in generation time across seasons for the Sydney location. Spring and winter also corresponded to significantly shorter generation times at Coffs Harbour ($F_{3,32} = 3506.47$, $p < 0.01$; Fig. 4.9; Table 4.4). There was no significant difference in salp abundance across seasons at Eden, however, generation times were significantly longer in winter ($F_{3,32} = 26.139$, $p < 0.01$). There was also a significant interaction between year and season for generation time at Eden ($F_{3,32} = 3.88$, $p = 0.02$), which is a result of longer generation times in spring and summer of 2011. Total salp abundance was significantly higher at Sydney and Eden compared to Coffs Harbour ($F_{2,477} = 6.04$, $p = 0.003$), whereas generation times were significantly longer in Coffs Harbour than the other two locations ($F_{2,115} = 36.01$, $p < 0.01$). Generation time (Pearson correlation: $r = -0.6$, $p = 0.04$) and blastozooid-to-oozoid ratio (Pearson correlation: $r = -0.63$, $p = 0.03$) were significantly negatively correlated to total salp abundance.

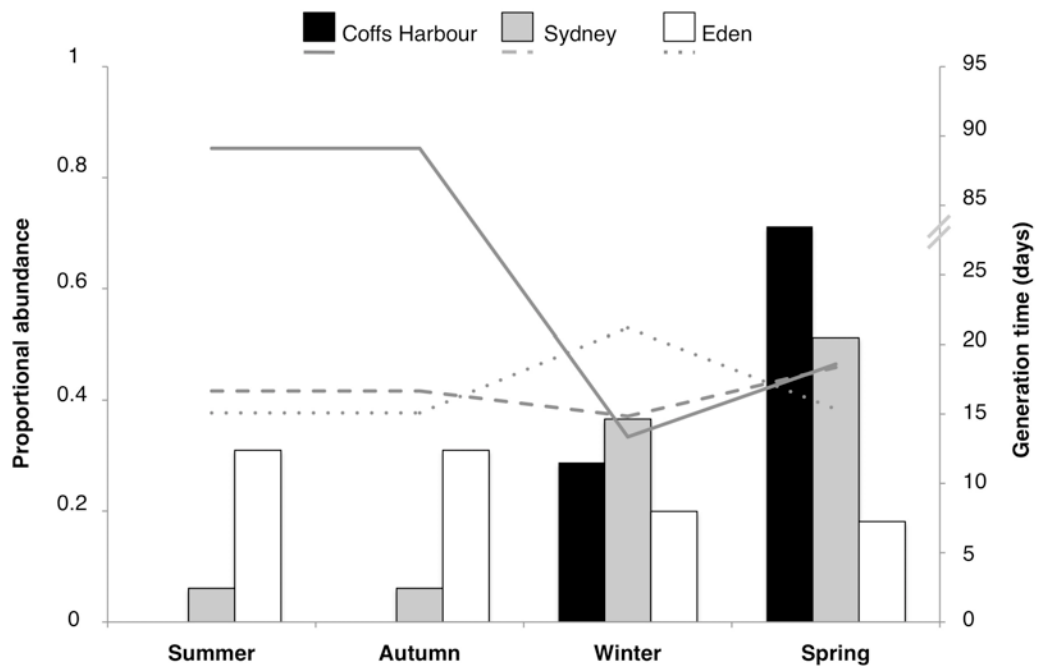


Figure 4.9. Proportional seasonal abundance of *Thalia democratica* (left-hand axis; bars) and mean seasonal generation time (right-hand axis; lines) derived from the time-series simulation for Coffs Harbour (black), Sydney (grey) and Eden (white). Note the right-hand axis is broken at 25 - 85 days.

4.4 Discussion

This size-structured population model in this study is the first *Thalia democratica* population model to incorporate food-based density dependence, and showed that temperature and chlorophyll *a* were appropriate drivers of *T. democratica* population dynamics. Juvenile oozoids were identified as the most influential life history stage to population biomass by both the Lefkovitch matrix and the size-structured population model. Increasing survival of juvenile oozoids resulted in increases in total salp abundance. Higher population abundances were also associated with shorter generation times (faster growth rates). This model further confirms why it is difficult to correlate salp abundance with chlorophyll *a* biomass and indicates that population-level traits such as the proportion of juvenile oozoids need to be considered when predicting the location and biomass of salp swarms.

4.4.1 Comparison of the modelled salp population with field estimates

The standard simulation of the size-structured population model, using an optimal temperature and chlorophyll *a* biomass, performed well in comparison with field observations. For example, the median and mean population abundances of *Thalia democratica* (491 and 2603 ind. m⁻³ respectively) correspond reasonably well to spring abundances found in the Tasman Sea (92 to 2444 ind. m⁻³; Henschke et al., 2011). Proportional abundances of oozoids (20%) were higher than found in the field (6%; Henschke, unpublished data), however the mean blastozooid-to-oozoid ratio (8.9) corresponds well with field data (8.8 to 11.2; Chapter 3). The variation in proportional abundances could be explained by the patchiness of salp swarms, and the undersampling of oozoids in the field due to their low abundances (Hamner et al., 1975).

Average generation times from the standard simulation (12 days) and from Sydney (17 days) and Eden (17 days) were shorter than those found in laboratory experiments (21 days; Braconnot, 1963; Deibel, 1982), and are more similar to those found in field estimates (2 - 14 days; Heron, 1972; Tsuda and Nemoto, 1992). Generation time is negatively correlated with growth rates, and the maximum growth rate used in this model (equation 14) should equate to a generation time of 2 days (Heron, 1972). Recently, Everett et al. (2011) demonstrated that it would be unsustainable for a salp swarm in the Tasman Sea to be growing as fast as suggested by Heron (1972) as they would deplete all nitrogen within the water column in less than a day. The generation times achieved in this model under optimum conditions (~12 days) appears to be a more realistic value, and correspond well to the shortest time that a salp swarm in the field can last (one week; Deibel and Paffenhofer, 2009). This suggests that the parameterisation between maximum growth rate and environmental conditions (temperature and chlorophyll *a* concentration) used in this model is appropriate. This is confirmed through the sensitivity analysis, which identified that generation time was most sensitive to changes in temperature and maximum growth rate.

4.4.2 Pattern of long-term and seasonal salp abundance

There is a lack of spatially inclusive zooplankton studies within the Tasman Sea. The most comprehensive studies sampling salps occurred from 1938 to 1942 (Thompson and Kesteven, 1942) and from 1957 to 1960 (Tranter, 1962). Similar to the time-series simulation output, mean salp abundances along the south-east coast of Australia (south from Sydney) were found to not differ significantly (Tranter, 1962). The time-series simulation also indicated that there were no significant differences in salp abundances

across years, which corresponds with a recent study which found seasonal but no yearly variation in *T. democratica* abundance off the coast of Sydney between 2002 – 2011 (Chapter 3). Interestingly, the timing of swarm formation in the time-series simulation appears to shift each year albeit within the same season, which could be related to small scale oceanographic variability. Mean abundances from the time-series simulation (38000 ind. m⁻³) are higher than maximum observed values of *T. democratica* (2444 ind. m⁻³; Everett et al., 2011), however, the proportional relationship between seasons corresponds well.

The time-series simulation showed strong seasonal variation at Coffs Harbour and Sydney, with *Thalia democratica* abundances significantly higher during winter and spring. There was no statistically significant seasonal variation at Eden, however, proportional *T. democratica* abundances were lower in winter and spring. As winter and spring were associated with lower temperatures and higher chlorophyll *a* biomass (Table 4.4), this suggests that higher salp abundances at Coffs Harbour and Sydney can be related to oceanographic conditions that promote phytoplankton blooms. Seasonal variation in *T. democratica* abundance is well documented off Sydney and Eden, with abundances of *T. democratica* generally being higher in spring off Sydney (Chapter 3; Thompson and Kesteven, 1942; Tranter, 1962; Baird et al., 2011) and higher in late spring and summer off Eden (Thompson and Kesteven, 1942; Tranter, 1962; Baird et al., 2011). Compared to other locations along the south-east Australian coast, Eden has a strong seasonal chlorophyll *a* signal, with higher chlorophyll *a* biomass observed in winter and spring (Everett et al., 2014). Therefore, proportionally lower winter and spring salp abundance at Eden in the time-series simulation is likely a result of sub-optimal temperatures during those seasons (mean = 16.7°C). Despite this, simulated

salp abundances were consistently high throughout the year at Eden, suggesting that environmental conditions are still sufficient to support salp populations. It has been suggested that the cooler waters at Eden would favour salps, compared to warmer waters further north, as it would promote more phytoplankton blooms (Baird et al., 2011). This is supported by the time-series simulation, at least during the first six months of the year.

Proportionally higher abundances and longer generation times in summer and autumn at Coffs Harbour suggests that this location has poor conditions for the formation of salp swarms, probably due to high water temperatures (mean = 24.3°C). Monthly zooplankton sampling at Stradbroke Island (27°S) found salps occurred in low abundances year round (<10 salps m⁻³; IMOS, 2014), and both Coffs Harbour and Stradbroke Island are dominated by the warm, oligotrophic East Australian Current (Malcolm et al., 2011). This could explain why the low abundances of salps at Stradbroke Island correspond well to modelled summer and autumn values for Coffs Harbour. Generation times in the time-series simulation at Coffs Harbour (~90 days) were substantially longer compared to Sydney and Eden (~17 days) and the maximum observed field value for *Thalia democratica* (21 days; Braconnot, 1963). There is no known data on how long a *T. democratica* population can last, however, as gelatinous zooplankton are difficult to culture within a laboratory (Heron, 1972; Harbison et al., 1986; Raskoff et al., 2003), it is possible that generation times in the field could be much longer than 21 days. Zooplankton surveys at Coffs Harbour generally found *T. democratica* in low abundances, however, opportunistic samples found higher abundances after upwelling events (Thompson and Kesteven, 1942; Baird et al., 2011). *T. democratica* are known to “overwinter” when conditions are poor, by slowing their

growth rate and reproductive release (Chapter 3; Heron and Benham, 1985), suggesting that very low abundances of *T. democratica* may occur in the slow growing Coffs Harbour populations until environmental conditions improve.

4.4.3 Population dynamics driving salp biomass

The time-series simulation showed that higher salp abundances were associated with lower blastozooid-to-oozoid ratios and shorter generation times. From the sensitivity analysis, the blastozooid-to-oozoid ratio does not appear to be influenced by environmental variables, but is instead dependent on the length at which 50% of females are reproducing (L_{50}). This was expected as environmental factors are believed to affect both blastozooids and oozoids in the same way (Menard et al., 1994). Prior to this study, there was no evidence to suggest that the blastozooid-to-oozoid ratio was associated with growth rate (Heron and Benham, 1985) or swarm abundance (Chapter 3), as it varies with swarm formation. For example, in the standard simulation, the blastozooid-to-oozoid ratio ranged from 1 to 110 depending on whether a new generation of female buds were released. To examine how the blastozooid-to-oozoid ratio in this model relates to swarm abundances, it is necessary to examine whether changes are driven by blastozooids or oozoids. In this study, higher blastozooid-to-oozoid ratios were driven by increasing proportions of oozoids and when conditions are kept stable (the Lefkovich matrix model), the survival of juvenile oozoids is the most influential life history stage to a salp population. Salp populations with low abundances have been found with a paucity of oozoid stages (Henschke et al., 2011; Loeb and Santora, 2012), confirming that oozoids are necessary to increase population abundances, as their high reproductive rates (up to 240 offspring per individual) allow populations of salps to increase rapidly (Heron, 1972). Therefore, the proportional

abundances of juvenile and post-release oozoids may be a more useful metric than the blastozooid-to-oozoid ratio for determining salp abundance.

4.4.4 Environmental factors driving salp biomass

Total salp biomass and the abundances of each stage are most sensitive to changes in temperature (T), chlorophyll a doubling time (DT) and the ingestion rate coefficient (o). Biomass was positively related to temperature, suggesting that higher abundances of *T. democratica* will occur as temperatures increase towards the optimum as a result of faster growth (due to the proportional relationship between temperature and growth) and thus lower length-dependent mortality. This relationship would reverse as temperatures increase above the optimum. The sensitivity analysis also showed that increases in phytoplankton growth rate (i.e. decreased chlorophyll a DT) and decreases in ingestion rate would result in increased *T. democratica* biomass. This would result in the *T. democratica* population consuming less efficiently while there is more chlorophyll a available, thus the availability of chlorophyll a would be higher overall. As *T. democratica* growth rates are proportional to the biomass of chlorophyll a relative to the biomass consumed (i.e. the available biomass of chlorophyll a), this would result in faster *T. democratica* growth rates.

4.4.5 Model limitations

Due to the lack of experimental data for *Thalia democratica*, many parameter values remain uncertain. Experimental data could improve the results of the model output, however, the sensitivity analysis showed that salp biomass and generation time were relatively insensitive to some uncertain parameters such as reproduction rates and mortality rates, so these should not be a priority for empirical research. The model

assumptions most in need of empirical support are: the input of chlorophyll *a* in the time-series and the tracking of cohorts instead of individuals.

Thalia democratica abundances corresponded well to field estimates in the standard simulation, but were at least ten-fold higher in the time-series simulation than any field observations. The higher abundances in the time-series simulation are likely a result of variation in chlorophyll *a*, given that all other variables were shared with the standard simulation. Chlorophyll *a* biomass in the time-series simulation is not derived from salp consumption in the previous time step (which it is in the standard simulation) and its input needs further refinement. This could result in an overestimation of chlorophyll *a* within the modelled system, and allow the *T. democratica* population to grow larger than is probable for a 1 m⁻³ volume. Correspondingly, this relationship could also result in a discrepancy between seasonal cycles of phytoplankton and salp abundance. In any case, the proportional abundances across seasons were appropriate in the time-series model, so this model can at least be applied to identify proportional variations in *T. democratica* abundances given a time-series of environmental data.

A caveat of the population model is that it tracks cohorts, not individuals, which means that generations occur independently. This was done as a mathematical convenience, and to better understand the role of individual life history stages. This is probably not realistic, as a naturally occurring population is likely to have numerous coexisting reproductive generations. To test how coexisting reproductive generations would influence the model outputs, the model was run with the addition of 30 generations (the average number of generations produced within a year) added at the halfway point for previously existing generations (~10 days apart). This meant that multiple reproductive

generations occurred simultaneously, and, at a given time-step, each generation would be at different life stages. However, after the model-spin up, there was no significant changes in the model outputs, most likely a result of the chlorophyll *a* concentration regulating the abundances of *T. democratica* until a quasi steady-state was reached. While not as comprehensive as an individual-based model, the model formulation used in this study offers the significant benefit of tracking individual cohorts to examine the temporal variation in population-level traits such as blastozoid-to-oozoid ratio and generation time.

4.4.6 Predicting *Thalia democratica* swarms

This model can be applied to predict conditions which will most likely promote swarms of *Thalia democratica*. This study suggests that for a salp population to develop and sustain itself, higher proportions of juvenile oozoids and faster growth (shorter generation times) are necessary. These population dynamics are driven by changes in temperature and chlorophyll *a* that generally occur during winter and spring. As salp swarms regularly form during phytoplankton blooms (Deibel and Paffenhofer, 2009) it would suggest that increases in chlorophyll *a* biomass would promote higher abundances of salps. However, to date, no studies have been able to correlate salp abundance with chlorophyll *a* biomass. From this model, it suggests that the discrepancy is likely due to offsets between when the chlorophyll *a* population peaks and the time taken for the salp population to respond; as well as the availability of chlorophyll *a* biomass (relative to salp consumption). Recent studies have also identified that salp abundances can vary depending on the availability of preferred phytoplankton food types (Chapter 3). Therefore, incorporating phytoplankton

functional groups into this model will increase the predictive capabilities of this population model.

4.4.7 Concluding remarks

The lack of long-term time-series data means that there is little understanding of how zooplankton populations will change with time, and as a result there is significant uncertainty around the trajectory of salp biomass in a changing ocean (Brotz et al., 2012; Condon et al., 2013). This model allows the analysis of seasonality of *Thalia democratica* swarms at different locations, and the prediction of changes in abundances as a result of changing oceanographic conditions. As the oceanographic predictors used in this study were derived from satellites, the model does not consider subsurface relationships. Although *Thalia democratica* does not exhibit vertical migration (Gibbons, 1997), incorporating vertical distribution of salps, phytoplankton and environmental variables will help to improve the model. This study confirms the importance of changes in environmental conditions to population-level traits and the relative population biomass of *T. democratica*. Future experiments should focus on understanding the relationship between salp growth rates and grazing rate, as well as identifying which environmental factors influence salp survivorship or mortality.

Chapter 5

Salp-falls in the Tasman Sea: a major food input to deep sea benthos

Abstract

Large, fast-sinking carcasses (food-falls) are an important source of nutrition to deep-sea benthic communities. In 2007 and 2009, mass depositions of the salp *Thetys vagina* were observed on the Tasman Sea floor between 200 and 2500 m depth, where benthic crustaceans were observed feeding on them. Analysis of a long-term (1981 to 2011) trawl survey database determined that salp biomass (wet weight, WW) in the eastern Tasman Sea regularly exceeds 100 t km^{-3} , with biomasses as high as 734 t km^{-3} recorded in a single trawl. With fast sinking rates, salp fluxes to the seafloor occur year-round. Salps, like jellyfish, have been considered to be of low nutritional value; however, biochemical analyses revealed that *T. vagina* has a high carbon (31% dry weight, DW) content, and an energy ($11.00 \text{ kJ g}^{-1} \text{ DW}$) content more similar to that of phytoplankton blooms, copepods and fish than to that of jellyfish, with which they are often grouped. The deposition of the mean yearly biomass ($4.81 \text{ t km}^{-2} \text{ WW}$) of salps recorded from the trawl database in the Tasman Sea represents a 330% increase to the carbon input normally estimated for this region. Given their abundance, rapid export to the seabed and high nutritional value, salp carcasses are likely to be a significant input of carbon to benthic food webs, which, until now, has been largely overlooked.

5.1 Introduction

Food-limited deep sea benthic ecosystems rely on depositions of organic matter from the euphotic zone (Gooday, 2002). Concentrated pulses of particulate organic matter (POM) derived from differing sources including phytoplankton blooms, other plant or algal matter, zooplankton faecal pellets and carcasses of larger fauna are major contributors of organic matter to the sea floor (Rowe and Staresinic, 1979; Smith et al., 2008). Despite the majority of particles being small (<5 mm; Alldredge and Silver, 1988), these pulses are an important source of nutrition for deep sea benthic communities, promoting both species richness and abundance (Butman et al., 1995). Benthic ecosystem functions are also positively related to increasing POM supply, including sediment community respiration rates and organic matter remineralisation (Witte and Pfannkuche, 2000; Smith et al., 2008; Sweetman and Witte, 2008).

Large, fast-sinking particles, such as carcasses, provide food fall events that augment the nutritional ecology of deep sea benthic communities (Rowe and Staresinic, 1979; Stockton and DeLaca, 1982; Smith and Baco, 2003). The “gelatinous pathway” (Billett et al., 2006; Lebrato et al., 2012) was first discovered by Moseley (1880) and illustrates the potential for sinking carcasses of gelatinous organisms to contribute a large flux of organic matter to the benthic environment. Due to their swarming nature, depositions of gelatinous carcasses generally accumulate in high densities to the benthic environment in areas underlying large and persistent gelatinous populations (Billett et al., 2006; Lebrato and Jones, 2009). For example, following swarms in surface waters (Wiebe et al., 1979; Grassle and Morse-Porteous, 1987), dense concentrations of salp carcasses were observed nearby on the seafloor in the outer Hudson Canyon (3240 m) in 1975 and 1986 (Cacchione et al., 1978). Similarly, pelagic cnidarian deposits (jelly-falls) have

been recorded on the sea floor off Oman (Billett et al., 2006), in the Sea of Japan (Yamamoto et al., 2008) and a Norwegian fjord (Sweetman and Chapman, 2011), while pyrosome carcasses have been observed on the Madeira Abyssal Plain (Roe et al., 1990) and on the seafloor off the Ivory Coast (Lebrato and Jones, 2009).

During two benthic sampling research voyages, mass depositions of the large salp *Thetys vagina* on the Tasman Sea floor were observed, prompting an examination into their subsequent fate and the nutritional value provided by the carcasses to the deep sea benthic communities. *T. vagina* reaches up to 306 mm in size (Nakamura and Yount, 1958) and has a distribution spanning the top 200 m (Thompson, 1948; Iguchi and Kidokoro, 2006) of sub-tropical and temperate waters of the Mediterranean Sea, Atlantic, Indian and Pacific Oceans (Berrill, 1950). Salp carcasses can potentially sink at rates of up to 1700 m d⁻¹ (Lebrato et al., 2013) suggesting that little if any decomposition occurs during descent, and mass depositions of salp carcasses may represent an important and substantial food-fall event for the benthic ecosystem. Although several reports indicate that gelatinous organisms such as salps are important to the diet of some marine organisms (eg. Duggins, 1981; Clark et al., 1989; Lyle and Smith, 1997; Gili et al., 2006), they are still generally thought to be of low nutritional value (Moline et al., 2004). Therefore, to determine whether salp carcasses can positively contribute to the benthic ecosystem, it is necessary to identify the quality of food they provide.

In particular, this study sought to: i) assess the frequency and abundance of salp swarms in the Tasman Sea and eastern New Zealand over 30 years; ii) quantify the biomass and relative abundance of *Thetys vagina* carcasses on the sea floor; and iii) compare the

energetic input and the biochemical composition of *T. vagina* carcasses with other gelatinous zooplankton.

5.2 Methods

5.2.1 Study region

Long term trawl surveys and two benthic sampling cruises were conducted in the southern Tasman Sea and Pacific Ocean east of New Zealand (Fig. 5.1a). For the first benthic study on board the R.V. *Tangaroa* in June 2007 (TAN0707), sampling was carried out on the Challenger Plateau, a large submarine plateau extending from the west coast of central New Zealand considered to be a region of low pelagic productivity (Wood, 1991). In October 2009, on the second benthic study on board the R.V. *Southern Surveyor* (SS03/2009), sampling occurred off south-east Australia in Bass Canyon, one of the largest submarine canyons in the world (Mitchell et al., 2007).

5.2.2 Trawl data analysis

Trawl data were available from two sources: a long-term data series (30 years) from the New Zealand fisheries research trawl database and pelagic trawls in the Tasman Sea over three years. Salp and pyrosome biomass was obtained from analysis of the New Zealand fisheries database (stock assessment, research and observer monitored commercial trawls) from 1981 to 2011 ($n = 2044$; for sampling locations see Fig. 5.1a). As the majority of data was opportunistically sampled, sampling periods within a year are variable but on average include every month per year. Trawls (midwater or benthic) were towed at a mean depth of 563.17 ± 342.40 , ranging from 33 to 2532 m. Where possible, recorded trawl dimensions and tow lengths were used. If details of trawl size or tow distance were not available, a standard averaged value calculated from all trawls was used (headline height = 8 m, wing distance = 30 m, tow distance = 4.4 km, tow speed = 6.5 km h^{-1}). Individuals were not classified into species. *Thetys vagina* biomass was obtained from three trans-Tasman cruises in 2008, 2009 and 2011 ($n = 12$). Depth-

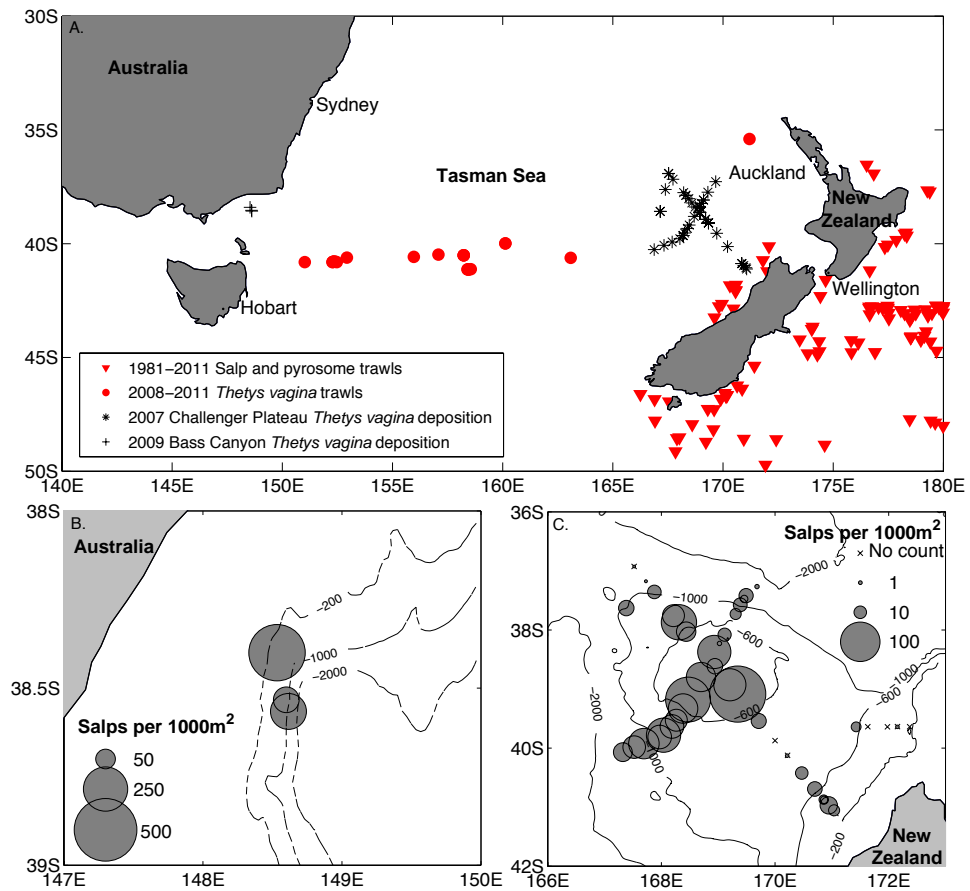


Figure 5.1 a) Survey area in the southern Tasman Sea and southwestern Pacific Ocean east of New Zealand showing trawl stations and benthic sampling stations. b-c) Density distribution based on video footage/camera stills of *Thetys vagina* (ind. 1000 m⁻²) at different stations in b) Bass Canyon and on the c) Challenger Plateau. Depth contours are displayed in metres.

stratified midwater tows with a pelagic trawl were made at 200 m intervals to a maximum depth of 1000 m from the surface, with equal 20 min tows at 6.5 km h⁻¹. The biomass estimates of *T. vagina* from the trans-Tasman pelagic trawls were calculated from the net area with the smallest mesh size capable of capturing them (minimum 40 mm mesh). Graded mesh area information was not available for the nets used in the New Zealand fisheries database, and as a result biomass estimates are more conservative than data obtained from the trans-Tasman pelagic trawls. All biomass estimates are represented in wet weight (WW).

5.2.3 Benthic sample collection and analysis

At both benthic sampling locations, video surveys were conducted using towed camera platforms with video and still image cameras. All individual salps observed on the seabed were counted along the full length of each video transect. If necessary, still camera images taken every 2 minutes along the transects were used to aid in identification of individuals. Deployments lasted between 30 to 60 minutes, at speeds of 0.25 to 0.50 m s⁻¹. On the Challenger Plateau, 46 deployments of the Deep Towed Imaging System (Hill, 2009) were conducted at a range of depths from 237 m to 1831 m. Both video and still cameras were oriented directly downwards, to facilitate scaling, and video frame width was calculated in ImageJ (<http://rsbweb.nih.gov/ij/>) by measuring widths of approximately 100 frame grabs using the camera's paired lasers (20 cm apart) as a reference. In Bass Canyon, the Benthic Optical and Acoustic Grab System (Sherlock et al., 2010) was deployed at three depths; 450, 650 and 1500 m. As the camera system did not have paired lasers, video frame width was measured by using average (\pm SD) length of *Thetys vagina* species caught from the subsequent Bass Canyon trawls (55.66 ± 5.90 mm, $n = 30$) to approximate frame size from 17 randomly

chosen screenshots containing *T. vagina*. Abundance of individuals per 1000 m² was calculated by determining salps per corrected area of deployments (corrected area = transect seabed area × percentage of usable video footage). Video analyses were run in OFOP (Ocean Floor Observation Protocol, www.ofop.texel.com); see methods in Bowden et al. (2011). Still image analyses used ImageJ software.

After each towed camera transect, benthic fauna were sampled at the same site using either a beam trawl (4 m mouth width, 10 mm mesh) or an epibenthic sled (1 m mouth width, 25 mm mesh). Trawls were towed for approximately 15 minutes at 0.75 ms⁻¹. Once back on deck, all fauna were sorted into species, weighed for biomass estimates and frozen (-20 °C).

Salps were thawed and total length and wet weight were measured for each individual. Guts were removed prior to biochemical analysis to ensure only body tissue was analysed. Randomly selected individuals from each site were then freeze-dried and their dry weights (DW) recorded. To determine ash-free dry weight (AFDW) of the specimens, tissue samples were taken and combusted at 550°C for 24 hours. All remaining tissue was ground in a ball mill to give a homogenous powder for biochemical analyses.

5.2.4 Biochemical analyses

Protein content of the salps was measured using the Bradford protein assay (Bradford, 1976) with bovine serum albumin (BSA) as the standard. Lipid content of the salps was estimated using a chloroform:methanol procedure after Folch et al. (1957) and carbohydrate content was estimated following Dubois et al. (1956) with D-glucose as

the standard. Energetic values of the salps were determined with a Parr 6200 Isooperibol Calorimeter (Parr Instrument Company, Moline USA) using a benzoic acid standard and as per the manufacturer's instructions (Parr, 2008).

Carbon and nitrogen contents were measured by combusting the material and using gas chromatography to separate the resulting N₂ and CO₂ gases. The gases were then analysed with an Isoprime isotope ratio mass spectrometer (IRMS) to give total carbon and nitrogen content. An average of the carbon content ($n = 68$, 31.35% DW) per salp for both locations was used to calculate carbon standing stock (mg C m⁻²) from the carcasses observed. All salps viewed in the video transects were assumed to have a dry weight of 0.38 g (the mean of $n = 27$ weighed individuals), allowing carbon standing stock to be calculated per square metre. While this is an approximation, all carcasses seen in the video and captured in benthic gear were of similar size.

5.3 Results

5.3.1 Observations of *Thetys vagina* on the sea floor

Carcasses of *Thetys vagina* were observed in all three video transects in Bass Canyon, and in 38 out of 46 transects on the Challenger Plateau. In total, 368 carcasses were recorded in Bass Canyon comprising 47.8% of the total observed fauna over an area of 2118 m². The mean (\pm SD) density of *T. vagina* was 219 ± 168 individuals (ind.) 1000 m⁻² with a minimum density of 85 and a maximum of 408 ind. 1000 m⁻² (Fig. 5.1b). On the Challenger Plateau 1400 individuals were observed, making up 9.8% of total observed fauna over an area of 72995 m². In 11 transects where abundances of *T. vagina* were high (>20 ind. 1000 m⁻²; Fig. 5.1b), *T. vagina* carcasses ranged from 19.6 to 48.7% of the total fauna observed, similar to that found in Bass Canyon. The mean (\pm SD) density of *T. vagina* on the Challenger Plateau was 26 ± 39 ind. 1000 m⁻², significantly lower than densities found in Bass Canyon ($F_{1,48} = 40.1$, $p < 0.01$), with a minimum density of 0 and a maximum of 202 ind. 1000 m⁻² (Fig. 5.1c). *T. vagina* comprised 19.0% of total haul biomass in Challenger Plateau and 42.6% of total haul biomass in Bass Canyon and were the dominant organisms in both locations. During one transect on the Challenger Plateau, the deep water spider crab, *Platymaia maoria*, was twice observed directly feeding on *T. vagina* carcasses (Fig. 5.2b; Table 5.1). On 17 occasions across 9 transects, demersal fish and sea stars were recorded near the carcasses (Table 5.2). The most common demersal fish were rattails (*Coelorinchus* spp.) and were found close to the carcasses on 10 occasions. At both locations, all *T. vagina* individuals observed on the sea floor were dead, whole and with no visible bacterial mats or biofilms.

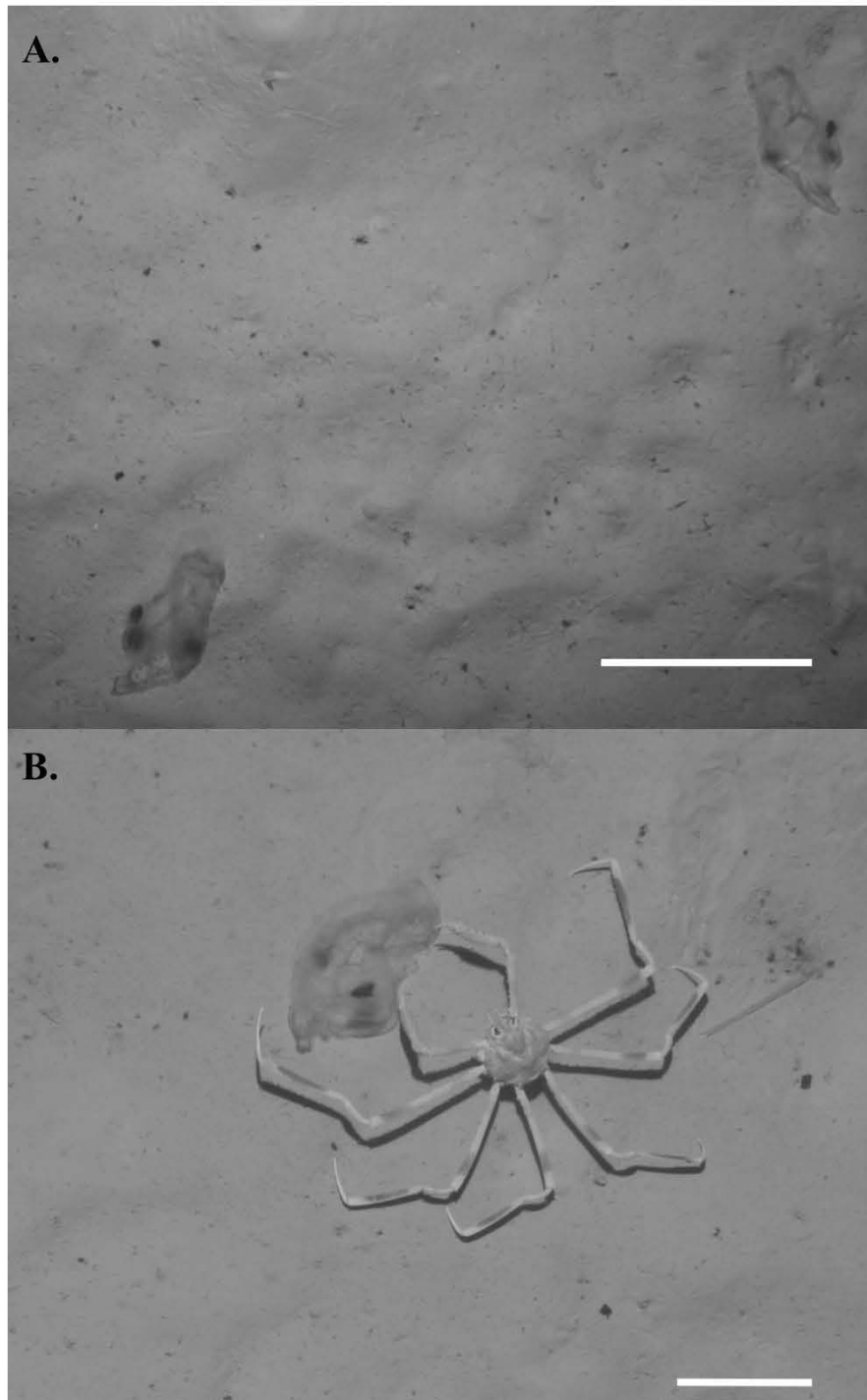


Figure 5.2 Sea floor photographs from the Tasman Sea. Scale bars refer to 10 cm. a) *Thetys vagina* carcasses at 1565 m depth taken in Bass Canyon. b) *Platymaia maora* feeding on *T. vagina* carcass at 482 m in Challenger Plateau.

Table 5.1 Megafaunal taxa observed directly feeding on or close to (potential feeders) *Thetys vagina* carcasses on the Challenger Plateau. Footnotes denote previous records of taxa feeding on salps.

Species	No. of events
Crustacea	
<i>Platymaia maoria</i>	2 ^a
Fish	
<i>Coelorinchus</i> sp. ^b	10
<i>Paraulopus</i> sp.	1
<i>Tripterothycis gilchristi</i>	1
<i>Helicolenus</i> sp. ^c	1
<i>Hoplichthys haswelli</i>	1
<i>Hydrolagus novaezelandiae</i> ^d	1
Echinodermata	
Ophiuroidea	2
Asteroidea ^e	1

^aDirect feeding observed; ^bClark (1985); ^cBax and Williams (2000); ^dDunn et al. (2010); ^eDomanski (1984)

5.3.2 Abundance of *Thetys vagina* and other large salps in the Tasman Sea

Analysis of the New Zealand fisheries database from 1981 – 2011 determined that salp and pyrosome biomass exceeded 100 t km⁻³ WW (56 t km⁻²) in approximately half of the years sampled (Fig. 5.3a). Biomass ranged from 0.006 t km⁻³ WW (0.003 t km⁻²) to 1464 t km⁻³ WW (824 t km⁻²) with a 30-year average (\pm SD) of 8.54 ± 51.79 t km⁻³ WW (4.81 t km⁻²). Salps and pyrosomes were present all year round but appear to form dense swarms an order of magnitude greater than their normal occurrence between December and June (Fig. 5.3b).

High densities of *Thetys vagina* were captured in three trans-Tasman cruises in 2008, 2009 and 2011 (Fig. 5.3a), with a maximum of 734 t km⁻³ WW (147 t km⁻²) caught in 2009 (minimum = 0.003 t km⁻³ WW, mean (\pm SD) = 44.82 ± 158.20 t km⁻³ WW). Depth stratified sampling showed that 98% of *T. vagina* biomass occurred in the top 200 m of the water column.

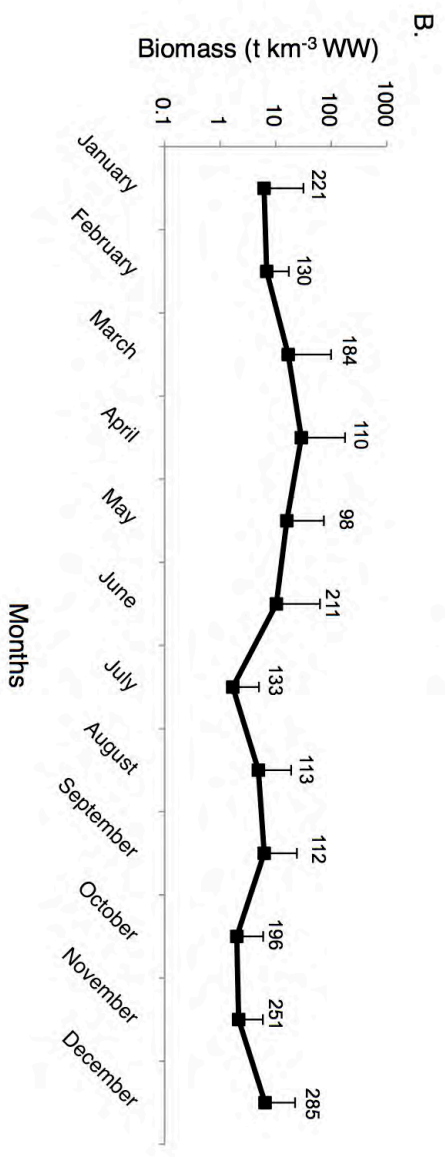
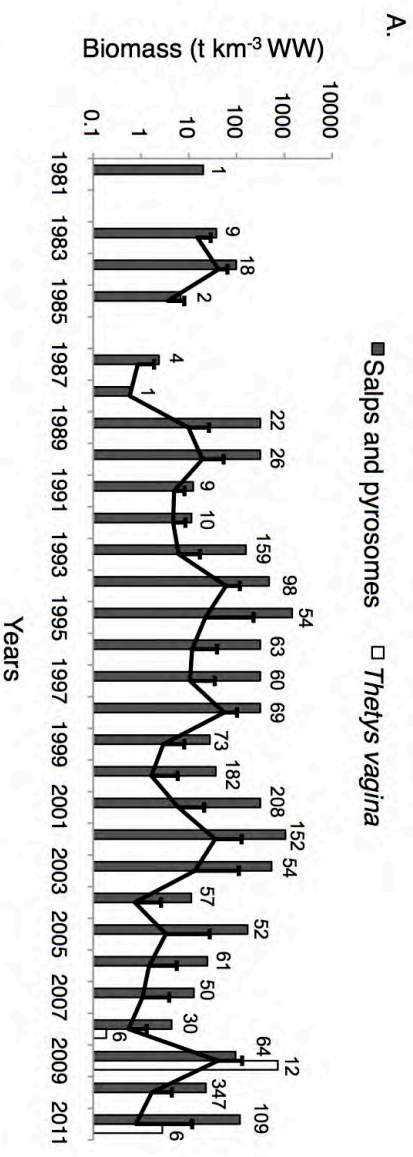


Figure 5.3 a) Maximum yearly biomass (Bars, t km⁻³ WW) for salps and pyrosomes (dark bars; New Zealand fisheries database) from 1981 - 2011, and *Thetyls vagina* (light bars; trans-Tasman pelagic trawls) in 2008, 2009 and 2011. Yearly mean (+SD) is represented by the solid line. Number of trawls per year are indicated above each bar. Station locations are presented in Figure 5.1. b) Mean (+SD) monthly biomass (t km⁻³ WW) of salps and pyrosomes from 1981 – 2011. Number of trawls per month are indicated above each bar.

5.3.3 Biochemical composition of *Thetys vagina*

Lipids accounted for the highest proportion of macronutrient, making up a mean (\pm SD) $10.5 \pm 2.8\%$ of dry weight (DW; Table 5.2). Protein constituted $3.4 \pm 1.5\%$ of DW, and carbohydrates $4.4 \pm 1.9\%$. The mean (\pm SD) energetic content of *Thetys vagina* was $11.0 \pm 1.4 \text{ kJ g}^{-1}$ DW. Ash-free dry weight (AFDW) was high, ranging from 33 - 88% DW and total organic content of *T. vagina* represented only 31% of AFDW.

Mean (\pm SD) carbon content for *Thetys vagina* ($31.4 \pm 5.4\%$ DW) was much higher than nitrogen content ($2.8 \pm 1.1\%$ DW; Table 5.2). Carbon standing stock of the *T. vagina* deposition in Bass Canyon was 26.1 mg C m^{-2} . On Challenger Plateau, carbon standing stock was lower, with a mean of 3.1 mg C m^{-2} , but reaching 24.1 mg C m^{-2} at some stations. Using energetic content as an indicator of nutritional quality, *T. vagina* is nutritionally similar to phytoplankton (Fig. 5.4). C:N ratio and energetic content values for *T. vagina* are much greater than reported values of cnidarians and ctenophores.

Table 5.2 Biochemical and elemental composition of *Thetys vagina* expressed either as a percentage of total dry weight (DW) or measured values. All values are means \pm SD. Ranges are displayed in brackets. *n* - number of individuals measured.

	<i>n</i>	<i>Thetys vagina</i>
Protein content (% DW)	68	3.42 ± 1.46 (1.10 – 7.34)
Lipid content (% DW)	31	10.50 ± 2.77 (6.19 – 16.48)
Carbohydrate content (% DW)	18	4.36 ± 1.92 (1.34 – 7.77)
Energetic content (kJ g⁻¹ DW)	9	11.00 ± 1.38 (8.91 – 13.33)
Carbon content (% DW)	68	31.35 ± 5.34 (18.77 – 42.68)
Nitrogen content (% DW)	68	2.82 ± 1.13 (1.52 – 8.09)
C:N	68	12.03 ± 3.03 (4.73 – 19.05)

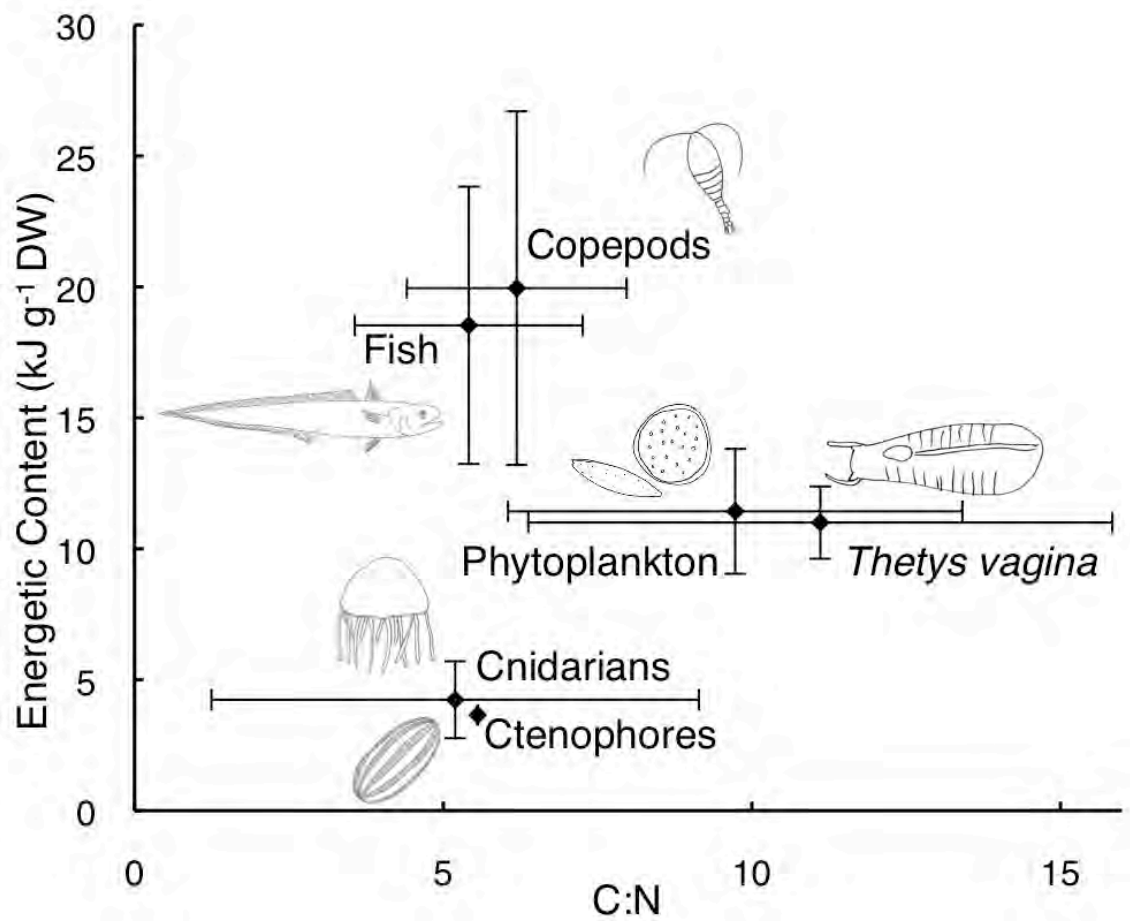


Figure 5.4 Relationship between mean (\pm SD) energetic content (kJ g^{-1} dry weight) and mean (\pm SD) C:N ratio as an indicator of quality of different marine organisms as a food item. Values for *Thetys vagina* obtained from this study. Other values obtained from previous studies: phytoplankton (Platt and Irwin, 1973), copepods (Donnelly et al., 1994; Ikeda et al., 2006), cnidarians and ctenophores (Clarke et al., 1992) and fish (Childress and Nygaard, 1973).

5.4 Discussion

5.4.1 Observations of *Thetys vagina* on the sea floor

Densities of *Thetys vagina* carcasses observed on the sea floor in this study are among the highest recorded for any gelatinous zooplankton deposition. These mean densities of *T. vagina* (26 and 219 ind. 1000 m⁻² for Challenger Plateau and Bass Canyon, respectively) are much greater than those found for depositions of the giant jellyfish *Nemopilema nomurai* in the sea of Japan (1.1 ind. 1000 m⁻²; Yamamoto et al., 2008) and the deep sea scyphozoan *Periphylla periphylla* in a Norwegian fjord (10 ind. 1000 m⁻²; Sweetman and Chapman, 2011). Densities were similar to that of *Pyrosoma atlanticum* carcasses off the Ivory Coast (70.6 ind. 1000 m⁻²) described by Lebrato and Jones (2009). The mass depositions of fresh carcasses observed in this study indicate the recent demise of swarms at both locations. On the Challenger Plateau, high densities of *T. vagina* were observed at the surface during sampling, suggesting that the swarm may still have been developing for several weeks after sampling. Sampling during an ongoing swarm may limit the accuracy of the deposition densities as some salp and pyrosome species are known to migrate to sea floor depths (Roe et al., 1990; Gili et al., 2006). As *T. vagina* mainly occurs in the top 200 m of the water column and all carcasses viewed on the video were dead or moribund, it is unlikely that deposition abundances were overstated.

5.4.2 Abundance of *Thetys vagina* and other large salps in the Tasman Sea

Other large salps such as *Salpa thompsoni* (Nishikawa et al., 1995; Perissinotto and Pakhomov, 1998) and *S. aspera* (Wiebe et al., 1979; Madin et al., 2006) frequently form large swarms, but records of *Thetys vagina* are sparse. The largest swarm recorded of *T. vagina* occurred in 2004 in the Sea of Japan, with biomasses as high as 900 t km⁻³ WW

(Iguchi and Kidokoro, 2006), comparable to the maximum of 734 t km^{-3} WW recorded in this study. As New Zealand fisheries surveys were designed for the capture of large pelagic and demersal fish, they are likely to under-represent the true abundances of salps. Trawls would only spend approximately 35% of their time in the 0 - 200 m depth range that is preferred by the majority of large salps in the Tasman Sea (Thompson, 1948). Regardless, abundances of salps across the 30-year dataset indicate that salp biomass in the Tasman Sea often exceeded 100 t km^{-3} WW, considerably higher than previously thought.

Tranter (1962) recorded an average zooplankton biomass (excluding salps) from 1959 – 1961 in the Tasman Sea of 36 t km^{-3} WW, with salps accounting for an additional 53 t km^{-3} WW. Using maximum swarm values from the present study, it can be seen that large salp and pyrosome swarms in the Tasman Sea can frequently exceed zooplankton biomass by 300%. Similarly, Young et al. (1996) sampled zooplankton in the Tasman Sea from 1992 – 1994 and found salps on average made up 30% of zooplankton biomass across the three years and at some times up to 90%. To put salp biomass into perspective, hoki (*Macruronus novaezealandiae*) constitutes New Zealand's largest fishery (O'Driscoll, 2004) with biomass estimated to be 1.2 t km^{-2} WW (based on an 8 year average) and representing 97% of all fish biomass in the mid-water depth range (Bull et al., 2001). The mean 30-year average of large salp biomass (4.81 t km^{-2} WW) for the Tasman Sea and New Zealand region not only exceeds this value, but also indicates the prevalence of salp swarms in the Tasman Sea.

5.4.3 Biochemical composition of large salps

This study provides the first data on the biochemical composition of *Thetys vagina*. Results obtained are within expected ranges observed for other large salps (Madin et al., 1981; Clarke et al., 1992; Dubischar et al., 2006). Similar to values from this study, higher proportions of lipids to protein are found in the Antarctic species, *Salpa thompsoni* (5.7 - 6.8% DW; Dubischar et al., 2006), while the opposite trend is observed for North Atlantic salp species, 0.96, 0.25 and 0.97% DW for *Pegea confoderata*, *S. cylindrica* and *S. maxima* respectively (Madin et al., 1981). Differences in the biochemical composition of salp species are likely to arise from either differing lipid concentrations within food sources (Larson and Harbison, 1989). Previous studies show carbohydrate contents for salps are generally low (0.8 - 1.3% DW; Madin et al., 1981; Clarke et al., 1992; Dubischar et al., 2006), however, this study recorded levels similar to that of protein. High carbohydrate values could be a result of only analysing the salp test, whereas Madin et al. (1981) could have been influenced by the addition of gut contents. This higher value is consistent with expected results, as the salp tunic is mainly comprised of proteins and polysaccharides (Smith and Dehnel, 1971).

Although the total organic content (lipids, proteins and carbohydrates) of an organism should equal its AFDW (Madin et al., 1981), high values of AFDW are characteristic for gelatinous zooplankton due to difficulties in removing “water of hydration” (Madin et al., 1981) when freeze-drying. Similar AFDW values have been found for other salps; 27 – 62.7% DW for *Salpa thompsoni* (Huntley et al., 1989; Donnelly et al., 1994) and 66.4% DW for *S. fusiformis* (Clarke et al., 1992) with total organic contents ranging from 19 – 51% of AFDW (Madin et al., 1981; Dubischar et al., 2006). Apart from residual water, the most likely causes for the “missing” compounds are those missed by

the methodology. For example, as the nitrogen content of protein can be assumed to be 16% (protein = N × 6.25; Madin et al., 1981), from the nitrogen values recorded here, protein content should have been as high as 17.6% DW, four times higher than detected values from this study. Similar problems detecting proteins in gelatinous zooplankton have been seen in previous studies (Clarke et al., 1992; Dubischar et al., 2006), and are thought to arise from problems with detecting cross-linked proteins.

5.4.4 Contribution to the benthic food web

Energetic content of *Thetys vagina* was higher than that of cnidarians and ctenophores (4.35 to 10.17 kJ g⁻¹ DW; Percy and Fife, 1981), other pelagic tunicates such as *Pyrosoma atlanticum* (4.94 ± 1.55 kJ g⁻¹ DW; Davenport and Balazs, 1991), and almost as high as some crustacean species (14.77 ± 1.67 kJ g⁻¹ DW; Wacasey and Atkinson, 1987). One issue that may arise when comparing energetic content of gelatinous and non-gelatinous zooplankton is whether dry weight specific metrics are comparable. Physiological rate functions between gelatinous and non-gelatinous zooplankton are more accurately compared using a carbon weight metric opposed to dry weight (Schneider, 1990), and it is possible that the same rules may follow for biogeochemical measurements. Using this analysis would result in values of 44 kJ g⁻¹ C for copepods and 35 kJ g⁻¹ C for *Thetys vagina*, which suggests that energetic contents for *T. vagina* may be more similar to copepods than calculated in this study.

Of all gelatinous zooplankton studied to date, carbon content for *T. vagina* was second only to *P. atlanticum* (Davenport and Balazs, 1991; Lebrato and Jones, 2009). The energetic content suggests that *T. vagina* carcasses have higher food value than other gelatinous zooplankton (cnidarians and ctenophores; Fig. 5.4) and nutritionally are more

similar to the phytoplankton blooms that normally sustain benthic communities (Rowe and Staresinic, 1979; Smith et al., 2008) as well as fish and copepods. As only the gelatinous tunic of *T. vagina* was analysed, nutritional quality has not been elevated by gut contents. Compared to smaller salps, the tunic of *T. vagina* is relatively thick and composed of densely packed fibrous material (Hirose et al., 1999), possibly resulting in elevated nutritional values. Based on maximum salp biomass values of 100 t km^{-3} WW, these deposition events can potentially export up to 616 GJ km^{-2} of energy, or 16 t km^{-2} of carbon, to the Tasman Sea benthos every year.

Several fish species feed exclusively on salps or have salps as a major component of their diets. These species tend to be opportunistic benthic-pelagic feeders, such as the black, smooth and spiky oreos, carinate rattail, and small-scaled brown slickhead (Clark et al., 1989; Lyle and Smith, 1997). As fish species, particularly rattails, were often found around the carcasses, these results suggest that the salp remains often found in these fish guts may result from scavenging at the seafloor. Apart from fish, other benthic feeders including sea-stars (Domanski, 1984), sea urchins (Duggins, 1981), octocorallians (Gili et al., 2006), mushroom corals (Hoeksema and Waheed, 2012) and from this study, the deep water spider crab *Platymaia maora*, have been observed feeding on salps. Similarly, pyrosome carcasses have provided food for a range of megafauna including crustaceans, arthropods, anemones and echinoderms (Roe et al., 1990; Lebrato and Jones, 2009) while anemones, shrimp, crabs and molluscs have been observed near and feeding on cnidarian carcasses (Yamamoto et al., 2008; Sweetman and Chapman, 2011). As salp carcasses can sink at rates up to 1700 m d^{-1} (Lebrato et al., 2013), they will be able to reach the seafloor in less than 2 to 3 days, before significant bacterial degradation can take place. Preliminary experimental data suggests

that at seafloor temperatures (4°C) *T. vagina* individuals will retain 68% of their mass after 28 days (Henschke, unpublished data). These results correspond to a model-calculated decomposition time of approximately 20 days for a gelatinous organism (including the more labile cnidaria) on the sea floor (Lebrato et al., 2011). As no bacterial mats or biofilms were observed on any of the *T. vagina* individuals viewed or collected in this study, slow decomposition rates of *T. vagina* would allow carcasses to remain on the sea floor until scavenged or eventually remineralised via the microbial loop.

5.4.5 Potential carbon standing stock

Studies in the world's oceans (Smith and Kaufmann, 1999), including the Pacific Ocean near New Zealand (Nodder et al., 2003), have identified that food demand in the benthic community (sediment community oxygen consumption) often exceeds food supply (POM). Salp carcasses are not detected by traditional methods of sampling water column nutrient fluxes, such as sediment traps (Lebrato and Jones, 2009), and consequently are not included in current carbon budget calculations, resulting in considerable underestimation of the total flux. Hence, salp carcasses may be supplementing the smaller POM that can be collected by sediment traps, and provide an extra source of nutrition for the benthic community. Since particles that generally make up the majority of measured carbon flux in the Tasman Sea are <1 mm (Kawahata and Ohta, 2000), these salp deposition events provide a substantial contribution of much larger carbon parcels to the benthos. As swarms of *Thetys vagina* were still in surface waters during sampling at Challenger Plateau, by the time the entire population had collapsed the input from both faecal pellets and carcasses would have been considerably higher than values estimated here.

Depositions of *Thetys vagina* on the Challenger Plateau in this study only represented 0.19% of the regional annual carbon flux, whereas carbon provided from the Bass Canyon deposition was tenfold greater, representing 1.5% of the annual flux (Kawahata and Ohta, 2000). Although gelatinous zooplankton depositions can occur across all bottom topographies, studies have identified much greater biomasses and carbon inputs when organisms are in environments that promote concentration such as canyons or structures such as pipelines (Cacchione et al., 1978; Lebrato and Jones, 2009). Carbon standing stocks in the Arabian Sea for cnidarian carcasses have been reported as high as 78 g C m⁻² in some areas, an order of magnitude higher than mean annual flux (Billett et al., 2006), and 22 g C m⁻² for *Pyrosoma atlanticum* carcasses off the Ivory Coast, 13 times greater than the annual flux (Lebrato and Jones, 2009). Future studies may benefit from incorporating bottom topographies when calculating the potential for gelatinous organisms to accumulate on the sea floor and their eventual contribution to carbon fluxes in the area.

5.4.6 Concluding remarks

Mass depositions of salp carcasses represent a significant pathway for the export of organic production from surface waters to the deep sea. Salp biomass in the Tasman Sea regularly exceeds 100 t km⁻³ WW with deposition events likely to export at least 16 t km⁻² of carbon, or 616 GJ km⁻² of energy, to the benthos every year. With higher organic content than depositions of other gelatinous organisms, the input of large salp carcasses (salp-fall) is likely to be important to the nutritional ecology the deep sea benthos.

Chapter 6

Conclusion: Understanding processes influencing salp swarms

6.1 General discussion

The main objective of this thesis was to further the understanding of processes influencing salp swarms. Predicting the location and magnitude of salp swarms will be important for management of the marine environment, particularly if future environmental conditions change to promote a dominance in gelatinous zooplankton (Hays et al., 2005). This thesis adds to a small body of literature concerning salps in the Tasman Sea, and is the first extensive Tasman Sea dataset on salp distribution in 70 years and salp ecology in 40 years. The response of *Thalia democratica* swarms to environmental conditions (temperature and chlorophyll *a*) were compared across water types (Chapter 3), and locations along the New South Wales coast (Chapter 4). The trophic role of salps within the Tasman Sea ecosystem (Chapter 2), and the potential for large salps to act as food falls to the benthos were also identified (Chapter 5). As salp swarms are prevalent around the world (Andersen, 1998), the results in this thesis are globally relevant.

Understanding the demographic characteristics of a salp population is necessary to determine how the population will swarm. Salp swarm abundance is related to asexual reproduction rates (Chapter 3), proportions of mature individuals (Chapter 3) and growth rates (generation time; Chapters 3 & 4). When salp populations are in low abundances, such as during winter, they will have slower growth rates, longer generation times and higher asexual reproduction (buds per chain). Although oozoids are producing longer chains of offspring, slower population growth results in increased

risk of mortality from factors such as predation. This will result in fewer blastozooids reaching maturity and the next generation of oozoid individuals being reduced. As oozoids are the key stage for population growth (Chapter 4), this will hinder the population's ability to swarm. When conditions improve, faster growth rates allow more salps to reach maturity and complete generations (see Fig. 3.1).

The conditions which promote salp swarms (i.e. faster growth, more reaching maturity and higher proportions of oozoids) are related to the availability of phytoplankton food (chlorophyll *a*). The availability of food does not necessarily relate to absolute abundances, but instead the abundances of preferred food (Chapter 3) related to the amount that can actually be ingested (Chapters 3 & 4). Higher salp abundances were found in years where there were increased proportions of preferred food, regardless of total food abundance and reduced proportions of zooplankton competitors. Therefore, this thesis emphasises the importance of the phytoplankton prey field driving salp swarm abundance and distribution, and confirms that salp populations are largely driven by bottom-up forcing.

When salp populations are large, they may compete with zooplankton for phytoplankton. As it is difficult to compare abundances of salps and other zooplankton through enumeration (Henschke et al., 2011), considering the isotopic signature of species is a better method to investigate competition as it can determine if salps and other zooplankton are consuming the same food source. From this thesis and previous work, it is unlikely that salps and krill are competitors (e.g. Chapter 2; Kawaguchi et al., 1998), and instead may be segregated in their distribution as they are consuming different phytoplankton species (Nishikawa et al., 1995). Salps and copepods are more likely to compete for food, due to their lack of niche differentiation (Chapter 2), and

salps can predate on copepod eggs and nauplii. However, as salp swarms are ephemeral, the resulting impact on the zooplankton community is likely to be small. Further experimental observations are necessary to reveal if copepods can mediate the strength of this competition by altering their foraging behaviour.

This thesis also identified that large salp carcasses are a major food-fall and carbon contributor to the benthic ecosystem. Large salps were found to be highly nutritious and carbon-rich, particularly when compared with other gelatinous organisms, and benthic crustaceans and fish were observed feeding on carcasses (Chapter 5). Swarms of large salps are a frequent occurrence in the Tasman Sea, and contribute a previously unknown source of nutritious carbon to the deep sea, up to 330% more per year in the Tasman Sea alone, which is equivalent to the energetic contribution of 36 minke whale carcasses (Henschke et al., 2012). Salps are an important prey item for several organisms, and would be nutritious for commercially important fisheries species such as sardines. Correspondingly, years with unusually high numbers of salps in the Tasman Sea coincided with high fisheries catches of sardines (Thompson and Kesteven, 1942). Understanding the relationship between salp abundance and fisheries catch would be of significant value to the commercial fisheries industry.

6.2 Avenues for future research

6.2.1 Defining “optimal conditions”

There is scope for the further development of predictive salp population models. Although the size-structured population model within this study could predict seasonality in salp swarms (Chapter 4), this model could be enhanced through experimental studies on life history traits such as growth, mortality and reproductive

rates, to confirm exactly which environmental conditions are “optimal”. In particular, it is necessary to identify the importance of the phytoplankton prey field in salp growth and reproduction – are there particular phytoplankton species which some salps prefer? Higher abundances of *Thalia democratica* were recently observed in the Derwent River, Tasmania, when abundances of flagellates are high (K. Swadling, pers. comm.), and gut pigment analysis could easily determine what phytoplankton species the salps are feeding on. However, there are no studies investigating the influence of phytoplankton food type on salp life history traits such as growth rates. Current research is investigating whether satellite ocean colour data (chlorophyll *a* biomass) can be correlated with phytoplankton species (NIWA, 2014). If this is possible, improvements can be made to the salp population model by incorporating phytoplankton type to predict variations in swarm magnitudes. As chlorophyll *a* biomass is difficult to correlate with salp abundances (Chapter 4), knowing the species composition of a phytoplankton bloom in an area may be a better proxy for predicting salp swarms, particularly if salp growth rates are not related to the abundance of food, but instead the availability of preferred food.

6.2.2 *The fate of small salp carcasses*

There is also scope to investigate the fate of smaller salps, such as *Thalia democratica*, after the collapse of a swarm. It is unlikely that they will be able to sink to the sea floor as rapidly as larger salps, so it is necessary to consider whether they remain in the euphotic zone and transfer their energy to other trophic levels through consumption, or if they will sink with aggregations of marine snow. Salps are often difficult to identify in stomach remains, and are usually identified through their muscle bands (M.R. Clark, pers. comm.). Smaller salps, such as *T. democratica*, would disintegrate before

identification could take place. Krill have been observed actively feeding on salps (Kawaguchi and Takahashi, 1996), and it has been found that *T. democratica* has a similar elemental composition to arthropods (Heron et al., 1988), suggesting there is potential for carnivorous zooplankton to feed on smaller salps. Alternatively, large amounts of marine snow are a common feature during a salp swarm, and are usually composed of salp faecal pellets, zooplankton carcasses and phytoplankton (Morris et al., 1988). If small salp carcasses become collected within these aggregations, their carbon contribution to the benthos could be as significant as the larger salps.

6.2.3 Incorporation of salps into biogeochemical models

Zooplankton dynamics have been shown to be one of the most poorly simulated state variables in biogeochemical models (Arhonditsis and Brett, 2004), most likely because of the diversity of species and life history stages occurring within the zooplankton. Despite the carbon sequestration potential of the carcasses of large salps, there is still little known about their basic ecology, such as growth rates, asexual fecundity and filtration rates. This makes estimating their abundance and seasonality in the marine environment very difficult. Recently, a salp swarm in the northeastern Pacific deposited faecal pellets and carcasses to the sea floor over a period of 6 months, providing up to 327% of the sediment community oxygen consumption demand and up to 38 mg C d^{-1} (Smith Jr et al., 2014). Although this highlights how prevalent the input of salp carcasses and faecal pellets to the benthos are, it remains unclear how global-scale models can incorporate these episodic events while maintaining reasonable complexity (Smith Jr et al., 2014). As not all salp species form swarms, there is need to further investigate the ecology of large salps in order to determine whether these mass deposition events are episodic in nature, or are occurring more regularly than previously

thought. Future consideration of salps within biogeochemical models should also take into account the relative contribution of larger and smaller species to determine if the carbon inputs from the faecal pellets of smaller salps (which occur in dense swarms) are greater than the carbon inputs of the faecal pellets and carcasses of larger, less abundant salps.

6.2.4 Salps are not jellyfish!

This thesis highlights how distinct salps are from the traditional jellyfish (cnidarians and ctenophores) and other gelatinous zooplankton they are commonly grouped with. The gelatinous zooplankton grouping does not have any taxonomic basis, but instead was created to describe a group of non-crustacean organisms that are difficult to collect with traditional sampling techniques (Haddock, 2004). For example, the evolutionary divergence time between cnidarians and tunicates occurred ~900 million years ago (mya), whereas humans diverged from elephants much more recently (~100 mya; Schopf, 1992). As an ecologist is unlikely to consider humans and elephants together for scientific analyses, similar care should be taken when collectively grouping salps with other gelatinous zooplankton. To better model the marine environment, future biogeochemical and ecosystem models should incorporate salps (and other thaliaceans) in their own category, separate to the broad gelatinous zooplankton grouping they are often included in (e.g. Fulton et al., 2004; Brotz et al., 2012).

References

- Aberle, N., Hansen, T., Boettger-Schnack, R., Burmeister, A., Post, A., and Sommer, U. (2010) Differential routing of 'new' nitrogen toward higher trophic levels within the marine food web of the Gulf of Aqaba, Northern Red Sea. *Mar. Biol.* **157**, 157-169
- Acuña, J. (2001) Pelagic tunicates: why gelatinous? *The American Naturalist* **158**, 100-107
- Ainley, D., Fraser, W., Smith Jr, W., and Hopkins, T. (1991) The structure of upper level pelagic food webs in the antarctic: effect of phytoplankton distribution. *J Mar Syst* **2**, 111-112
- Allredge, A.L., and Madin, L.P. (1982) Pelagic tunicates: Unique herbivores in the marine plankton. *Bioscience* **32**, 655-663
- Allredge, A.L., and Silver, M.W. (1988) Characteristics, dynamics and significance of marine snow. *Prog. Oceanogr.* **20**, 41-82
- Altabet, M.A. (1988) Variations in nitrogen isotopic composition between sinking and suspended particles: implications for nitrogen cycling and particle transformation in the open ocean. *Deep Sea Res* **35**, 535-554
- Altabet, M.A., and Francois, R. (1994) Sedimentary nitrogen isotopic ratio as a recorder for surface ocean nitrate utilization. *Global Biogeochemical Cycles* **8**, 103-116
- Andersen, V. (1998) Salp and pyrosomid blooms and their importance in biogeochemical cycles. In *The Biology of Pelagic Tunicates* (Bone, Q., ed), 125-138, Oxford University Press, New York
- Andersen, V., and Nival, P. (1986) A model of the population-dynamics of salps in coastal waters of the Ligurian Sea. *J. Plankton Res.* **8**, 1091-1110
- Arhonditsis, G.B., and Brett, M.T. (2004) Evaluation of the current state of mechanistic aquatic biogeochemical modelling. *Mar. Ecol. Prog. Ser.* **271**, 13-26

- Baird, M.E., Everett, J.D., and Suthers, I.M. (2011) Analysis of southeast Australian zooplankton observations of 1938-42 using synoptic oceanographic conditions. *Deep Sea Res. Part II* **58**, 699-711
- Baird, M.E., Timko, P.G., Middleton, J.H., Mullaney, T.J., Cox, D.R., and Suthers, I.M. (2008) Biological Properties across the Tasman Front off southeast Australia. *Deep Sea Res. Part I* **55**, 1438-1455
- Barange, M. (1990) Vertical migration and habitat partitioning of six euphausiid species in the northern Benguela upwelling system. *J. Plankton Res.* **12**, 1223-1237
- Barlow, R.G., Mantoura, R.F.C., Gough, M.A., and Fileman, T.W. (1993) Pigment signatures of the phytoplankton composition in the northeastern Atlantic during the 1990 spring bloom. *Deep Sea Res. Part II* **40**, 459-477
- Bautista, B., Harris, R.P., Tranter, P.R.G., and Harbour, D. (1992) In situ copepod feeding and grazing rates during a spring bloom dominated by *Phaeocystis* sp. in the English Channel. *J. Plankton Res.* **14**, 691-703
- Bax, N., and Williams, A. (2000) Habitat and fisheries production in the south east fishery ecosystem. *Final Report, Fisheries Research and Development Corporation Project 94*, 40
- Beaglehole, J.C., ed (1963) *The Endeavour Journal of Joseph Banks 1768-1771*. Public Library of NSW, Sydney
- Bearhop, S., Adams, C.E., Waldron, S., Fuller, R.A., and Macleod, H. (2004) Determining trophic niche width: a novel approach using stable isotope analysis. *J. Anim. Ecol.* **73**, 1007-1012
- Berner, L. (1957) Studies on the Thaliacea of the temperate northeast Pacific Ocean. Ph.D. thesis. *University of California San Diego*
- Berrill, N.J. (1950) Order Salpida (Demomyaria). In *The Tunicata, with an account of the British species*, 286-301, The Ray Society, London
- Billett, D.S.M., Bett, B.J., Jacobs, C.L., Rouse, I.P., and Wigham, B.D. (2006) Mass deposition of jellyfish in the deep Arabian Sea. *Limnol. Oceanogr.* **51**, 2077-2083

- Blackburn, M. (1979) Thaliacea of the California Current region: Relations to temperature, chlorophyll, currents, and upwelling. *California Cooperative Oceanic Fisheries Investigations Reports* **20**, 184-193
- Bowden, D.A., Schiaparelli, S., Clark, M.R., and Rickard, G.J. (2011) A lost world? Archaic crinoid-dominated assemblages on an Antarctic seamount. *Deep Sea Res. Part II* **58**, 119-127
- Braconnot, J.C. (1963) Study of the annual cycle of salps and doliolids in Rade de Villefranche-sur-mer. *ICES/CIEM Int. Counc. Explor. Sea* **28**, 21-36
- Bradford, M.M. (1976) A rapid and sensitive method for the quantitation of microgram quantities of protein utilizing the principle of protein-dye binding. *Anal. Biochem.* **72**, 248-254
- Brett, M. (2004) When is a correlation between non-independent variables "spurious"? *Oikos* **105**, 647-656
- Brotz, L., Cheung, W.W.L., Kleisner, K., Pakhomov, E., and Pauly, D. (2012) Increasing jellyfish populations: trends in Large Marine Ecosystems. *Hydrobiologia* **690**, 3-20
- Bruland, K.W., and Silver, M.W. (1981) Sinking rates of fecal pellets from gelatinous zooplankton (Salps, Pteropods, Doliolids). *Mar. Biol.* **63**, 295-300
- Bull, B., Livingston, M.E., Hurst, R., and Bagley, N. (2001) Upper-slope fish communities on the Chatham Rise, New Zealand, 1992-99. *N. Z. J. Mar. Freshwat. Res.* **35**, 795-815
- Butman, C.A., Carlton, J.T., and Palumbi, S.R. (1995) Whaling effects on deep-sea biodiversity. *Conserv. Biol.* **9**, 462-464
- Cacchione, D.A., Rowe, G.T., and Malahoff, A. (1978) Submersible investigation of outer Hudson submarine canyon. In *Sedimentation in submarine canyons, fans and trenches*. (Stanley, D.J., and Kelling, G., eds), 42-50, Hutchinson and Ross, Dowden
- Chase, J.M., and Leibold, M.A. (2003) *Ecological Niches*. University of Chicago Press, Chicago, USA.

Childress, J.J., and Nygaard, M.H. (1973) The chemical composition of midwater fishes as a function of depth of occurrence off southern California. *Deep Sea Res* **20**, 1093-1109

Clark, M.R. (1985) The food and feeding of seven fish species from the Campbell Plateau, New Zealand. *N. Z. J. Mar. Freshwat. Res.* **19**, 339-363

Clark, M.R., King, K.J., and McMillan, P.J. (1989) The food and feeding relationships of black oreo, *Allocyttus niger*, smooth oreo, *Pseudocyttus maculatus*, and eight other fish species from the continental slope of the south-west Chatham Rise, New Zealand. *J. Fish Biol.* **35**, 465-484

Clarke, A., Holmes, L.J., and Gore, D.J. (1992) Proximate and elemental composition of gelatinous zooplankton from the Southern Ocean. *J Exp Mar Biol Ecol* **155**, 55-68

Clarke, K.R., Somerfield, P.J., and Gorley, R.N. (2008) Testing of null hypotheses in exploratory community analyses: similarity profiles and biota-environment linkage. *J Exp Mar Biol Ecol* **366**, 56-69

Clarke, K.R., and Warwick, R.M. (2001) *Changes in marine communities: an approach to statistical analysis and interpretation*. PRIMER-E, Plymouth

Condie, S.A., and Dunn, J.R. (2006) Seasonal characteristics of the surface mixed layer in the Australasian region: implications for primary production regimes and biogeography. *Mar. Freshwat. Res.* **57**, 569-590

Condon, R.H., Duarte, C.M., Pitt, K.A., Robinson, K.L., Lucas, C.H., Sutherland, K.R., Mianzan, H., Bogeberg, M., Purcell, J.E., Decker, M.B., Uye, S., Madin, L.P., Brodeur, R.D., Haddock, S.H.D., Malej, A., Parry, G.D., Eriksen, E., Quiñones, J., Acha, M., Harvey, M., Arthur, J.M., and Graham, W.M. (2013) Recurrent jellyfish blooms are a consequence of global oscillations. *Proc. Natl. Acad. Sci. U. S. A.* **110**, 1000-1005

Condon, R.H., Graham, W.M., Duarte, C.M., Pitt, K.A., Lucas, C.H., Haddock, S.H.D., Sutherland, K.R., Robinson, K.L., Dawson, M.N., Decker, M.B., Mills, C.E., Purcell, J.E., Malej, A., Mianzan, H., Uye, S., Gelcich, S., and Madin, L.P. (2012) Questioning the rise of gelatinous zooplankton in the world's oceans. *Bioscience* **62**, 160-169

- Cresswell, G.R. (1994) Nutrient enrichment of the Sydney continental shelf. *Mar. Freshwat. Res.* **45**, 677-691
- Davenport, J., and Balazs, G.H. (1991) 'Fiery bodies' - Are pyrosomas an important component of the diet of leatherback turtles? *Brit. Herp. Soc. Bull.* **37**, 33-38
- Davenport, S.R., and Bax, N.J. (2002) A trophic study of a marine ecosystem off southeastern Australia using stable isotopes of carbon and nitrogen. *Can. J. Fish. Aquat. Sci.* **59**, 514-530
- Deibel, D. (1982) Laboratory determined mortality, fecundity and growth-rates of *Thalia democratica* Forskal and *Dolioletta gegenbauri* Uljanin (Tunicata, Thaliacea). *J. Plankton Res.* **4**, 143-153
- Deibel, D., and Lowen, B. (2012) A review of the life cycles and life-history adaptations of pelagic tunicates to environmental conditions. *ICES J Mar Sci* **69**, 358-369
- Deibel, D., and Paffenhofer, G.A. (2009) Predictability of patches of neritic salps and doliolids (Tunicata, Thaliacea). *J. Plankton Res.* **31**, 1571-1579
- del Giorgio, P.A., and France, R.L. (1996) Ecosystem-specific patterns in the relationship between zooplankton and POM or microplankton $\delta^{13}C$. *Limnol. Oceanogr.* **41**, 359-365
- Dela-Cruz, J., Middleton, J.H., and Suthers, I.M. (2008) The influence of upwelling, coastal currents and water temperature on the distribution of the red tide dinoflagellate, *Noctiluca scintillans*, along the east coast of Australia. *Hydrobiologia* **598**, 59-75
- Doblin, M.A., Petrou, K.L., Shelly, K., Westwood, K., van den Enden, R., Wright, S., Griffiths, B., and Ralph, P.J. (2011) Diel variation of chlorophyll-*a* fluorescence, phytoplankton pigments and productivity in the Sub-Antarctic and Polar Front Zones south of Tasmania, Australia. *Deep Sea Res. Part II* **58**, 2189-2199
- Doi, H., Kobari, T., Fukumori, K., Nishibe, Y., and Nakano, S. (2010) Trophic niche breadth variability differs among three *Neocalanus* species in the subarctic Pacific Ocean. *J. Plankton Res.* **32**, 1733-1737

- Domanski, P.A. (1984) Giant larvae: prolonged planktonic larval phase in the asteroid *Luidia sarsi*. *Mar. Biol.* **80**
- Donnelly, J., Torres, J.J., Hopkins, T.L., and Lancraft, T.M. (1994) Chemical composition of Antarctic zooplankton during austral fall and winter. *Polar Biol.* **14**, 171-183
- Dubischar, C.D., and Bathmann, U.V. (1997) Grazing impact of copepods and salps on phytoplankton in the Atlantic sector of the Southern Ocean. *Deep-Sea Research Part II -Topical Studies in Oceanography* **44**, 415-433
- Dubischar, C.D., Pakhomov, E., and Bathmann, U.V. (2006) The tunicate *Salpa thompsoni* ecology in the Southern Ocean II. Proximate and elemental composition. *Mar. Biol.* **149**, 625-632
- Dubois, M., Gilles, K.A., Hamilton, J.K., Rebers, P.A., and Smith, F. (1956) Colorimetric method for determination of sugars and related substances. *Anal. Chem.* **28**, 350-356
- Duggins, D.O. (1981) Sea urchins and kelp: The effects of short term changes in urchin diet. *Limnol. Oceanogr.* **26**, 391-394
- Dunn, M.R., Griggs, L., Forman, J., and Horn, P.L. (2010) Feeding habits and niche separation among the deep-sea chimaeroid fishes *Harriotta raleighana*, *Hydrolagus bemisi* and *Hydrolagus novaezealandiae*. *Mar. Ecol. Prog. Ser.* **407**, 209-225
- Elton, C.S. (1927) *Animal Ecology*. Sidgewick & Jackson, London
- Everett, J.D., Baird, M.E., Oke, P.R., and Suthers, I.M. (2012) An avenue of eddies: Quantifying the biophysical properties of mesoscale eddies in the Tasman Sea. *Geophys. Res. Lett.* **39**, L16608
- Everett, J.D., Baird, M.E., Roughan, M., Suthers, I.M., and Doblin, M.A. (2014) Relative impact of seasonal and oceanographic drivers on surface chlorophyll *a* along a Western Boundary Current. *Prog. Oceanogr.* **120**, 340-351

- Everett, J.D., Baird, M.E., and Suthers, I.M. (2011) Three-dimensional structure of a swarm of the salp *Thalia democratica* within a cold-core eddy off southeast Australia. *J. Geophys. Res.* **116**, C12046
- Fanelli, E., Papiol, V., Cartes, J.E., Rumolo, P., Brunet, C., and Sprovieri, M. (2011) Food web structure of the epibenthic and infaunal invertebrates on the Catalan slope (NW Mediterranean): Evidence from $\delta^{13}\text{C}$ and $\delta^{15}\text{N}$ analysis. *Deep Sea Res. Part I* **58**, 98-109
- Fischer, G., Futterer, D., Gersonde, R., Honjo, S., Ostermann, D., and Wefer, G. (1988) Seasonal variability of particle flux in the Weddell Sea and its relation to ice cover. *Nature* **335**, 426-428
- Folch, J., Lees, M., and Sloane Stanley, G.H. (1957) A simple method for the isolation and purification of total lipides from animal tissues. *J. Biol. Chem.* **226**, 497-509
- Foxton, P. (1966) The distribution and life-history of *Salpa thompsoni* Foxton with observations on a related species, *Salpa gerlachei* Foxton. *Discov Rep* **34**, 1-116
- Fraser, J. (1962) The role of ctenophores and salps in zooplankton production and standing crop. *Rapports et Proces Verbaux des Reunions du Conseil permanent International pour l'Exploration de la Mer* **153**, 121-123
- Frederiksen, M., Edwards, M., Richardson, A.J., Halliday, N.C., and Wanless, S. (2006) From plankton to top predators: bottom-up control of a marine food web across four trophic levels. *J. Anim. Ecol.* **75**, 1259-1268
- Fry, B., and Wainright, S.C. (1991) Diatom sources of ^{13}C -rich carbon in marine food webs. *Mar. Ecol. Prog. Ser.* **76**, 149-157
- Fulton, E.A., Smith, A.D.M., and Punt, A.E. (2004) Ecological indicators of the ecosystem effects of fishing: Final Report. *Report No. R99/1546, Australian Fisheries Management Authority, Canberra*
- Gibbons, M.J. (1997) Vertical distribution and feeding of *Thalia democratica* on the Agulhas Bank during March 1994. *J. Mar. Biol. Assoc. U.K.* **77**, 493-505

- Gibbons, M.J., and Richardson, A.J. (2013) Beyond the jellyfish joyride and global oscillations: advancing jellyfish research. *J. Plankton Res.* **35**, 929-938
- Gili, J.M., Rossi, S., Pages, F., Orejas, C., Teixido, N., Lopez-Gonzalez, P.J., and Arntz, W.E. (2006) A new trophic link between the pelagic and benthic systems on the Antarctic shelf. *Mar. Ecol. Prog. Ser.* **322**, 43-49
- Godeaux, J. (1965) Observations sur la tunique des tuniciers pelagiques. *Rapports et Proces Verbaux des Reunions* **18**, 457-460
- Godeaux, J.E.A., Bone, Q., and Braconnot, J.C. (1998) Anatomy of Thaliacea. In *The Biology of Pelagic Tunicates* (Bone, Q., ed), 1-24, Oxford University Press, New York
- Godfrey, J.S., Cresswell, G.R., Golding, T.J., Pearce, A.F., and Boyd, R. (1980) The Separation of the East Australian Current. *J. Phys. Oceanogr.* **10**, 430-440
- Goericke, R., Montoya, J.P., and Fry, B. (1994) Physiology of isotopic fractionation in algae and cyanobacteria. In *Stable isotopes in ecology and environmental science*, 187-221, Blackwell, Oxford
- Goericke, R., and Repeta, D.J. (1992) The pigments of *Prochlorococcus marinus* - the presence of divinyl chlorophyll-*a* and chlorophyll-*b* in a marine prokaryote. *Limnol. Oceanogr.* **37**, 425-433
- Gooday, A.J. (2002) Biological responses to seasonally varying fluxes of organic matter to the ocean floor: A review. *J. Oceanogr.* **58**, 305-332
- Grassle, J.F., and Morse-Porteous, L.S. (1987) Macrofaunal colonization of disturbed deep-sea environments and the structure of deep-sea benthic communities. *Deep Sea Res. Part A* **34**, 1911-1950
- Haddock, S.H.D. (2004) A golden age of gelata: past and future research on planktonic ctenophores and cnidarians. *Hydrobiologia* **530/531**, 549-556
- Hamner, W.M., Madin, L.P., Alldredge, A.L., Gilmer, R.W., and Hamner, P.P. (1975) Underwater observations of gelatinous zooplankton: Sampling problems, feeding biology, and behavior. *Limnol. Oceanogr.* **20**, 907 - 917

- Harbison, G., and Gilmer, R. (1976) The feeding rates of the pelagic tunicate *Pegea confederata* and two other salps. *Limnol. Oceanogr.* **21**, 517-528
- Harbison, G.R., McAlister, V.L., and Gilmer, R.W. (1986) The response of the salp, *Pegea confoederata*, to high levels of particulate material: Starvation in the midst of plenty. *Limnol. Oceanogr.* **31**, 371-382
- Harris, G., Griffiths, F., Clementson, L., Lyne, V., and Van der Doe, H. (1991) Seasonal and interannual variability in physical processes, nutrient cycling and the structure of the food chain in Tasmanian shelf waters. *J. Plankton Res.* **13**, 109-131
- Hastie, T.J., and Tibshirani, R.J. (1990) *Generalized additive models*. Chapman & Hall, London
- Hay, S. (2006) Marine ecology: Gelatinous bells may ring change in marine ecosystems. *Curr Biol* **16**, R679-R682
- Hays, G.C., Richardson, A.J., and Robinson, C. (2005) Climate change and marine plankton. *Trends Ecol. Evol.* **20**, 337-344
- Henschke, N., Bowden, D.A., Everett, J.D., Holmes, S.P., Kloser, R.J., Lee, R.W., and Suthers, I.M. (Year) Pelagic-benthic coupling: The fate of moribund mega salps (*Thetys vagina* (Tunicata, Thaliacea)) and their importance as food fall in the deep sea. In Australian Marine Science Association - New Zealand Marine Science Society, Hobart, Australia. , 1-5 July 2012,
- Henschke, N., Bowden, D.A., Everett, J.D., Holmes, S.P., Kloser, R.J., Lee, R.W., and Suthers, I.M. (2013) Salp-falls in the Tasman Sea: a major food input to deep sea benthos. *Mar. Ecol. Prog. Ser.* **491**, 165-175
- Henschke, N., Everett, J.D., Baird, M.E., Taylor, M.D., and Suthers, I.M. (2011) Distribution of life history stages of the salp *Thalia democratica* in shelf waters during a spring bloom. *Mar. Ecol. Prog. Ser.* **430**, 49-62
- Heron, A.C. (1972) Population ecology of a colonizing species - pelagic tunicate *Thalia democratica*. 1. Individual growth-rate and generation time. *Oecologia* **10**, 269-293

- Heron, A.C. (1982) A vertical free fall plankton net with no mouth obstructions. *Limnol. Oceanogr.* **27**, 380-383
- Heron, A.C., and Benham, E.E. (1984) Individual growth rates of salps in three populations. *J. Plankton Res.* **6**, 811-828
- Heron, A.C., and Benham, E.E. (1985) Life history parameters as indicators of growth rate in three salp populations. *J. Plankton Res.* **7**, 365-379
- Heron, A.C., McWilliam, P.S., and Dalpont, G. (1988) Length weight relation in the salp *Thalia democratica* and potential of salps as a source of food. *Mar. Ecol. Prog. Ser.* **42**, 125-132
- Hill, P. (2009) Designing a deep-towed camera vehicle using single conductor cable. *Sea Technol.* **50**, 49-51
- Hirose, E., Kimura, S., Itoh, T., and Nishikawa, J. (1999) Tunic morphology and cellulosic components of pyrosomas, doliolids, and salps (Thaliacea, Urochordata). *Biol. Bull.* **196**, 113-120
- Hobday, A.J., Okey, T.A., Poloczanska, E.S., Kunz, T.J., and Richardson, A.J. (2006) Impacts of climate change on Australian marine life, Australian Greenhouse Office, Canberra, Australia.
- Hoeksema, B.W., and Waheed, Z. (2012) It pays to have a big mouth: mushroom corals ingesting salps at northwest Borneo. *Mar. Biodiv.* **22**, 297-302
- Hopcroft, R.R., and Roff, J.C. (1995) Zooplankton growth rates: extraordinary production by the larvacean *Oikopleura dioica* in tropical waters. *J. Plankton Res.* **17**, 205-220
- Hopkins, T. (1985) Food web of an Antarctic midwater ecosystem. *Mar. Biol.* **89**, 197-212
- Humphrey, G.F. (1963) Seasonal variation in plankton pigments in waters off Sydney. *Australian Journal of Marine and Freshwater Research* **14**, 24-36

- Huntley, M.E., Sykes, P.F., and Marin, V. (1989) Biometry and trophodynamics of *Salpa thompsoni* Foxton (Tunicata, Thaliacea) near the Antarctic Peninsula in austral summer, 1983-1984. *Polar Biol.* **10**, 59-70
- Iguchi, N., and Kidokoro, H. (2006) Horizontal distribution of *Thetys vagina* Tilesius (Tunicata, Thaliacea) in the Japan Sea during spring 2004. *J. Plankton Res.* **28**, 537-541
- Ikeda, T., Yamaguchi, A., and Matsuishi, T. (2006) Chemical composition and energy content of deep-sea calanoid copepods in the western North Pacific Ocean. *Deep Sea Res. Part I* **53**, 1791-1809
- IMOS (2014) National Reference Station zooplankton counts. <http://imos.aodn.org.au/>. accessed 09/05/2014
- Jackson, A.L., Inger, R., Parnell, A.C., and Bearhop, S. (2011) Comparing isotopic niche widths among and within communities: SIBER - Stable Isotope Bayesian Ellipses in R. *J. Anim. Ecol.* **80**, 595-602
- Jeffrey, S.W., Mantoura, R.F.C., and Wright, S.W. (1997) *Phytoplankton pigments in oceanography: Guidelines to modern methods monographs on oceanographic methodology*. UNESCO Publishing, Paris
- Johnson, C.R., Banks, S.C., Barrett, N.S., Cazassus, F., Dunstan, P.K., Edgar, G.J., Frusher, S.D., Gardner, C., Haddon, M., Helidoniotis, F., Hill, K.J., Holbrook, N.J., Hosie, G.W., Last, P.R., Ling, S.D., Melbourne-Thomas, J., Miller, K., Pecl, G.T., Richardson, A.J., Ridgway, K.R., Rintoul, S.R., Ritz, D.A., Ross, D.J., Sanderson, J.C., Shepherd, S.A., Slotwinski, A., Swadling, K.M., and Taw, N. (2011) Climate change cascades: Shifts in oceanography, species' ranges and subtidal marine community dynamics in eastern Tasmania. *J Exp Mar Biol Ecol* **400**, 17-32
- Kasai, A., Kimura, S., Nakata, H., and Okazaki, Y. (2002) Entrainment of coastal water into a frontal eddy of the Kuroshio and its biological significance. *J Mar Syst* **37**, 185-198
- Kashkina, A.A. (1986) Feeding of Fishes on Salps (Tunicata, Thaliacea). *Voprosy Iktiologii* **3**, 440-447

- Kawaguchi, S., Ichii, T., and Naganobu, M. (1998) Do krill and salps compete? Contrary evidence from the krill fisheries. *CCAMLR Sci.* **5**, 205-216
- Kawaguchi, S., and Takahashi, Y. (1996) Antarctic krill (*Euphausia superba* Dana) eat salps. *Polar Biol.* **16**, 479-481
- Kawahata, H., and Ohta, H. (2000) Sinking and suspended particles in the South-west Pacific. *Mar. Freshwat. Res.* **51**, 113-126
- Kemp, S., and Hardy, M.A. (1929) The ships, their equipment and the methods used in research. *Discov Rep* **1**, 181-189
- Kimura, S., Nakata, H., and Okazaki, Y. (2000) Biological production in meso-scale eddies caused by frontal disturbances of the Kuroshio Extension. *ICES J Mar Sci* **57**, 133-142
- Kleijnen, J.P.C. (1997) Sensitivity analysis and related analyses: A review of some statistical techniques. *J. Statist. Comput. Simulation* **57**, 111-142
- Koski, M., Moller, E., Maar, M., and Visser, A. (2007) The fate of discarded appendicularian houses: degradation by the copepod, *Microsetella norvegica*, and other agents. *J. Plankton Res.* **29**, 641-654
- Kouwenberg, J.H.M. (1994) Copepod distribution in relation to seasonal hydrographics and spatial structure in the North-western Mediterranean (Golfe du Lion). *Estuar. Coast. Shelf Sci.* **38**, 69-90
- Landry, M.R. (1981) Switching between herbivory and carnivory by the planktonic marine copepod *Calanus pacificus*. *Mar. Biol.* **65**, 77-82
- Larson, R.J., and Harbison, G.R. (1989) Source and fate of lipids in polar gelatinous zooplankton. *Arctic* **42**, 339-346
- Lavaniegos, B.E., and Ohman, M.D. (2003) Long-term changes in pelagic tunicates of the California Current. *Deep Sea Res. Part II* **50**, 2473-2498

- Layman, C.A., Arrington, D.A., Montaña, C.G., and Post, D.M. (2007a) Can stable isotope ratios provide for community-wide measures of trophic structure? *Ecology* **88**, 42-48
- Layman, C.A., Quattrochi, J.P., Peyer, C.M., and Allgeier, J.E. (2007b) Niche width collapse in a resilient top predator following ecosystem fragmentation. *Ecol. Lett.* **10**, 937-944
- Le Borgne, R., and Moll, P. (1986) Growth rates of the salp *Thalia democratica* in Tikehau atoll (Tuamotu is.). *Océanographie Tropicale* **21**, 23-29
- Lebrato, M., de Jesus Mendes, P., Steinberg, D.K., Cartes, J.E., Jones, B.M., Birsa, L.B., Benavides, R., and Oschlies, A. (2013) Jelly biomass sinking speed reveals a fast carbon export mechanism. *Limnol. Oceanogr.* **58**, 1113-1122
- Lebrato, M., and Jones, D.O.B. (2009) Mass deposition event of *Pyrosoma atlanticum* carcasses off Ivory Coast (West Africa). *Limnol. Oceanogr.* **54**, 1197-1209
- Lebrato, M., Pahlow, M., Oschlies, A., Pitt, K.A., Jones, D.O.B., Molinero, J.C., and Condon, R.H. (2011) Depth attenuation of organic matter export associated with jelly falls. *Limnol. Oceanogr.* **56**, 1917-1928
- Lebrato, M., Pitt, K., Sweetman, A., Jones, D., Cartes, J., Oschlies, A., Condon, R., Molinero, J., Adler, L., Gaillard, C., Lloris, D., and Billett, D. (2012) Jelly-falls historic and recent observations: a review to drive future research directions. *Hydrobiologia* **690**, 227-245
- Lefkovich, L.P. (1965) The study of population growth in organisms grouped by stages. *Biometrics* **21**, 1-18
- Leibold, M.A. (1995) The niche concept revisited - mechanistic models and community context. *Ecology* **76**, 1371-1382
- Lewontin, R.C. (1965) Selection for colonizing ability. In *The genetics of colonizing species* (Baker, H.G., and Stebbins, G.L., eds), 77-94, Academic Press, New York

- Licandro, P., Ibanez, F., and Etienne, M. (2006) Long-term fluctuations (1974-1999) of the salps *Thalia democratica* and *Salpa fusiformis* in the northwestern Mediterranean Sea: Relationships with hydroclimatic variability. *Limnol. Oceanogr.* **51**, 1832-1848
- Loeb, V.J., and Santora, J.A. (2012) Population dynamics of *Salpa thompsoni* near the Antarctic Peninsula: Growth rates and interannual variations in reproductive activity (1993 - 2009). *Prog. Oceanogr.* **96**, 93-107
- Longhurst, A.R. (1985) Relationship between diversity and the vertical structure of the upper ocean. *Deep Sea Res* **32**, 1535-1570
- Lotka, A.J. (1925) *Elements of mathematical biology*. Dover Publishers, New York
- Lyle, J.M., and Smith, D.C. (1997) Abundance and biology of warty oreo (*Allocyttus verrucosus*) and spikey oreo (*Neocyttus rhomboidalis*)(Oreosomatidae) off south-eastern Australia. *Mar. Freshwat. Res.* **48**, 91-102
- Maciejewska, K. (1993) Feeding of Antarctic krill *Euphausia superba* in Weddell Sea. *Polish Polar Research* **14**, 52-54
- Madin, L.P., Cetta, C.M., and McAlister, V.L. (1981) Elemental and Biochemical Composition of Salps (Tunicata: Thaliacea). *Mar. Biol.* **63**, 217-226
- Madin, L.P., and Deibel, D. (1998) Feeding and energetics of Thaliaceans. In *The Biology of Pelagic Tunicates* (Bone, Q., ed), 43-64, Oxford University Press, New York
- Madin, L.P., Kremer, P., Wiebe, P.H., Purcell, J.E., Horgan, E.H., and Nemazie, D.A. (2006) Periodic swarms of the salp *Salpa aspera* in the Slope Water off the NE United States: Biovolume, vertical migration, grazing, and vertical flux. *Deep Sea Res. Part I* **53**, 804-819
- Malcolm, H.A., Davies, P.L., Jordan, A., and Smith, S.D.A. (2011) Variation in sea temperature and the East Australian Current in the Solitary Islands region between 2001-2008. *Deep Sea Res. Part II* **58**, 616-627
- Mantoura, R.F.C., and Llewellyn, C.A. (1983) The rapid determination of algal chlorophyll and carotenoid pigments and their breakdown products in natural waters by reverse-phase high-performance liquid chromatography. *Anal. Chim. Acta* **151**, 297-314

- Menard, F., Dallot, S., Thomas, G., and Braconnot, J.C. (1994) Temporal fluctuations of two Mediterranean salp populations from 1967 to 1990 - Analysis of the influence of environmental variables using a Markov-chain model. *Mar. Ecol. Prog. Ser.* **104**, 139-152
- Miller, R.L., and Cosson, J. (1997) Timing of sperm shedding and release of aggregates in the salp *Thalia democratica* (Urochordata: Thaliacea). *Mar. Biol.* **129**, 607-614
- Minagawa, M., and Wada, E. (1984) Stepwise enrichment of ^{15}N along food chains: Further evidence and the relation between $\delta^{15}\text{N}$ and animal age. *Geochim. Cosmochim. Acta* **48**, 1135-1140
- Mitchell, J.K., Holdgate, G.R., Wallace, M.W., and Gallagher, S.J. (2007) Marine geology of the Quaternary Bass Canyon system, southeast Australia: A cool-water carbonate system. *Mar. Geol.* **237**, 71-96
- Moline, M.A., Claustre, H., Frazer, T.K., Schofield, O., and Vernet, M. (2004) Alteration of the food web along the Antarctic Peninsula in response to a regional warming trend. *Global Change Biol.* **10**, 1973-1980
- Morris, R.J., Bone, Q., Head, R., Braconnot, J.C., and Nival, P. (1988) Role of salps in the flux of organic matter to the bottom of the Ligurian Sea. *Mar. Biol.* **97**, 237-241
- Moseley, H.N. (1880) Deep-sea dredging and life in the deep sea. *Nature* **21**, 591-593
- Mullaney, T.J., and Suthers, I.M. (2013) Entrainment and retention of the coastal larval fish assemblage by a short-lived, submesoscale, frontal eddy of the East Australian Current. *Limnol. Oceanogr.* **58**, 1546-1556
- Mullin, M.M. (1983) In situ measurement of filtering rates of the salp, *Thalia democratica*, on phytoplankton and bacteria. *J. Plankton Res.* **5**, 279-288
- Nakamura, E.L., and Yount, J.L. (1958) An unusually large salp. *Pac. Sci.* **12**, 181
- Nichols, P., Mooney, B., Virtue, P., and Elliott, N. (1998) Nutritional value of Australian fish: oil, fatty acid and cholesterol of edible species. *Final Report, Fisheries Research and Development Corporation Project 95/122*

- Nilsson, C.S., and Cresswell, G.R. (1981) The formation and evolution of East Australian current warm-core eddies. *Prog. Oceanogr.* **9**, 133-183
- Nishikawa, J., Naganobu, M., Ichii, T., Ishii, H., Terazaki, M., and Kawaguchi, K. (1995) Distribution of salps near the south Shetland Islands during austral summer, 1990–1991 with special reference to krill distribution. *Polar Biol.* **15**, 31-39
- NIWA (2014) Remote sensing of phytoplankton biomass and productivity. <https://www.niwa.co.nz/environmental-information/research-projects/remote-sensing-of-phytoplankton-biomass-and-productivity>. accessed 14/07/2014.
- Nodder, S.D., Pilditch, C.A., Probert, P.K., and Hall, J.A. (2003) Variability in benthic biomass and activity beneath the Subtropical Front, Chatham Rise, SW Pacific Ocean. *Deep Sea Res. Part I* **50**, 959-985
- O'Driscoll, R.L. (2004) Estimating uncertainty associated with acoustic surveys of spawning hoki (*Macruronus novaezelandiae*) in Cook Strait, New Zealand. *ICES J Mar Sci* **61**, 84-97
- Oke, P.R., and Sakov, P. (2012) Assessing the footprint of a regional ocean observing system. *J Mar Syst* **105-108**, 30-51
- Paffenhofer, G.A., and Lewis, K.D. (1989) Feeding behaviour of nauplii of the genus *Eucalanus* (Copepoda, Calanoida). *Mar. Ecol. Prog. Ser.* **57**, 129-136
- Pakhomov, E.A., Froneman, P.W., and Perissinotto, R. (2002) Salp/krill interactions in the Southern Ocean: spatial segregation and implications for the carbon flux. *Deep Sea Res. Part II* **49**, 1881-1907
- Park, C., and Wormuth, J.H. (1993) Distribution of Antarctic zooplankton around Elephant Island during the austral summers of 1988, 1989, and 1990. *Polar Biol.* **13**, 215-225
- Park, T. (1994) Geographic distribution of the bathypelagic genus *paraeuchaeta* (Copepoda, Calanoida). *Hydrobiologia* **292/293**, 317-332
- Parnell, A.C., Inger, R., Bearhop, S., and Jackson, A.L. (2010) Source partitioning using stable isotopes: coping with too much variation. *PLoS One* **5**, e9672

- Parr (2008) 6200 Calorimeter Operating Instruction Manual No. 442M. Parr Instrument Company
- Partridge, L., Gems, D., and Withers, D.J. (2005) Sex and Death: What Is the Connection? *Cell* **120**, 461-472
- Percy, J.A., and Fife, F.J. (1981) The biochemical composition and energy content of Arctic marine macrozooplankton. *Arctic* **34**, 307-313
- Perissinotto, R., and Pakhomov, E.A. (1998) Contribution of salps to carbon flux of marginal ice zone of the Lazarev Sea, Southern Ocean. *Mar. Biol.* **131**, 25-32
- Peterson, B.J., and Fry, B. (1987) Stable isotopes in ecosystem studies. *Annu. Rev. Ecol. Syst.* **18**, 293-320
- Peterson, W.T., Painting, S.J., and Hutchings, L. (1990) Diel variations in gut pigment content, diel vertical migration and estimates of grazing impact for copepods in the southern Benguela upwelling region in October 1987. *J. Plankton Res.* **12**, 259-281
- Pillar, S.C., Stuart, V., Barange, M., and Gibbons, M.J. (1992) Community structure and trophic ecology of euphausiids in the Benguela ecosystem. *South African Journal of Marine Science* **12**, 393-409
- Platt, T., and Irwin, B. (1973) Caloric content of phytoplankton. *Limnol. Oceanogr.* **18**, 306-310
- Poloczanska, E.S., Babcock, R.C., Butler, A., Hobday, A.J., Hoegh-Guldberg, O., Kunz, T.J., Matear, R., Milton, D.A., Okey, T.A., and Richardson, A.J. (2007) Climate change and Australian marine life. *Oceanogr. Mar. Biol. Annu. Rev.* **45**, 407-478
- Post, D.M. (2002) Using stable isotopes to estimate trophic position: Models, methods, and assumptions. *Ecology* **83**, 703-718
- Ragueneau, O., Treguer, P., Leynaert, A., Anderson, R.F., Brzezinski, M.A., DeMaster, D.J., Dugdale, R.C., Dymond, J., Fischer, G., Francois, R., Heinze, C., Maier-Reimer, E., Martin-Jezequel, V., Nelson, D.M., and Queguiner, B. (2000) A review of the Si cycle in the modern ocean: recent progress and missing gaps in the application of biogenic opal as a paleoproductivity proxy. *Global Planet. Change* **26**, 317-365

- Raskoff, K.A., Sommer, F.A., Hamner, W.M., and Cross, K.M. (2003) Collection and culture techniques for gelatinous zooplankton. *Biol. Bull.* **204**, 68-80
- Rau, G.H., Teyssie, J.-L., Rassoulzadegan, F., and Fowler, S.W. (1990) $^{13}\text{C}/^{12}\text{C}$ and $^{15}\text{N}/^{14}\text{N}$ variations among size-fractionated marine particles: implications for their origin and trophic relationships. *Mar. Ecol. Prog. Ser.* **59**, 33-38
- Revill, A.T., Young, J.W., and Lansdell, M. (2009) Stable isotopic evidence for trophic groupings and bio-regionalization of predators and their prey in oceanic waters off eastern Australia. *Mar. Biol.* **156**, 1241-1253
- Richardson, A.J., Bakun, A., Hays, G.C., and Gibbons, M.J. (2009) The jellyfish joyride: causes, consequences and management actions. *Trends Ecol. Evol.* **24**, 312-322
- Richoux, N.B., and Froneman, P.W. (2009) Plankton trophodynamics at the subtropical convergence, Southern Ocean. *J. Plankton Res.* **31**, 1059-1073
- Robison, B.H., Reisenbichler, K.R., and Sherlock, R.E. (2005) Giant larvacean houses: Rapid carbon transport to the deep sea floor. *Science* **308**, 1609-1611
- Roe, H.S.J., Billett, D.S.M., and Lampitt, R.S. (1990) Benthic/midwater interactions on the Madeira Abyssal Plain; evidence for biological transport pathways. *Prog. Oceanogr.* **24**, 127-140
- Rolff, C. (2000) Seasonal variation in $\delta^{13}\text{C}$ and $\delta^{15}\text{N}$ of size-fractionated plankton at a coastal station in the northern Baltic proper. *Mar. Ecol. Prog. Ser.* **203**, 47-65
- Rowe, G.T., and Staresinic, N. (1979) Sources of organic matter to the deep-sea benthos. *Ambio Special Report* **6**, 19-23
- Sano, M., Maki, K., Nishibe, Y., Nagata, T., and Nishida, S. (2013) Feeding habits of mesopelagic copepods in Sagami Bay: Insights from integrative analysis. *Prog. Oceanogr.* **110**, 11-26
- Schneider, G. (1990) A comparison of carbon based ammonia excretion rates between gelatinous and non-gelatinous zooplankton: implications and consequences. *Mar. Biol.* **106**, 219-225

Schopf, J.W. (1992) *Major events in the history of life*. Jones & Bartlett Learning, Boston

Sheard, K. (1949) Plankton characteristics at the Cronulla onshore station, New South Wales, 1943-46. *Commonwealth Scientific and Industrial Research Organisation* **246**

Sherlock, M., Kloser, R., Williams, A., and Ryan, T. (Year) A combined benthic grab and observation system for rapid assessment of water column and seabed. In Proceedings of the OCEANS'10 Institute of Electrical and Electronics Engineers Conference, Sydney, Australia, 24-27 May 2010, 1-5

Siegel, V., and Harm, U. (1996) The composition, abundance, biomass and diversity of the epipelagic zooplankton communities of the southern Bellinghousen Sea (Antarctic) with special reference to krill and salps. *Archive of Fishery and Marine Research* **44**, 115-139

Smith, C.R., and Baco, A.R. (2003) *Ecology of whale falls at the deep-sea floor*. Taylor & Francis, London

Smith, C.R., De Leo, F.C., Bernardino, A.F., Sweetman, A.K., and Arbizu, P.M. (2008) Abyssal food limitation, ecosystem structure and climate change. *Trends Ecol. Evol.* **23**, 518-528

Smith, J.A., Baumgartner, L.J., Suthers, I.M., Ives, M.C., and Taylor, M.D. (2012) Estimating the stocking potential of fish in impoundments by modelling supply and steady-state demand. *Freshwat. Biol.* **57**, 1482-1499

Smith Jr, K.L., Sherman, A.D., Huffard, C.L., McGill, P.R., Henthorn, R., Von Thun, S., Ruhl, H.A., Kahru, M., and Ohman, M.D. (2014) Large salp bloom export from the upper ocean and benthic community response in the abyssal northeast Pacific: Day to week resolution. *Limnol. Oceanogr.* **59**, 745-757

Smith, K.L., and Kaufmann, R.S. (1999) Long-term discrepancy between food supply and demand in the deep eastern North Pacific. *Science* **284**, 1174-1177

- Smith, M.J., and Dehnel, P.A. (1971) The composition of tunic from four species of ascidians. *Comparative Biochemistry and Physiology B-Biochemistry & Molecular Biology* **40B**, 615-622
- Stockton, W.L., and DeLaca, T.E. (1982) Food falls in the deep sea: occurrence, quality, and significance. *Deep Sea Res. Part I* **29**, 157-169
- Stowasser, G., Atkinson, A., McGill, R.A.R., Phillips, R.A., Collins, M.A., and Pond, D.W. (2012) Food web dynamics in the Scotia Sea in summer: A stable isotope study. *Deep Sea Res. Part II* **59-60**, 208-221
- Sutherland, K.R., Madin, L.P., and Stocker, R. (2010) Filtration of submicrometer particles by pelagic tunicates. *Proc. Natl. Acad. Sci. U. S. A.* **107**, 15129-15134
- Suthers, I.M., J.W., Y., Baird, M.E., Roughan, M., Everett, J.D., Brassington, G.B., Byrne, M., Oke, P.R., Condie, S.A., Hartog, J.R., Hassler, C.S., Holbrook, N.J., and Malcolm, H.A. (2011) The strengthening East Australian Current, its eddies and biological effects—An introduction and overview. *Deep Sea Res. Part II* **58**, 538-546
- Sweetman, A.K., and Chapman, A. (2011) First observations of jelly-falls at the seafloor in a deep-sea fjord. *Deep Sea Res. Part I* **58**, 1206-1211
- Sweetman, A.K., and Witte, U. (2008) Response of an abyssal macrofaunal community to a phytodetrital pulse. *Mar. Ecol. Prog. Ser.* **355**, 73-84
- Terazaki, M. (1998) Life history, distribution, seasonal variability and feeding of the pelagic chaetognath *Sagitta elegans* in the Subarctic Pacific: A review. *Plankton Biol. Ecol.* **45**, 1-17
- Thompson, H. (1948) *Pelagic tunicates of Australia*. Commonwealth Council for Scientific and Industrial Research, Melbourne
- Thompson, H., and Kesteven, G.L. (1942) Pelagic tunicates in the plankton of south-eastern Australian waters, and their place in oceanographic studies. In *Bulletin*, 153: 151-156, Council for Scientific and Industrial Research
- Threlkeld, S.T. (1976) Starvation and the size structure of zooplankton communities. *Freshwat. Biol.* **6**, 489-496

- Timonin, A.G. (1971) The structure of plankton communities of the Indian Ocean. *Mar. Biol.* **9**, 281-289
- Tranter, D.J. (1962) Zooplankton abundance in Australasian waters. *Mar. Freshwat. Res.* **13**, 106-142
- Troedsson, C., Bouquet, J.-M., Aksnes, D.L., and Thompson, E.M. (2002) Resource allocation between somatic growth and reproductive output in the pelagic chordate *Oikopleura dioica* allows opportunistic response to nutritional variation. *Mar. Ecol. Prog. Ser.* **243**, 83-91
- Tsuda, A., and Nemoto, T. (1992) Distribution and growth of salps in a Kuroshio warm-core ring during summer 1987. *Deep Sea Res. Part A* **39**, **Supplement 1**, S219-S229
- Uitz, J., Huot, Y., Bruyant, F., Babin, M., Claustre, H., and Claustre, H. (2008) Relating phytoplankton photophysiological properties to community structure on large scales. *Limnol. Oceanogr.* **53**, 614-630
- Vander Zanden, M.J., and Rasmussen, J.B. (1999) Primary consumer $\delta^{13}\text{C}$ and $\delta^{15}\text{N}$ and the trophic position of aquatic consumers. *Ecology* **80**, 1395-1404
- Vanderklift, M.A., and Ponsard, S. (2003) Sources of variation in consumer-diet $\delta^{15}\text{N}$ enrichment: a meta-analysis. *Stable Isotope Ecology* **136**, 169-182
- Vargas, C.A., and Madin, L.P. (2004) Zooplankton feeding ecology: clearance and ingestion rates of the salps *Thalia democratica*, *Cyclosalpa affinis* and *Salpa cylindrica* on naturally occurring particles in the Mid-Atlantic Bight. *J. Plankton Res.* **26**, 827-833
- von Vaupel Klein, J.C. (1998) Cases of niche-partitioning and of habitat-segregation in pelagic marine calanoids of the genus *Euchirella* (Crustacea: Copepoda). *Zoologische Verhandelingen*, 383-400
- Voronina, N.M. (1998) Comparative abundance and distribution of major filter-feeders in the Antarctic pelagic zone. *J Mar Syst* **17**, 375-390
- Wacasey, J.W., and Atkinson, E.G. (1987) Energy values of marine benthic invertebrates from the Canadian Arctic. *Mar. Ecol. Prog. Ser.* **39**, 243-250

- Waite, A.M., Muhling, B.A., Holl, C.M., Beckley, L.E., Montoya, J.P., Strzelecki, J., Thompson, P.A., and Pesant, S. (2007a) Food web structure in two counter-rotating eddies based on $\delta^{15}\text{N}$ and $\delta^{13}\text{C}$ isotopic analyses. *Deep Sea Res. Part II* **54**, 1055-1075
- Waite, A.M., Pesant, S., Griffin, D.A., Thompson, P.A., and Holl, C.M. (2007b) Oceanography, primary production and dissolved inorganic nitrogen uptake in two Leeuwin Current eddies. *Deep Sea Res. Part II* **54**, 981-1002
- Wickstead, J.H. (1962) Food and feeding in pelagic copepods. *Proceedings of the Zoological Society of London* **139**, 545-555
- Wiebe, P.H., Madin, L.P., Haury, L.R., Harbison, G.R., and Philbin, L.M. (1979) Diel vertical migration by *Salpa aspera* and its potential for large-scale particulate organic matter transport to the deep-sea. *Mar. Biol.* **53**, 249-255
- Witte, U., and Pfannkuche, O. (2000) High rates of benthic carbon remineralisation in the abyssal Arabian Sea. *Deep Sea Res. Part II* **47**, 2785-2804
- Wong, W.W., and Sackett, W.M. (1978) Fractionation of stable carbon isotopes by marine phytoplankton. *Geochim. Cosmochim. Acta* **42**, 1809-1815
- Wood, R.A. (1991) Structure and seismic stratigraphy of the western Challenger Plateau. *N. Z. J. Geol. Geophys.* **34**, 1-9
- Wood, S.N. (2006) *Generalized additive models: An introduction with R*. Chapman & Hall/CRC, Boca Raton
- Yamamoto, J., Hirose, M., Ohtani, T., Sugimoto, K., Hirase, K., Shimamoto, N., Shimura, T., Honda, N., Fujimori, Y., and Mukai, T. (2008) Transportation of organic matter to the sea floor by carrion falls of the giant jellyfish *Nemopilema nomurai* in the Sea of Japan. *Mar. Biol.* **153**, 311-317
- Young, J.W. (1989) The distribution of hyperiid amphipods (Crustacea: Peracarida) in relation to warm-core eddy J in the Tasman Sea. *J. Plankton Res.* **11**, 711-728
- Young, J.W., Bradford, R.W., Lamb, T.D., and Lyne, V.D. (1996) Biomass of zooplankton and micronekton in the southern bluefin tuna fishing grounds off eastern Tasmania, Australia. *Mar. Ecol. Prog. Ser.* **138**, 1-14

Zeldis, J., James, M.R., Grieve, J., and Richards, L. (2002) Omnivory by copepods in the New Zealand Subtropical Frontal Zone. *J. Plankton Res.* **24**, 9-23

Zuur, A.F., Ieno, E.N., Walker, N.J., Saveliev, A.A., and Smith, G.M. (2009) *Mixed Effects Models and Extensions in Ecology with R (Statistics for Biology and Health)*. Springer-Verlag, New York